





# รายงานวิจัยฉบับสมบูรณ์

# โครงการ ความหลากหลายทางโครงสร้าง โครงสร้างเชิงพลวัติและสมบัติทางแม่เหล็กของ โคออร์ดิเนชันพอลิเมอร์ที่ประกอบด้วย pyrazole-3,5-dicarboxylate และตัวเชื่อมอินทรีย์ชนิด *N,N*'-ditopic

โดย ผศ.ดร. เจ้าทรัพย์ บุญมาก และคณะ

เมษายน 2561

# รายงานวิจัยฉบับสมบูรณ์

# โครงการ ความหลากหลายทางโครงสร้าง โครงสร้างเชิงพลวัติและสมบัติทางแม่เหล็กของ โคออร์ดิเนชันพอลิเมอร์ที่ประกอบด้วย pyrazole-3,5-dicarboxylate และตัวเชื่อมอินทรีย์ชนิด *N,N*'-ditopic

|    | คณะผู้วิจัย             | สังกัด             |
|----|-------------------------|--------------------|
| 1. | ผศ.ดร.เจ้าทรัพย์ บุญมาก | มหาวิทยาลัยขอนแก่น |
| 2. | ศ.ดร.สุจิตรา ยังมี      | มหาวิทยาลัยขอนแก่น |

สนับสนุนโดยสำนักงานคณะกรรมการอุดมศึกษา และสำนักงานกองทุนสนับสนุนการวิจัย (ความเห็นในรายงานนี้เป็นของผู้วิจัย สกอ. และ สกว. ไม่จำเป็นต้องเห็นด้วยเสมอไป)

#### ABSTRACT

Project Code: MRG5980237

Project Title: Structural diversity, structural dynamics and magnetic properties of coordination

polymers containing pyrazole-3,5-dicarboxylate and different N,N'-ditopic organic spacers

**Investigator:** Asst. Dr. Jaursup Boonmak, Khon Kaen University

E-mail Address: jaursup@kku.ac.th

**Project Period:** May 2, 2016 - May 1, 2018

A novel series of copper coordination polymers (CPs) containing pyrazole-3,5dicarboxylic acid (H<sub>3</sub>pzdc) with pyrazine (I-1), 4,4'-bipyridine (I-2, I-3), 2-aminopyrazine (I-4), and 1,2-di(4-pyridyl)ethylene (II-1-6) were successfully synthesized and characterized. The single crystal X-ray structural analysis demonstrated that various distorted geometries of Cu(II) centers, diverse coordination modes of H<sub>3</sub>pzdc and, N,N'-ditopic coligands play a key role on their structural diversity. The reaction temperature also has a great influence on the structural assembly. Furthermore, by utilizing a H<sub>3</sub>pzdc and flexible 1,2-di(4-pyridyl)ethylene (dpe) with various copper(II) salts under the same solvothermal synthetic condition, six novel CPs, namely,  $\{[Cu_2(pzdc)(dpe)_2]X\}_n$  (X = NO<sub>3</sub> (II-1),  $ClO_4$  (II-2),  $BF_4$  (II-3), SCN (II-4)),  $\{[Cu(II)_4Cu(I)_4 (pzdc)_4 (dpe)_6](H_2O)_4\}_{2n}$  (II-5), and  $\{[Cu_5(HPO_4)_2(pzdc)_2(dpe)_3](H_2O)_5\}_n$  (II-6) were obtained. The structural diversity of **II-1-6** depends on starting Cu(II) salts. Compounds **II-1-4** are isostructural and exhibit 3D porous cationic pillar-layered coordination framework. The anion-exchange properties of II-1-4 were studied. Interestingly, II-1-4 exhibit the irreversible chemisorption of thiocyanate anion instead of anion exchange without the destruction of their structural framework as confirmed by PXRD, IR, UV-Vis, and AA spectroscopy. Moreover, the anion-induced structural transformation of **II-1-4** was observed when exchanging by an azide anion. The luminescent and magnetic properties of the products were also studied.

**Keywords:** coordination polymers, pyrazole-3,5-dicarboxylic acid, structural diversity, luminescent properties, magnetic properties

# บทคัดย่อ

**รหัสโครงการ:** MRG5980237

**ชื่อโครงการ:** ความหลากหลายทางโครงสร้าง โครงสร้างเชิงพลวัติ และสมบัติทางแม่เหล็กของโคออร์ดิเนชันพอลิ

เมอร์ที่ประกอบด้วย pyrazole-3,5-dicarboxylate และตัวเชื่อมอินทรีย์ชนิด N,N'-ditopic

ชื่อนักวิจัย: ผศ.ดร.เจ้าทรัพย์ บุญมาก มหาวิทยาลัยขอนแก่น

อีเมล: jaursup@kku.ac.th

ระยะเวลาโครงการ: 2 พฤษภาคม 2559 - 1 พฤษภาคม 2561

งานวิจัยนี้เป็นการออกแบบ สังเคราะห์ พิสูจน์เอกลักษณ์ทางสเปกโทรสโกปีและวิเคราะห์โครงสร้าง ผลึกของคอปเปอร์โคออร์ดิเนชันพอลิเมอร์ชนิดใหม่ที่ประกอบด้วยไพราโซ-3,5-ไดคาร์บอกซิเลต (pzdc) ร่วมกับ สะพานอินทรีย์ชนิด N,N' ทำให้ได้โคออร์ดิเนชันพอลิเมอร์ชนิดใหม่จำนวน 10 สาร ดังต่อไปนี้ ซีรีย์ของคอป เปอร์(II)โคออร์ดิเนชันพอลิเมอร์ที่มีสมบัติทางแม่เหล็ก ได้แก่ {[Cu<sub>3</sub>(pzdc)<sub>2</sub>(pyz) (H<sub>2</sub>O)<sub>6</sub>](H<sub>2</sub>O)}<sub>0</sub> (I-1)  $\{ [Cu_3(pzdc)_2(bpy)(H_2O)_8](H_2O)_6 \}_n \ (I-2) \ \{ [Cu_4(Hpzdc)_2(pzdc)_2(bpy)_2] [Cu(bpy)(H_2O)_4]_n (H_2O)_4 \}_n \ (I-3) \}_n (I-3)_n ($  $\{[Cu_3(pzdc)_2(ampy)(H_2O)_5](H_2O)_3\}_n$  (I-4) และซีรีย์ของคอปเปอร์(II) โคออร์ดิเนชันพอลิเมอร์ที่มีการรวมตัว ทางโครงสร้างที่ขึ้นกับไอออนลบ ได้แก่ {[Cu2(pzdc)(dpe)2] NO3}ก (II-1) {[Cu2(pzdc)(dpe)2]ClO4}ก (II-2)  $\{[Cu_2(pzdc)(dpe)_2]BF_4\}_n (II-3) \{[Cu_2(pzdc)(dpe)_2]SCN\}_n (II-4) \{[Cu_4Cu_4(pzdc)_4(dpe)_6](H_2O)_4\}_n (II-5)\}$  $\{[Cu_5(HPO_4)_2(pzdc)_2(dpe)_3(H_2O)](H_2O)_4\}_n$  (II-6) (เมื่อ pyz คือ pyrazine bpy คือ 4,4'-bipyridyl ampy คือ 2-aminopyrazine และ dpe คือ 1,2-di(4-pyridyl)ethylene) สาร I-1-4 แสดงโครงสร้างหนึ่งมิติที่มีทอ พอโลยีแตกต่างกัน ส่วนสาร II-1-4 มีโครงสร้างแบบเดียวกันซึ่งเป็นโครงข่ายโคออร์ดิเนชันประจุบวกสามมิติที่มีรู พรุนและมีไอออนประจุลบหนึ่งบรรจุภายในรูพรุนของโครงข่าย เมื่อใช้คอปเปอร์(II)ซัลเฟตเป็นสารตั้งต้นจะทำให้ เกิดสาร II-5 ซึ่งเป็นโครงข่ายเลเยอร์สองมิติที่แทรกสอดกันที่ประกอบด้วยไอออนคอปเปอร์(I) และคอปเปอร์(II) และหากใช้ไอออนประจุลบสามจะทำให้เกิดโครงข่ายสามมิติของสาร **II-6** ที่ประกอบด้วย  $\mu_4$ -HPO $_4^{2-}$  เชื่อม ระหว่างไอออนคอปเปอร์(II) สมบัติทางแม่เหล็กของสาร I-1 I-2 และ I-4 แสดงอันตรกิริยาชนิดแอนติเฟร์โรแมก เนติกแบบอ่อน สาร II-1-4 แสดงการดูดซับทางเคมีต่อไอออนไซโอไซยาเนตโดยไม่ทำลายโครงสร้างผลึกและ แสดงการเปลี่ยนเฟสทางโครงสร้างเมื่อถูกเหนี่ยวนำโดยการแลกเปลี่ยนไอออนลบกับไอออนเอไซด์ ซึ่งพฤติกรรม ้นี้สอดคล้องกับการเปลี่ยนแปลงสมบัติเชิงแสงของสารผลิตภัณฑ์

**คำหลัก:** โคออร์ดิเนชันพอลิเมอร์ ไพราโซ-3,5-ไดคาร์บอกซิเลต สมบัติเชิงแสง สมบัติทางแม่เหล็ก

#### EXECUTIVE SUMMARY

Project Code: MRG5980237

Project Title: Structural diversity, structural dynamics and magnetic properties of coordination

polymers containing pyrazole-3,5-dicarboxylate and different N,N'-ditopic organic spacers

**Investigator:** Asst. Dr. Jaursup Boonmak, Khon Kaen University

E-mail Address: jaursup@kku.ac.th

**Project Period:** May 2, 2016 - May 1, 2018

Coordination polymers (CPs) have gained considerable attention in recent decades for not only their interesting structural diversities but also their applications in various fields, such as ion and guest exchange, catalysis, magnetism, luminescence, and gas storage. The successful construction of CPs usually depends on ligands, metal ions, pH, temperature, counteranions, and solvent. It is well known that the coordination polymers containing carboxylates show various dimensional networks with interesting properties. This diversity results from the fact that the carboxylate groups can bind metal centers in various ways and may account for the possible intermolecular hydrogen bonds spreading low dimensional material to higher dimensional supramolecular frameworks. The coordination geometries of the metal center also play an important role in the construction of coordination polymers. Particularly Cu(II) ion usually exhibits versatile of coordination geometries with different coordination numbers in one compound because of Jahn-Teller distortion.

In this research, the pyrazole-3,5-dicarboxylic acid (H<sub>3</sub>pzdc) is used as a ligand for binding copper ion via carboxylate and pyrazole ring. H<sub>3</sub>pzdc is an intriguing multidentate ligand and rich coordination modes. It has six potential coordination sites consisting of four carboxylate oxygen atoms from two carboxylate groups and two nitrogen atoms from pyrazole ring when it is fully deprotonated. Its ability acts as M···M bridges generating a wide variety of nuclearity and dimensionality of coordination compounds. The close proximity of the two metal centers bridging the pyrazolate moiety is considered to be a crucial parameter in the construction of polynuclear compounds where the metal centers would be able to magnetically and electronically interact. In addition, different coordination modes of pyrazole-3,5-dicarboxylate can contribute different forms of cooperative coupling which can be principally used to modulate the overall magnetic behavior in coordination network. The incorporation of Cu(II) ions with H<sub>3</sub>pzdc ligands can generate metallacyclic dinuclear and linear trinuclear secondary building units and also provide the extended structures. Apart from carboxylate linkers, the N,N'-ditopic spacers are frequently used as ancillary ligands for a dimensional extension. Their length, rigidity and functional groups have consequential effects on the final structures of coordination networks. However, the structures and properties of the copper coordination polymers containing both H<sub>3</sub>pzdc and N,N'ditopic coligands have been less documented. Therefore, herein N,N'-ditopic coligands were used to build the extended structures of Cu(II) pyrazole-3,5-dicarboxylate clusters.

In order to study the effect of different N,N'-ditopic spacers and starting copper(II) salts on the self-assembly of ternary CPs. Herein, the pyrazole-3,5-dicarboxylate and different neutral N,N'-coligands including pyrazine (pyz), 4,4'-bipyridyl (bpy), 2-aminopyrazine (ampy), and 1,2-di(4-pyridyl)ethylene (dpe) were incorporated in Cu(II) systems. In the case of starting copper(II) salts, various copper(II) salts were used including  $NO_3$ ,  $ClO_4$ ,  $BF_4$ ,  $SCN_5$ ,  $SO_4$ , and  $PO_4$ 

anions. Consequently, a new series of coordination polymers were successfully synthesized. The characterizations have been done through X-ray crystallography, infrared spectroscopy (IR), solid-state (diffuse reflectance) electronic spectra, elemental analyses, thermogravimetric analyses (TGA) and X-ray powder diffraction (XRPD). This research can be separated into two parts, as follow:

**Part** I: Four novel copper(II) coordination polymers, namely  $\{[Cu_3(pzdc)_2(pyz)(H_2O)_6](H_2O)\}_n$  (1),  $\{[Cu_3(pzdc)_2(bpy)(H_2O)_8](H_2O)_6\}_n$  (2),  $\{[Cu_4(Hpzdc)_2(pyz)(H_2O)_8](H_2O)_6\}_n$  (2),  $\{[Cu_4(Hpzdc)_2(pyz)(H_2O)_8](H_2O)_6\}_n$  (2),  $\{[Cu_4(Hpzdc)_2(pyz)(H_2O)_8](H_2O)_6\}_n$  (2),  $\{[Cu_4(Hpzdc)_2(pyz)(H_2O)_8](H_2O)_6\}_n$  (2),  $\{[Cu_4(Hpzdc)_2(pyz)(H_2O)_8](H_2O)_6\}_n$  (3)  $(pzdc)_2(bpy)_2[Cu(bpy)(H_2O)_4]_n(H_2O)_4]_n$  (3), and  $\{[Cu_3(pzdc)_2(ampy)(H_2O)_5](H_2O)_5]_n$  (4)  $(H_3pzdc = pyrazole-3,5-dicarboxylic acid, pyz = pyrazine, bpy = 4,4'-bipyridine and ampy = 2$ aminopyrazine) were synthesized and characterized. Compounds 1, 2 and 4 were synthesized by layering method at room temperature while 3 was prepared under solvothermal reaction. Compounds 1 and 2 are one-dimensional (1D) chain coordination polymers, while 3 shows 1D cationic chain coordination polymer with anionic tetranuclear Cu(II) cluster. Compound 4 exhibits 1D ladder-like chain structure. Compounds 1, 2 and 4 consist of neutral trinuclear  $[Cu_3(pzdc)_2]$  building unit which is constructed by  $\mu_2$ -pzdc<sup>3</sup>- bridging (5-6-5), (6-6-6), and (6-5-5) sequences of Cu(II) geometries for 1, 2 and 4, respectively. Each trinuclear unit is extended via N,N'-linkers giving polymeric chain structure. In contrast, an anionic tetranuclear cluster of 3 is built up from two anionic dinuclear metallacyclic [Cu<sub>2</sub>(Hpzdc)(pzdc)] building units and double  $\mu_2$ -bpy spacers. The magnetic properties of 1, 2 and 4 exhibit weak antiferromagnetic interactions among Cu(II) centers.

**Part II:** By utilizing a pyrazole-3,5-dicarboxylic acid (H<sub>3</sub>pzdc) and flexible 1,2-di(4-pyridyl)ethylene (dpe) with various copper(II) salts under the same solvothermal synthetic condition, six novel coordination polymers, namely, {[Cu<sub>2</sub>(pzdc)(dpe)<sub>2</sub>]X}<sub>n</sub> (X = NO<sub>3</sub> (1), ClO<sub>4</sub> (2), BF<sub>4</sub> (3), SCN (4)), {[Cu(II)<sub>4</sub>Cu(I)<sub>4</sub>(pzdc)<sub>4</sub>(dpe)<sub>6</sub>](H<sub>2</sub>O)<sub>4</sub>}<sub>2n</sub> (5), and {[Cu<sub>5</sub>(HPO<sub>4</sub>)<sub>2</sub> (pzdc)<sub>2</sub>(dpe)<sub>3</sub>](H<sub>2</sub>O)<sub>5</sub>}<sub>n</sub> (6) were obtained. The structural diversity of compounds **1-6** depends on starting Cu(II) salts. Compounds **1-4** are isostructural and exhibit 3D porous cationic pillar-layered coordination framework with lattice monoanions incorporated into the channels of the framework. When using copper(II) sulfate as a reagent, a neutral mixed-valence Cu(I, II) 2D+2D  $\rightarrow$  2D parallel interpenetrated layer of **5** was obtained. In the case of phosphate trianion, compound **6** shows 3D coordination framework which contains  $\mu_4$ -HPO<sub>4</sub><sup>2-</sup> linking between Cu(II) centers. The anion-exchange properties of **1-4** were studied. Interestingly, compounds **1-4** exhibit the irreversible chemisorption of thiocyanate anion instead of anion exchange without the destruction of their structural framework. Moreover, the anion-induced structural transformation of **1-4** was observed when exchanging by an azide anion. The luminescent properties of **1-6** and exchanged products were also investigated.

**Output:** The research outcome includes two international publication papers.

- 1) F. Klongdee, <u>J. Boonmak</u>\*, S. Youngme, Anion-dependent self-assembly of copper coordination polymers based on pyrazole3,5-dicarboxylate and 1,2-di(4-pyridyl)ethylene, *Dalton Transactions*, 2017, 46, 4806-4815. (IF 2016 = 4.029, Q1)
- 2) F. Klongdee, <u>J. Boonmak</u>\*, B. Moubaraki, K. S. Murray, S. Youngme, Copper(II) coordination polymers containing neutral trinuclear or anionic dinuclear building units based on pyrazole-3,5-dicarboxylate: Synthesis, structures and magnetic properties, *Polyhedron*, 2017, 126, 8-16. (IF 2016 = 1.926, Q2)

# **TABLE OF CONTENTS**

|         |   | Page |
|---------|---|------|
| ABSTRAC | CT (IN THAI)  |      |
| ABSTRAC | CT (IN ENGLISH)   |      |
| EXECUTI | VE SUMMARY  |      |
|         |   |      |
| PART I  | Copper(II) coordination polymers containing neutral trinuclear or     |      |
|         | anionic dinuclear building units based on pyrazole-3,5-dicarboxylate: |      |
|         | Synthesis, structures and magnetic properties                         | 1    |
|         | Introduction  | 1    |
|         | Experimental  | 2    |
|         | Results and Discussion  | 4    |
|         | Conclusions   | 13   |
|         | References  | 14   |
|         | Supporting Information  | 16   |
| PART II | Anion-dependent self-assembly of copper coordination polymers         |      |
|         | based on pyrazole-3,5-dicarboxylate and 1,2-di(4-pyridyl) ethylene    | 25   |
|         | Introduction  | 25   |
|         | Experimental  | 26   |
|         | Results and Discussion  | 30   |
|         | Conclusions   | 40   |
|         | References  | 41   |
|         | Supporting Information  | 43   |
|         |   |      |

OUTPUT OF THE RESEARCH

APPENDICES

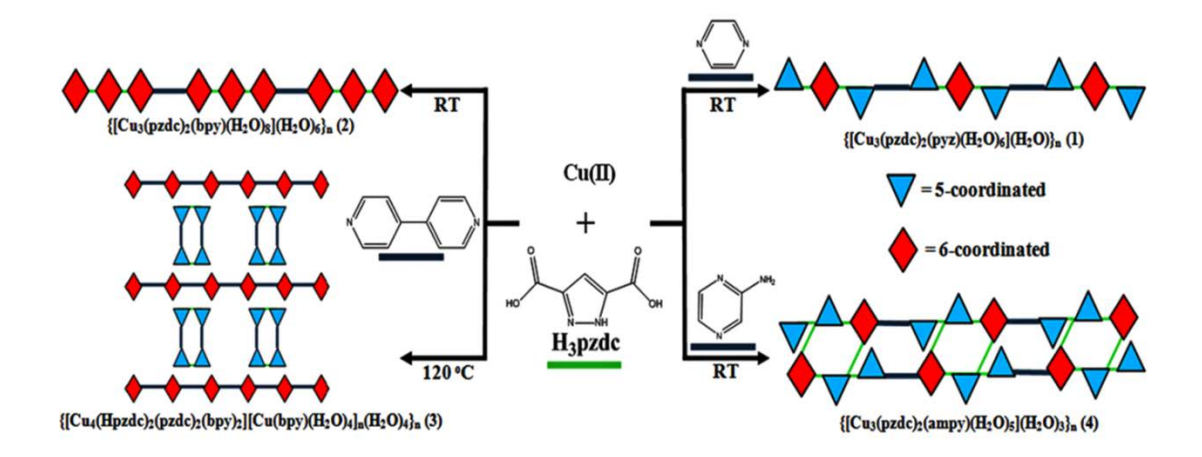
# **PART I**

# Copper(II) coordination polymers containing neutral trinuclear or anionic dinuclear building units based on pyrazole-3,5-dicarboxylate: Synthesis, structures and magnetic properties

# Introduction

In the last few decades, coordination polymers (CPs) have attracted wide attention due to their diverse structures and many potential applications in the areas of gas storage, catalysis, ion-exchange, luminescence, and magnetism. [1-10] CPs have been constructed by primary building unit, i.e., metal ions and organic bridging ligands, and it is well known that metal center, ligand, pH, temperature, and solvent have strongly affected on construction and versatile structures of CPs.[11-16] CPs with short bridging ligands such as azide, pyrazole, and carboxylate are especially favorable for creating new magnetic materials because they are able to efficiently transfer magnetic interactions between neighboring magnetic centers. [17-20] Pyrazole-3,5-dicarboxylic acid (H<sub>3</sub>pzdc) is a multifunctional ligand and exhibits diverse coordination modes.[21, 22] It has six potential coordination sites consisting of four carboxylate oxygen atoms from two carboxylate groups and two nitrogen atoms from pyrazole ring when it is fully deprotonated. A variety of coordination compounds based on H<sub>3</sub>pzdc have been reported.[23-26] Generally, incorporation of Cu(II) ions with H<sub>3</sub>pzdc ligands can generate metallacyclic dinuclear [23, 27] and trinuclear secondary building units[28, 29] (Figure 1), such as  $(Et_3NH)_2[Cu_2(pzdc)_2(H_2O)_2]$ ,[23]  $[Cu_3(pzdc)_2(H_2O)_2]$  $(MeOH)_6(H_2O)_4$ [28] and  $[Cu_3(2,2'-bipy)_2(pzdc)_2(H_2O)_2](H_2O)_2$ [29] complexes. addition, the pyrazole-3,5-dicarboxylic acid can also provide the extended structures, such as, 3D frameworks of  $\{[Na_2(\mu-H_2O)_2][Cu_2(pzdc)_2]\}_n[23]$  and  $[Cu_3(pzdc)_2(H_2O)_4]_n[30]$ . However the structures and properties of the ternary Cu(II)-CPs containing both H<sub>3</sub>pzdc and organic coligands have been less documented.[31] In this work, N,N'-ditopic coligands were used to build the extended structures of Cu(II) pyrazole-3,5-dicarboxylate based on tri- and dinuclear secondary building units.

Based on above consideration, we synthesized four novel ternary copper(II) coordination polymers with H<sub>3</sub>pzdc and N,N'-ditopic ligands (Scheme 1), namely  $\{[Cu_3(pzdc)_2(pyz)(H_2O)_6](H_2O)\}_n$  $\{[Cu_3(pzdc)_2(bpy)(H_2O)_8](H_2O)_6\}_n$ **(1)**, (2), $\{[Cu_4(Hpzdc)_2$  $(pzdc)_2(bpy)_2[Cu(bpy)(H_2O)_4]_n(H_2O)_4\}_n$  $\{Cu_3(pzdc)_2(ampy)(H_2O)_5\}(H_2O)_3\}_n$  (4) (pyz = pyrazine, bpy = 4,4'-bipyridine, and ampy = 4,4'-bipyridine, ampy =2-aminopyrazine). Combining Cu(II) ions and H<sub>3</sub>pzdc ligands can generate neutral trinuclear [Cu<sub>3</sub>(pzdc)<sub>2</sub>] secondary building unit for 1, 2 and 4 and anionic dinuclear metallacyclic [Cu<sub>2</sub>(Hpzdc)<sub>2</sub>] building unit for 3. A variety of coordination geometries and distinct sequences of Cu(II) geometries in each building unit has been demonstrated. Moreover, each building unit was extended by N,N'-ditopic coligands, giving rise to 1D chain CPs for 1 and 2, tetranuclear anionic cluster for 3, and ladder-like chain structure for 4. The effects of coligands, geometry of Cu(II) center, reaction temperature and various coordination modes of H<sub>3</sub>pzdc play an important role in the construction of chain coordination polymers. In addition, the magnetic properties of 1, 2 and 4 containing trinuclear Cu(II) building unit have been studied.



Scheme 1. A series of Cu(II) coordination polymers 1-4.

# **Experimental section**

# Physical measurements

All chemicals and solvents used for synthesis were obtained from commercial sources and were used without further purification. FT-IR spectra were obtained in KBr disks on a PerkinElmer Spectrum One FT-IR spectrophotometer in 4000-450 cm<sup>-1</sup> spectral range. Solid-state (diffuse reflectance) electronic spectra were measured as polycrystalline samples on a PerkinElmer Lambda2S spectrophotometer, within the range 400-1100 nm. Elemental analyses (C, H, N) were carried out with a PerkinElmer PE 2400CHNS analyzer. The X-ray powder diffraction (XRPD) data were collected on a PANalytical EMPYREAN using monochromatic CuKα radiation, and the recording speed was 0.5 s/step over the 2θ range of 5-50° at room temperature. Thermogravimetric analyses (TGA) were performed using a TG-DTA 2010S MAC apparatus between 35 and 750 °C in N2 atmosphere with heating rate of 10 °C min<sup>-1</sup>. Magnetic susceptibility measurements (2–300 K) were carried out using a Quantum design MPMS-5S SQUID magnetometer. Measurements carried out using a 1 kOe dc field. Accurately weighed samples of ~25 mg were contained in a gel capsule that was held in the center of a soda straw that was attached to the end of the sample rod. Data were corrected for magnetization of the sample holder and for diamagnetic contributions, which were estimated from Pascal constants.

# Preparation of compounds 1-4

### $\{[Cu_3(pzdc)_2(pyz)(H_2O)_6](H_2O)\}_n$ (1)

The deionized water (3 mL) was slowly dropped over the mixture solution containing  $Cu(NO_3)_2 \cdot 3H_2O$  (0.2 mmol, 48 mg) and pyrazine (0.2 mmol, 16 mg) in water and DMF (4 mL, 1:1 v/v) in 15 mL of glass vial. Then, the solution of pyrazole-3,5-dicarboxylic acid (0.2 mmol, 35 mg) in deionized water and ethanol (5 mL, 1:1 v/v) was carefully layered over the mixture layer. Then, the vial was sealed and allowed to stand undisturbed at room temperature. The blue crystals of **1** were obtained after 2 days. Yield: 16 mg (34%) based on copper salt. Anal. Calcd for  $Cu_3C_{14}H_{20}N_6O_{15}$ : C, 23.92; H, 2.87; N, 11.95. Found: C, 24.40; H, 2.80; N, 11.73%. FT-IR peaks (KBr, cm<sup>-1</sup>): 3367br (v(OH)), 1622s ( $v_{as}(OCO)$ ), 1609s

(v(C=N)), 1509m, 1423w, 1395m  $(v_s(OCO))$ , 1341s, 1330s, 1297s, 1157w, 1127w, 1100w, 1063w, 1028w, 1017w, 930w, 828w, 797w. UV-vis (diffuse reflectance, cm<sup>-1</sup>): 14049.

# ${[Cu_3(pzdc)_2(bpy)(H_2O)_8](H_2O)_6}_n$ (2)

The preparation of **2** was similar to that of **1**, except 4, 4'-bipyridine (0.2 mmol, 31 mg) replaced pyrazine. After 2 days, light blue crystals of **2** were obtained. Yield: 14 mg (23%) based on copper salt. Anal. Calcd for  $Cu_3C_{20}H_{38}N_6O_{22}$ : C, 26.54; H, 4.23; N, 9.28. Found: C, 26.37; H, 4.00; N, 9.30%. FT-IR peaks (KBr, cm<sup>-1</sup>): 3405br (v(OH)), 1620s ( $v_{as}(OCO)$ ), 1615s (v(C=N)), 1520m, 1415w, 1390m ( $v_{s}(OCO)$ ), 1339s, 1293m, 1223m, 1127w, 1060w, 1028w, 1015w, 828w,781m, 643w. UV-vis (diffuse reflectance, cm<sup>-1</sup>): 14384.

# ${[Cu_4(Hpzdc)_2(pzdc)_2(bpy)_2][Cu(bpy)(H_2O)_4]_n(H_2O)_4}_n$ (3)

The mixture solution of  $\text{Cu(NO}_3)_2 \cdot 3\text{H}_2\text{O}$  (0.2 mmol, 48 mg), 4,4′-bipyridine (0.2 mmol, 31 mg) and pyrazole-3,5-dicarboxylic acid (0.2 mmol, 35 mg) in the deionized water (7 mL), DMF (2 mL) and ethanol (3mL) was sealed in a 20 mL glass vial. Then, the mixture was heated at 120 °C for 1 day and then slowly cooled down to room temperature. The blue crystals of **3** were obtained. Yield: 10 mg (16 %) based on copper salt Anal. Calcd for  $\text{Cu}_5\text{C}_{50}\text{H}_{46}\text{N}_{14}\text{O}_{24}$ : C, 38.88; H, 3.00; N, 12.69. Found: C, 38.79; H, 2.85; N, 13.00%. FT-IR peaks (KBr, cm<sup>-1</sup>): 3368br (v(OH)), 1646s (v<sub>as</sub>(OCO)), 1599s (v(C=N)), 1533w, 1481w, 1407w, 1387m (v<sub>s</sub>(OCO)), 1288s, 1224m, 1065w, 1020w, 817w, 806w, 778m. UV-vis (diffuse reflectance, cm<sup>-1</sup>): 14407.

# ${[Cu_3(pzdc)_2(ampy)(H_2O)_5](H_2O)_3}_n$ (4)

The preparation of **4** was similar to that of **1**, except aminopyrazine (0.2 mmol, 19 mg) replaced pyrazine. The dark green crystals of **4** were obtained after 2 days. Yield: 17 mg (35%) based on copper salt. Anal. Calcd for  $Cu_3C_{14}H_{23}N_7O_{16}$ : C, 22.97; H, 3.17; N, 13.39. Found: C, 23.10; H, 3.11; N, 13.10%. FT-IR peaks (KBr, cm<sup>-1</sup>): 3336br (v(OH)), 1635s (v<sub>as</sub>(OCO)), 1607s (v(C=N)), 1541m, 1511m, 1383m (v<sub>s</sub>(OCO)), 1327s, 1314s, 1282s, 1229m, 1078w, 1028w, 1012w, 850w, 785m. UV-vis (diffuse reflectance, cm<sup>-1</sup>): 14389.

# X-ray crystallography

The X-ray reflection data of 1–4 were collected on a Bruker D8 Quest PHOTON100 CMOS detector with graphite-monochromated MoKα radiation using the APEX2 program.[32] Raw data frame integration was performed with SAINT,[33] which also applied correction for Lorentz and polarization effects. An empirical absorption correction by using the SADABS program[34] was applied. The structure was solved by direct methods and refined by full-matrix least-squares method on  $F^2$  with anisotropic thermal parameters for all non-hydrogen atoms using the SHELXTL software package.[35] All hydrogen atoms were placed in calculated positions and refined isotropically, with the exception of the hydrogen atoms of all water molecules in 1–4 were found *via* difference Fourier maps, then restrained at fixed positions and refined isotropically. The hydrogen atoms on the disordered lattice water molecules in 3 (O4) and 4 (O14) could not be located. The highly disordered lattice water molecules in 3 (O4) and 4 (O14) could not be resolved. The pzdc/Hpzdc ligand in 3 lies across a mirror plane so the disordered hydrogen atom (H2) on carboxylic oxygen was refined with quarter occupancy. The details of crystal data, selected bond lengths and angles for compounds 1–4 are listed in Tables 1 and S1.

Table 1. Crystallographic data for compounds 1-4

| compound                              | 1  | 2   | 3                              | 4  |
|---------------------------------------|--|---|--------------------------------|--|
| formula                               | $-\frac{\text{Cu}_{3}\text{C}_{14}\text{H}_{20}\text{N}_{6}\text{O}_{15}}{\text{Cu}_{3}\text{C}_{14}\text{H}_{20}\text{N}_{6}\text{O}_{15}}$ | $-\frac{-}{\text{Cu}_{3}\text{C}_{20}\text{H}_{38}\text{N}_{6}\text{O}_{22}}$ | $Cu_5C_{50}H_{46}N_{14}O_{24}$ | Cu <sub>3</sub> C <sub>14</sub> H <sub>23</sub> N <sub>7</sub> O <sub>16</sub> |
| molecular                             | 702.98   | 905.18  | 1544.71                        | 736.01   |
| weight                                |  |   |                                |  |
| T(K)                                  | 293(2)   | 293(2)  | 293(2)                         | 293(2)   |
| crystal                               | triclinic  | monoclinic  | orthorhombic                   | triclinic  |
| system                                |  |   |                                |  |
| space group                           | P-1  | $P2_{1}/c$  | Cmmm                           | <i>P</i> -1  |
| a (Å)                                 | 7.1902(2)  | 8.8968(7)   | 15.6847(5)                     | 7.8991(3)  |
| b (Å)                                 | 8.8370(2)  | 10.1970(8)  | 18.6369(7)                     | 12.9067(5)   |
| c (Å)                                 | 9.5076(2)  | 18.2364(14)   | 11.1125(4)                     | 13.6852(5)   |
| $\alpha$ (deg)                        | 72.1460(10)  | 90  | 90                             | 110.648(1)   |
| $\beta$ (deg)                         | 75.8720(10)  | 93.682(2)   | 90                             | 97.878(1)  |
| γ (deg)                               | 82.1560(10)  | 90  | 90                             | 100.755(1)   |
| $V(\mathring{A}^3)$                   | 556.38(2)  | 1651.0(2)   | 3248.3(2)                      | 1251.0(1)  |
| Z                                     | 1  | 2   | 2                              | 2  |
| $ ho_{ m cald}$ (g cm <sup>-3</sup> ) | 2.098  | 1.813   | 1.571                          | 1.954  |
| μ (Μο Κα)                             | 2.933  | 2.014   | 1.696                          | 2.617  |
| $(mm^{-1})$                           |  |   |                                |  |
| data                                  | 3895   | 4119  | 1879                           | 5540   |
| collected                             |  |   |                                |  |
| unique data                           | 3433(0.0172)   | 3350(0.0480)  | 1530(0.0228)                   | 3802(0.0634)   |
| $(R_{\rm int})$                       |  |   |                                |  |
| $R_1^a / wR_2^b$                      | 0.0252/0.0659  | 0.0504/0.1365   | 0.0606/0.1885                  | 0.0530/ 0.1249   |
| $[I > 2\sigma(I)]$                    |  |   |                                |  |
| $R_1^a / wR_2^b$                      | 0.0315/0.0684  | 0.0649/0.1460   | 0.0754/ 0.1994                 | 0.0941/0.1408  |
| [all data]                            |  |   |                                |  |
| GOF                                   | 1.102  | 0.994   | 1.115                          | 1.059  |
| max/min                               | 0.525/-0.307   | 1.392/-1.305  | 1.623/-0.843                   | 2.290/ -0.518  |
| electron                              |  |   |                                |  |
| density (e Å                          |  |   |                                |  |
| 3)                                    |  |   |                                |  |

 ${}^{a}R = \sum ||F_0| - |F_c|| / \sum |F_0|, {}^{b}R_w = \{\sum [w(|F_0| - |F_c|)]^2 / \sum [w|F_0|^2]\}^{1/2}$ 

# Results and discussion

# Structural description of $\{[Cu_3(pzdc)_2(pyz)(H_2O)_6](H_2O)\}_n$ (1)

X-ray crystallographic analysis reveals that 1 crystalizes in the triclinic system with P-1 space group. Asymmetric unit of 1 consists of two independent Cu(II) centers (Cu1 and Cu2), one pzdc<sup>3-</sup> ligand, a half of pyz ligand, three coordination water molecules and one lattice water molecule. Each Cu1 ion lies on a crystallographic inversion center adopting an elongated octahedral CuN<sub>2</sub>O<sub>4</sub> geometry which is coordinated by two oxygen atoms and two nitrogen atoms from two different pzdc<sup>3-</sup> ligands in the equatorial plane. The axial position is occupied by two oxygen atoms from two coordination water molecules. Whereas the terminal Cu2 center is five-coordinated showing distorted square pyramidal CuN<sub>2</sub>O<sub>3</sub> geometry ( $\tau$  = 0.33, Addison's parameter  $\tau$  = 0 for square pyramid and  $\tau$  = 1 for trigonal bipyramid).[36]

The basal plane is surrounded by carboxylic oxygen and pyrazoyl nitrogen atoms from pzdc<sup>3</sup>- ligand, one pyrazine nitrogen atom and one oxygen atom from coordination water molecule, while the apical position is occupied by oxygen atom from another coordination water molecule (O5). The Cu–N and Cu–O distances are in the range of 1.9619(11)-2.1734(15) Å, while the axial Cu1–O distance of 2.4957(14) Å is significantly longer, indicating the presence of a common Jahn-Teller effect in the Cu(II) ion.[30] The Cu2N<sub>2</sub>O<sub>2</sub> square plane is not completely planar with tetrahedral twist between the planes of 29.64°. The Cu2 is shifted by 0.3268(2) Å from the mean equatorial plane toward the apical position. The Cu1 and two Cu2 ions are connected by pzdc<sup>3-</sup> in a  $\mu_2$ - $\eta^2$ N, O,  $\eta^2$ N',O'coordination mode (type I, Figure S1) to form a neutral trinuclear Cu(II) unit containing (5-6-5) sequences of Cu(II) geometries with the Cu1···Cu2 distance of 4.4102(2) Å (Figure 2a). Each trinuclear Cu(II) unit is linked by  $\mu_2$ -pyrazine spacer to form a 1D chain structure of 1 with the Cu2···Cu2 distance of 6.8462(3) Å (Figure 2b). Furthermore, the 3D packing motif of 1 is stabilized by various interchain hydrogen bonding interactions between pzdc<sup>3-</sup>, pyz, coordination and lattice water molecules (Figure S2 and Table S2).

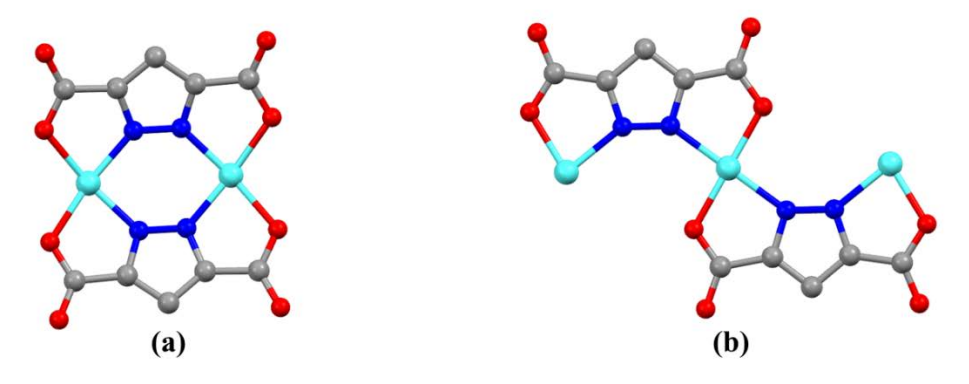


**Figure 1.** (a) Metallacyclic dinuclear Cu(II) secondary building unit (b) trinuclear Cu(II) secondary building unit.

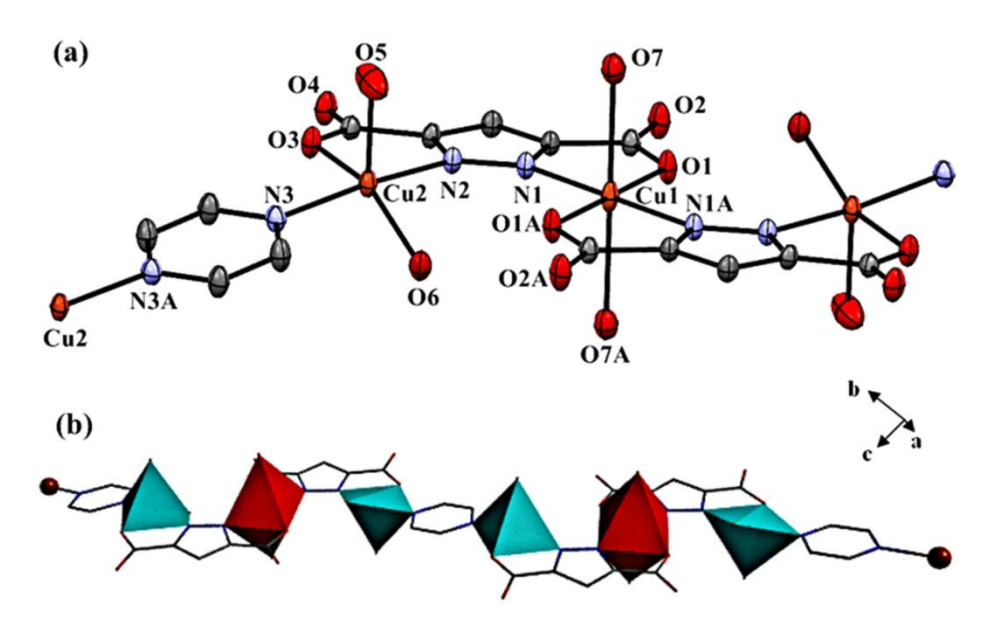


**Figure 2**. (a) A trinuclear Cu(II) building unit and atom labeling scheme of **1**. The ellipsoids are shown at 50% probability level. All hydrogen atoms and lattice water molecules are omitted for clarity (symmetry code: A = 1-x, 2-y, 2-z). (b) The 1D coordination polymer of **1**.

The blue and red polygons represent five- and six-coordination geometries of Cu(II) centers, respectively.

# Structural description of $\{[Cu_3(pzdc)_2(bpy)(H_2O)_8](H_2O)_6\}_n$ (2)

Compound 2 crystallizes in monoclinic system and  $P2_1/c$  space group. asymmetric unit contains two independent Cu(II) ions (Cu1 and Cu2), one pzdc3-, one-half of bpy, four coordination water molecules and three lattice water molecules. Both Cu(II) ions reveal an elongated octahedral geometry, Cu1 is six-coordinated surrounded by O and N atoms from pzdc<sup>3-</sup> ligand, one pyridine nitrogen atom and one oxygen atom from coordination water molecule in the basal plane. The axial position is located by two oxygen atoms from two coordination water molecules. While the Cu2 is located in crystallographic inversion center and occupied by two N atoms and two O atoms from two different pzdc3- ligands in the equatorial plane. The apical site is occupied by two oxygen atoms from two coordination water molecules. The Cu-N and Cu-O distances are in the range of 1.959(3)-2.6715(3) Å which are within the range of those reported for elongated octahedral geometry of Cu(II) complexes containing pzdc<sup>3</sup>-.[28, 30] The Cu1N<sub>2</sub>O<sub>2</sub> square base is not completely planar with tetrahedral twist between the planes of 5.35°. The pzdc<sup>3</sup>- ligand acting as a  $\mu_2$ - $\eta^2$ -N,O,  $\eta^2$ -N',O' fashion (type I, Figure S1) link between two Cu1 and Cu2 ions forming a neutral trinuclear Cu(II) unit with (6-6-6) sequences of Cu(II) geometries. The Cu1···Cu2 distance is 4.5207(5) Å (Figure 3a). In addition, each trinuclear Cu(II) unit is connected by  $\mu_2$ -bpy ligands to generate a 1D chain (Figure 3b) with Cu1···Cu1 distance of 11.1146(9) Å. The two pyridine rings of bipyridyl moieties are perfectly coplanar, being located on a crystallographic center of symmetry. The 3D supramolecular structure of 2 is generated via various hydrogen bonding interactions between pzdc<sup>3-</sup>, bpy, coordination and lattice water molecules (Figure S3 and Table S2).

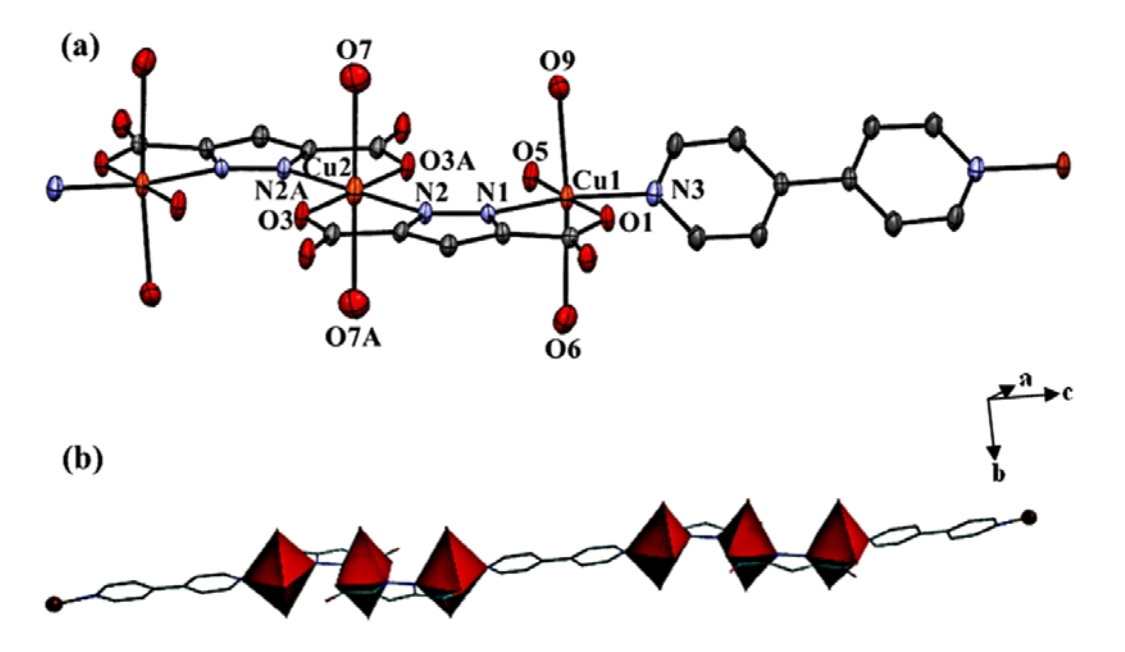


**Figure 3.** (a) A trinuclear Cu(II) building unit and atom labeling scheme of **2**. The ellipsoids are shown at 50% probability level. All hydrogen atoms and lattice water molecules are omitted for clarity (symmetry code: A = 2-x, 1-y, 1-z). (b) The 1D coordination polymer of **2**. The red polygon represents six-coordination geometries of Cu(II) centers.

# $Structural\ description\ of\ \{[Cu_4(Hpzdc)_2(pzdc)_2(bpy)_2][Cu(bpy)(H_2O)_4]_n(H_2O)_4\}_n\ (3)$

Compound 3 crystallizes the orthorhombic, Cmmm space group which consists of  $[Cu(bpy)(H_2O)_4]_n^{2+}$ cationic chain coordination polymer anionic  $[Cu_4(Hpzdc)_2(pzdc)_2(bpy)_2]^{2-}$  units. The anionic tetranuclear Cu(II) unit contains four Cu(II)centers (Cu1), two Hpzdc<sup>2-</sup>, two pzdc<sup>3-</sup> and two bpy ligands. Each Cu1 is located in crystallographic mirror plane adopting a distorted square pyramidal geometry. The Cu(II) center is coordinated by two carboxylate O and two pyrazoyl N atoms from two different pyrazole-3,5-dicarboxylates in equatorial plane and one N atom from  $\mu_2$ -bpy in the axial site (Figure 4a). The Cu1N<sub>2</sub>O<sub>2</sub> square base is not completely planar with tetrahedral twist between the planes of 24.98°. The Cu1 is shift by 0.3277(7) Å from the mean equatorial plane toward the axial position. The calculation of the bond valence sum (BVS)[37, 38] for Cu1 was performed. The analysis resulted in the value of 2.11, thus confirming the formal oxidation states of +2 for copper center. Two Cu1 centers are connected by Hpzdc<sup>2-</sup> and pzdc<sup>3-</sup> ligands in  $\mu_2$ - $\eta^2$ N,O,  $\eta^2$ N',O'coordination modes (type I, Figure S1), resulting to metallacyclic dinuclear Cu(II) unit with Cu-Cu distance of 3.995(1) Å. Moreover, these two dinuclear Cu(II) units are linked by two  $\mu_2$ -bpy linkers, forming tetranuclear anionic cluster (Figure 4a). The metallacyclic anionic dinuclear Cu(II) building unit containing pzdc3- has been found in such  $(Et_3NH)_2[Cu_2(pzdc)_2(H_2O)_2],[23]$ the literature, as,  $\{[Cu_2(pzdc)_2] (C_{10}H_{10}N_2)\}_n[31]$  While  $H_2O_2$ { $Cu_2(pzdc)_2$ }]<sub>n</sub>[23] and a neutral [Cu<sub>2</sub>(Hpzdc)<sub>2</sub>] building unit is less reported.[39] In this work, we show the first example of metallacyclic anionic dinuclear Cu(II) building unit containing both Hpzdc<sup>2-</sup> and pzdc<sup>3-</sup> ligands. In the cationic 1D coordination polymer, the Cu2 is surrounded by four O atoms from four coordination water molecules in basal plane and two N atoms from two different  $\mu_2$ -bpy linkers in apical position, adopting elongated octahedral geometry (Figure 4b). Each Cu2 is connected by  $\mu_2$ -bpy to generate a 1D cationic linear chain (Figure 4c). The Cu–N and Cu–O distances are in the normal range between 1.933(4)-2.201(9) Å.[23] The two pyridine rings of all bipyridyl moieties are perfectly coplanar, being located on a crystallographic mirror plane. In the 3D packing diagram of 3, besides electronic interaction between cationic chain and anionic tetranuclear unit of 3, the molecular structure hydrogen bonding interaction between bpy, pyrazole-dicarboxylate and coordination water molecule stabilize entire 3D supramolecular structure (Figure 5 and Table S2).

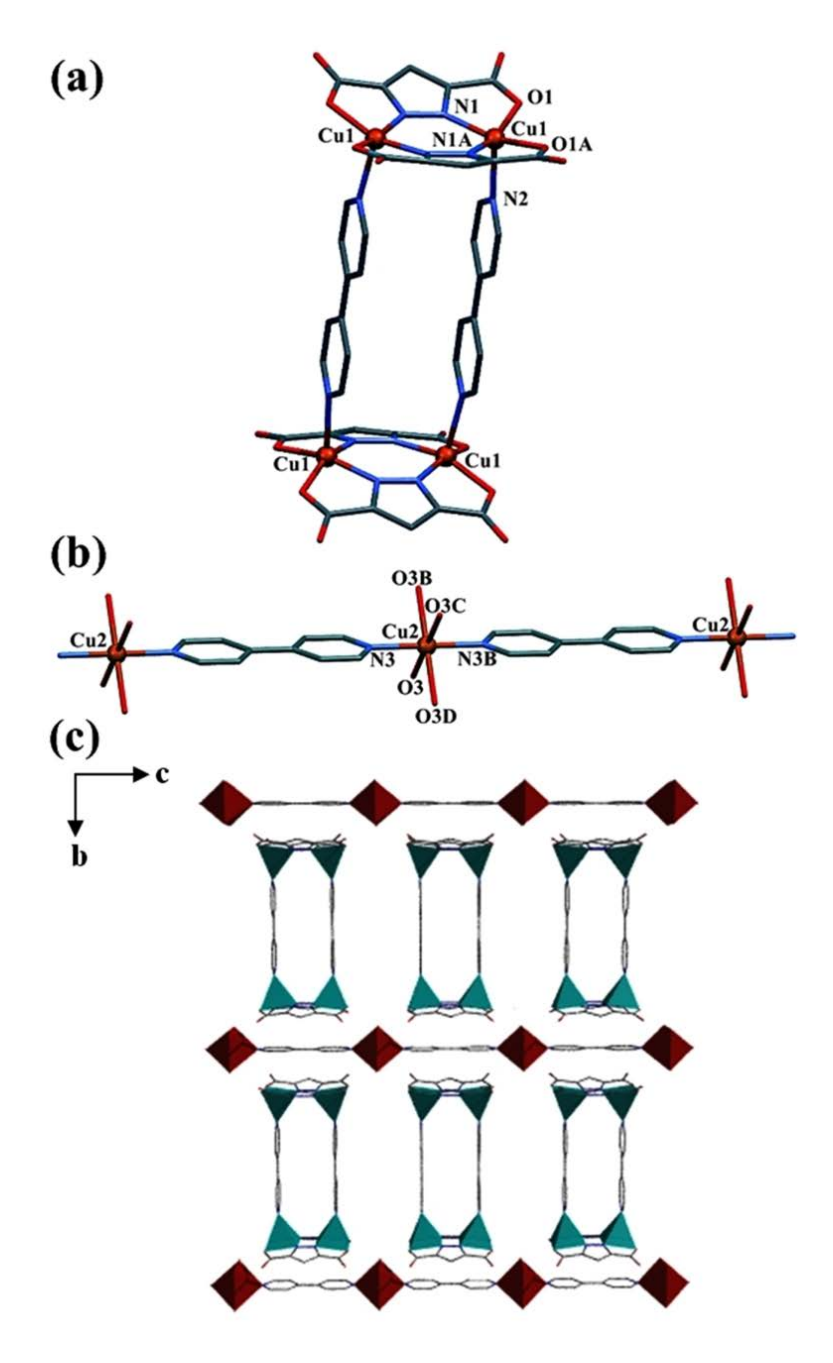


**Figure 4.** (a) Anionic tetranuclear Cu(II) unit of  $\{[Cu_4(Hpzdc)_2(pzdc)_2(bpy)_2]^{2-}, (b) \text{ Cationic chain coordination polymer of } [Cu(bpy)(H_2O)_4]_n^{2+} \text{ with atom labeling scheme of } 3. All hydrogen atoms and lattice water molecules are omitted for clarity (symmetry codes: <math>A = -x$ , y, z; B = 1-x, 1-y, -z; C = x, 1-y, z; D = 1-x, y, -z. (c) Anionic tetranuclear Cu(II) units stabilizing with cationic 1D chain coordination polymers. The blue and red polygons represent five- and six-coordination geometries of Cu(II) centers, respectively.

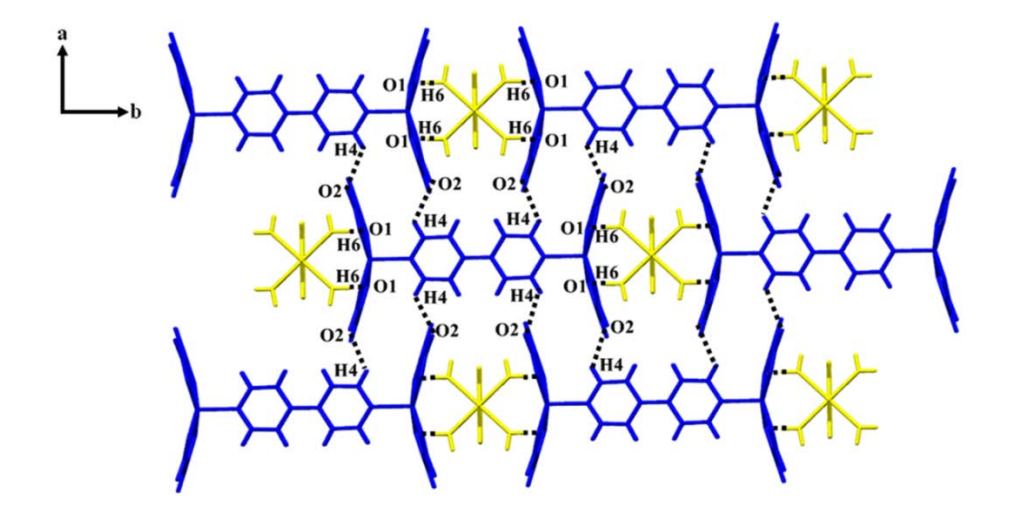
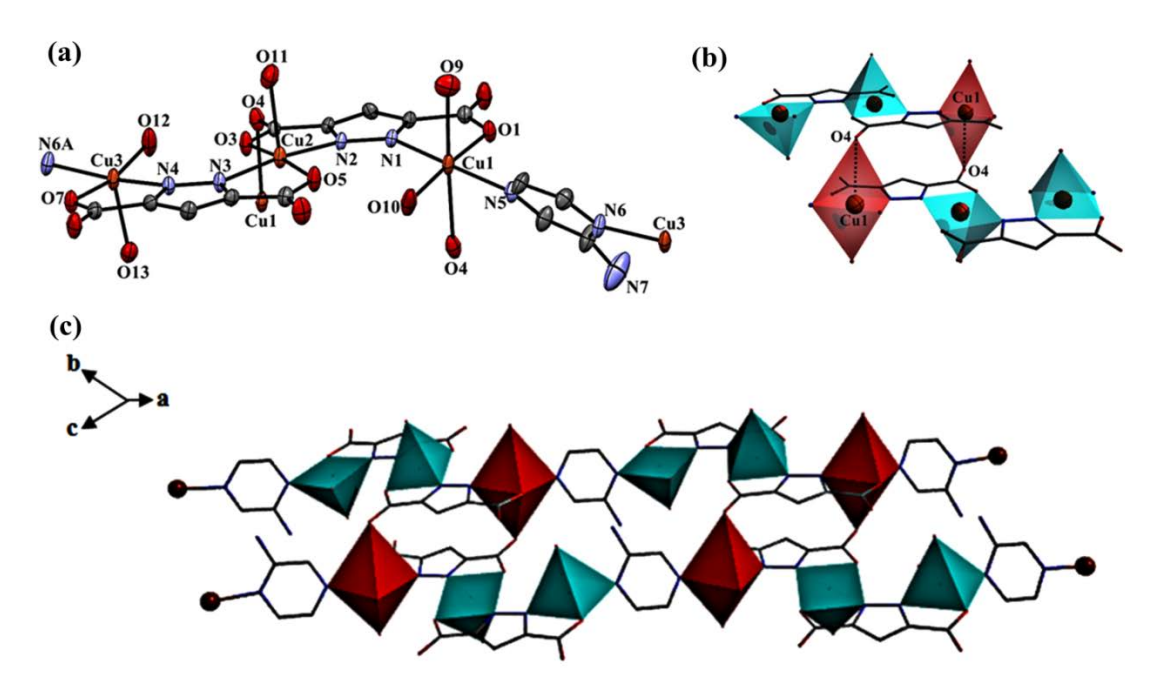


Figure 5. 3D packing diagram of 3 formed by intermolecular hydrogen bonding.

# Structural description of $\{[Cu_3(pzdc)_2(ampy)(H_2O)_5](H_2O)_3\}_n$ (4)

Single crystal X-ray analysis reveals that compound 4 crystallizes in triclinic crystal system, P-1 space group. Asymmetric unit of 4 contains three independent Cu(II) ions, two pzdc<sup>3</sup>-, one ampy ligand, five coordination water molecules and three lattice water molecules. Each Cu1 center is occupied by O and N atoms from pzdc<sup>3</sup>, one pyrazine nitrogen atom from ampy ligand and one oxygen from coordination water molecule in the basal plane, while the apical positions are occupied by an O atom from coordination water molecule giving rise to square pyramidal CuN<sub>2</sub>O geometry. In addition, the semi-coordinated O4 atom from pzdc<sup>3</sup>weakly interacts to copper center with the longest Cu1...O4 distance of 2.800(3) Å, forming an elongated octahedral geometry. The Cu2 and Cu3 centers show distorted square pyramidal geometries ( $\tau = 0.02$  and 0.03 for Cu2 and Cu3, respectively). Each Cu2 center is coordinated by two carboxylate oxygen and two nitrogen atoms from two different pzdc3- ligands at equatorial plane. The axial site is occupied by one oxygen from coordination water molecule. The basal plane around the Cu3 center is composed of O and N atoms from pzdc3-, one pyrazine nitrogen from ampy and one oxygen from coordination water molecule. The apical site is taken by oxygen from coordination water molecule. The Cu-N and Cu-O distances are in the range of 1.931(4)-2.472(5) Å which are well within their normal ranges for pyrazolatobridged trinuclear Cu(II) complexes.[30] While the longest Cu1-O4 distance of 2.800(3) Å shows very weak coordination bond.[31, 40] The CuN<sub>2</sub>O<sub>2</sub> square base shows tetrahedral twists between the planes of 7.19°, 11.01°, and 17.76° for Cu1-Cu3, respectively. The pzdc<sup>3</sup>ligand exhibits  $\mu_3$ - $\eta^2$ N,O,  $\eta^2$ N',O',  $\eta^1$ O bridging mode (type II, Figure S1) connecting three Cu(II) centers to form a neutral trinuclear Cu(II) unit containing (6-5-5) sequences of Cu(II) geometries with the Cu1···Cu2, Cu2···Cu3 distances of 4.4634(5) and 4.4765(6) Å, respectively (Figure 6a). In addition, each trinuclear Cu(II) building unit is linked together by weak  $\mu_3$ -syn,anti-pzdc<sup>3-</sup> bridging mode (Cu1-O4) forming hexanuclear Cu(II) cluster (Figure 6b). Moreover, the adjacent hexanuclear Cu(II) units are connected by double  $\mu_2$ -ampy spacers to generate 1D ladder-like chain structure with the shortest Cu···Cu distance of 6.8089(2) Å (Figure 6c). In addition, the intramolecular hydrogen bond between NH<sub>2</sub> group of  $\mu_2$ -ampy and coordination water molecules stabilizes the ladder-like chain structure of **4.**The 3D packing structure of **4** is assembled by various weak interchain hydrogen bonding

interactions between pzdc<sup>3-</sup>, ampy, coordination and lattice water molecules (Figure S4 and Table S2).



**Figure 6.** (a) A trinuclear Cu(II) building unit and atom labeling scheme of **4**. The ellipsoids are shown at 50% probability level. All hydrogen atoms and lattice water molecules are omitted for clarity (symmetry code: A = x, -1+y, -1+z). (b) A hexanuclear Cu(II) building unit composed of weak Cu1-O4 bond. (c) The 1D ladder-like chain of **4**. The blue and red polygons represent five- and six-coordination geometries of Cu(II) centers, respectively.

# **Thermal Analyses**

Thermogravimetric analysis (TGA) of 1-4 were performed in N<sub>2</sub> atmosphere from 35-750 °C. Compound 1 shows a weight loss of 15.50% in the range of 70-110 °C, which is due to the loss of six water molecules (calcd. 15.36%). After 250 °C, the sample gradually starts to lose the remaining water molecule and decompose to the unidentified species. Compounds 2 and 4 show the first weight loss of 17.85 % and 4.66% varying from 35-80 °C for 2 and 35-60 °C for 4 corresponding to the loss of nine water molecules for 2 (calcd. 17.91%) and two water molecules for 4 (calcd. 4.89%). Subsequently, the second weight loss process of 9.91% and 14.74% varies from 80-295 °C and 60-290 °C for 2 and 4, respectively, corresponding to the removal of all remaining water molecules (calcd. 9.95% for 2 and 14.69% for 4). Then the samples start to decompose after about 290 °C. Finally, compound 3 shows gradual weight loss of 9.51% in the range of 35-250 °C, corresponding to the escape of all coordination and lattice water molecules (calcd. 9.33%). Then the structures decompose to some unidentified species (Figure 7).

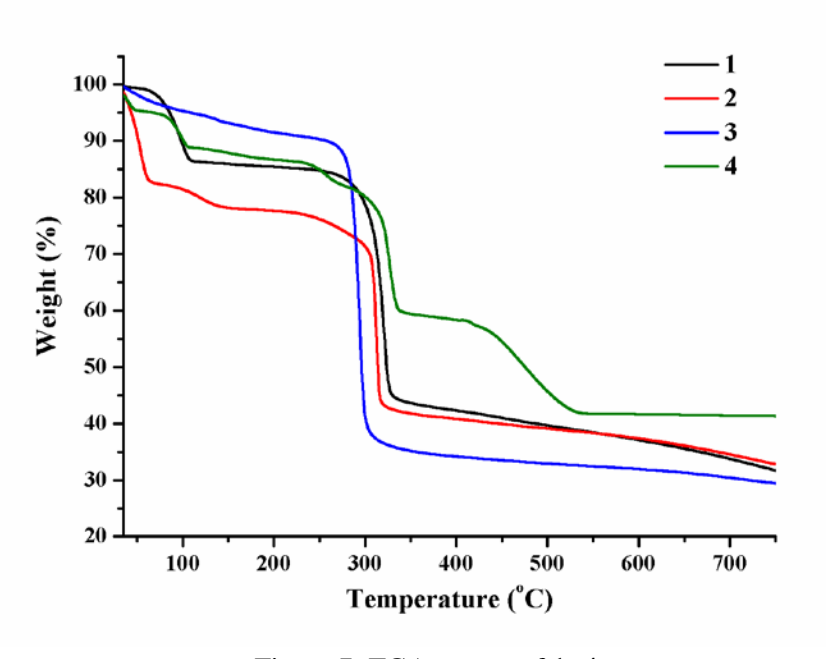


Figure 7. TGA curves of 1–4.

# XRPD patterns

To confirm whether the crystal structures of **1-4** are truly representative of the bulk materials, X-ray powder diffraction experiments have been performed at room temperature. The experimental and simulated (from the single crystal data) patterns are identical confirming the phase purity of the bulk samples (Figure S6-S9).

### **Structural discussion**

By the combination of  $Cu(NO_3)_2 \cdot 3H_2O$  with  $H_3pzdc$  and N,N'-ditopic coligands in a 1:1:1 molar ratio in the mixture solution of H<sub>2</sub>O/DMF/EtOH, the ternary Cu(II) coordination polymers 1-4 were obtained. Compounds 1, 2 and 4 were synthesized by layering method at room temperature. They exhibit 1D chain coordination polymers comprised of pyrazolatobridged trinuclear Cu(II) building unit with the unique (5-6-5), (6-6-6) and (6-5-5) sequences of Cu(II) coordination number for 1, 2 and 4, respectively. While 3 was synthesized by solvothermal method at 120 °C that contains both anionic tetranuclear Cu(II) cluster and cationic 1D coordination polymer. The  $\mu_2$ - $N_1N'$ -bridges link Cu<sub>3</sub> secondary building unit in compounds 1 and 2 giving rise to 1D chain structure. While each trinuclear unit in 4 is assembled to hexanuclear cluster by weak syn, anti-bridging mode of pzdc3- and further extended by  $\mu_2$ -ampy forming 1D ladder-like chain structure. The neutral trinuclear [Cu<sub>3</sub>(pzdc)<sub>2</sub>] building unit with various sequences of Cu(II) coordination numbers have been reported, such as,  $[Cu_3(pzdc)_2(Me_2en)_2(H_2O)_2](H_2O)_8,[28]$   $[Cu_3(dien)_2(pzdc)_2CH_3OH]_2$  $(CH_3OH)_6,[41]$   $[Cu_3(pzdc)_2(H_2O)_4]_n,[30]$  with (5-4-5), (5-5-5), and (5-6-5) sequences of Cu(II) coordination numbers, respectively. It can be seen that 5-coordinated Cu(II) geometry is more favorable in the neutral Cu<sub>3</sub> system, however, 6-coordinated octahedral geometry may be adopted by using long rigid bpy spacer in 2 where is less steric hindrance between neighboring Cu<sub>3</sub> units. Besides versatile of distorted coordination geometries of Cu(II) centers, and various coordination modes of H<sub>3</sub>pzdc play a key role on the construction of Cu(II) secondary building unit, the reaction temperature also have a significant influence on

the structural assembly. When using the bpy as a coligand, compound 3 was synthesized at high temperature, giving the cationic 1D chain CPs with the unique anionic tetranuclear Cu(II) cluster constructed from metallacyclic dinuclear Cu(II) building unit while 2 was prepared at room temperature, generating a simple 1D chain structure. The coordination geometries of Cu(II) centers were also confirmed by electronic diffuse reflectance spectra which agree with the  ${}^2E_g$  to  ${}^2T_{2g}$  (parent) transition for distorted octahedral and square pyramidal geometry (Figure S5).[7, 40]

## **Magnetic properties**

The temperature dependent magnetic susceptibilities for the 1D coordination polymers **1**, **2** and **4** are all very similar and indicative of the neutral trinuclear, pyrazolato-bridged moieties showing weak antiferromagnetic coupling with little or no coupling across the N,N'-ditopic linkers in the 1D species. Taking compound **4** as a typical example (Figure 8, the other plots are in Figure S10-S11),  $\chi_{\rm M}T$ , per Cu<sub>3</sub>, is ~ 1.25 cm<sup>3</sup> mol<sup>-1</sup> K at room temperature, as expected for three weakly coupled Cu(II) ions, with g on each Cu(II) of 2.1. The  $\chi_{\rm M}T$  values decrease gradually between 300 K and 100 K, then more rapidly reaching a plateau at 0.4 cm<sup>3</sup> mol<sup>-1</sup> K at 10 K, indicative of a S = ½ ground state for the Cu<sub>3</sub> species. Below 5 K, there is a further decrease that is possible indicative of weak antiferromagnetic inter-trinuclear coupling, across the linking N,N'-ditopic coligands.

Focusing, first, on the 5-300 K data, we have used a linear trinuclear  $S=\frac{1}{2}$  model with spin Hamiltonian containing exchange and Zeeman terms: [30, 42]

$$\mathbf{H} = -2J\{\mathbf{S}_1.\mathbf{S}_2 + \mathbf{S}_1.\mathbf{S}_2'\} + g\mu_B S_{Tz} H_z$$

Where the Cu(II) centers are arranged Cu2-Cu1(center)-Cu2'. J is the exchange interaction between adjacent Cu(II) ions in the trimer,  $S_i$  the spin operator for each S = 1/2 Cu(II),  $S_T$  the total spin operator of the trimer with  $S_T = S_1 + S_2 + S_2$  and  $S_{Tz}$  is the z component of the  $S_T$  operator. This leads to three energy levels  $S = \frac{1}{2}$  (energy zero);  $S = \frac{1}{2}$  (E = -2J) and S = 3/2 (E = -3J). We have also included a J' (Cu2-Cu2') term in the fitting but it is insensitive compared to setting it at zero (Table 2).

In Figure 8 it can be seen that the best fit line (solid line) reproduces the  $\chi_{\rm M}T$  values extremely well, the plateau at low temperatures indicative of population of the  $S = \frac{1}{2}$  state. Perusal of the literature of pyrazolate-bridged Cu(II) compounds reveals few singlypyrazolate bridged examples for comparison. The 3D complex [Cu<sub>3</sub>(pzdc)<sub>2</sub>(H<sub>2</sub>O)<sub>4</sub>]<sub>n</sub>,[30] obtained hydrothermally, shows similar trinuclear core units to the present 1D CPs, but forms a 3D array via bridging through the carboxylate O atoms. The J value obtained in fitting the 50–300 K data to the present trinuclear model is -22 cm<sup>-1</sup>, a little higher than those found here which is agree with the shorter. Cu-Cu separation in the trinuclear moiety of  $[Cu_3(pzdc)_2(H_2O)_4]_n$  (4.356 Å) comparing to 4.4102(2)-4.5207(2) Å for 1, 2 and 4. A singly- $K[Cu_2L_2(pz)]H_2O$  ( $H_2L$  = 6-amino-1,3-dimethyl-5-(2'-carboxy bridged complex, phenyl)azouracil and pz = pyrazole), with pseudotetrahedral geometry around the Cu(II) centers, showed  $J = -2.7 \text{ cm}^{-1}$  and g = 2.1,[43] J being much lower in magnitude than those in Table 2. In contrast, double-pyrazolate bridging, in (Bu<sub>4</sub>N)<sub>2</sub>[Cu<sub>2</sub>(pzdc)<sub>2</sub>], with Cu···Cu separation of 3.98 Å,[44] or mixed {pyrazolate/alkoxide}[45] or {pyrazolate/azide}[46] bridging leads to much stronger antiferromagnetic coupling and larger negative J values (≥-100 cm<sup>-1</sup>) than those found here, no doubt because of the extra bridging contribution and

smaller Cu···Cu separation. A marked difference is observed in the  $\chi_{\rm M}T$  plots for 1, 2 and 4 compared to that of  $[{\rm Cu_3(pzdc)_2(H_2O)_4}]n$ ,[30] at very low temperatures. In the latter, the  $\chi_{\rm M}T$  values are similar to the present ones above ~50 K, but increase sharply below ~20 K due to long-range magnetic order of the  $S = \frac{1}{2}$  ground states ( $J(2D = +1.9 \text{ cm}^{-1}; J(3D) = -0.06 \text{ cm}^{-1})$  brought about by the carboxylate bridging that forms the 3D array. We do not see such behaviour here, the linking pyrazine and bipyridine that form the 1D chains, do not provide strong enough superexchange pathways between the Cu<sub>3</sub> units to induce long range order. Indeed, the small decrease in  $\chi_{\rm M}T$  at very low temperatures is indicative of weak intertrinuclear coupling.

**Table 2.** Best fit *J* values. A constant  $N\alpha$  (temperature independent susceptibility) of 65 x 10<sup>-6</sup> cm<sup>3</sup> mol<sup>-1</sup> was fixed in the susceptibility expression

| CPs | J (cm <sup>-1</sup> ) | g    |
|-----|-----------------------|------|
| 1   | -16.4                 | 2.10 |
| 2   | -16.5                 | 2.14 |
| 4   | -18.0                 | 2.17 |

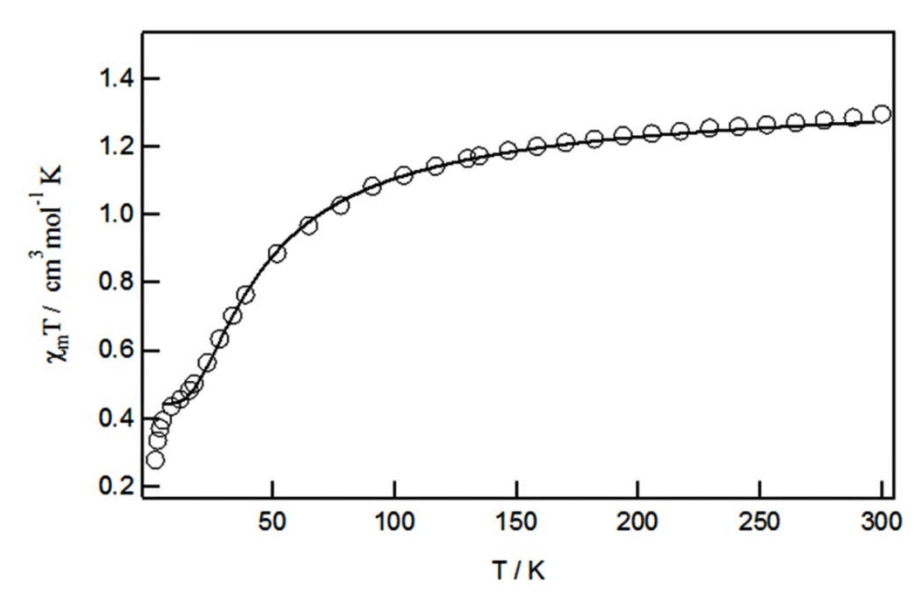


**Figure 8.** Experimental values of  $\chi_M T$ , per Cu<sub>3</sub>, (open circles) versus temperature (K) plot for compound 4. The solid lines is the best fit using the linear  $S = \frac{1}{2}$  trimer model described in the text that does not include an inter-trimer term,  $\theta$ .

# Conclusions

Four new copper(II) coordination polymers constructed by self-assembly of dinuclear or trinuclear building units based on pzdc ligand and auxiliary *N,N'*-ditopic spacers have been structurally characterized. Compounds **1** and **2** exhibit 1D chains while **3** shows 1D chain cationic coordination polymer and anionic tetranuclear Cu(II) cluster. Compound **4** exhibits 1D ladder-like chain structure. Compounds **1** and **2** consist of trinuclear Cu(II) building units

constructed by Cu(II) ions and pzdc<sup>3-</sup> ligands with (5-6-5), (6-6-6) sequences of Cu(II) geometries, respectively. These Cu<sub>3</sub> units are extended *via* pyz or bpy linkers giving 1D chain structures. In **4**, the hexanuclear Cu(II) cluster is generated by the combination of two Cu<sub>3</sub> units based on pzdc<sup>3-</sup> and ampy spacer extend the hexanuclear unit to 1D ladder-like chain structure. In contrast, anionic tetranuclear Cu(II) cluster of **3** is built up from two  $[Cu_2(Hpzdc)(pzdc)]^-$  units and two bpy linkers, stabilizing with 1D chain of  $[Cu(bpy)(H_2O)_4]_n^{2+}$ . This result demonstrated that various distorted geometries of Cu(II) centers, diverse coordination modes of  $H_3pzdc$  and, N,N'-ditopic coligands play a key role on their structural diversity. Furthermore the reaction temperature also have a great influence on the structural assembly of **2** and **3**. The magnetic studies of **1**, **2** and **4** revealed weak antiferromagnetic coupling interactions within Cu(II) trimer.

### References

- [1] M. Arıcı, O.Z. Yeşilel, M. Taş, H. Demiral, Inorg. Chem. 54 (2015) 11283-11291.
- [2] L. Bromberg, X. Su, T.A. Hatton, *Chem. Mater.* 26 (2014) 6257–6264.
- [3] E. Lee, H. Ju, S. Kim, K.-M. Park, S.S. Lee, Cryst. Growth Des. 15 (2015) 5427-5436.
- [4] J.-J. Liu, Y.-F. Guan, M.-J. Lin, C.-C. Huang, W.-X. Dai, Cryst. Growth Des. 15 (2015) 5040-5046.
- [5] G. Kang, Y. Jeon, K.Y. Lee, J. Kim, T.H. Kim, Cryst. Growth Des. 15 (2015) 5183-5187.
- [6] H.-Y. Wang, Y. Wu, C.F. Leong, D.M. D'Alessandro, J.-L. Zuo, Inorg. Chem. 54 (2015) 10766-10775.
- [7] P. Suvanvapee, J. Boonmak, F. Klongdee, C. Pakawatchai, B. Moubaraki, K.S. Murray, S. Youngme, Cryst. Growth Des. 15 (2015) 3804–3812.
- [8] J. Wu, L. Zhao, M. Guo, J. Tang, Chem. Commun. 51 (2015) 17317-17320.
- [9] C. Wang, S.-Y. Lin, W. Shi, P. Cheng, J. Tang, *Dalton Trans.* 44 (2015) 5364-5368.
- [10] J. Wu, L. Zhao, L. Zhang, X.-L. Li, M. Guo, A.K. Powell, J. Tang, *Angew. Chem. Int. Ed.* 55 (2016) 15574 –15578.
- [11] B. Mohapatra, S. Verma, Cryst. Growth Des. 16 (2016) 696-704.
- [12] L. Liu, C. Huang, X. Xue, M. Li, H. Hou, Y. Fan, *Cryst. Growth Des.* 15 (2015) 4507-4517.
- [13] J.-X. Yang, X. Zhang, J.-K. Cheng, J. Zhang, Y.-G. Yao, Cryst. Growth Des. 12 (2012) 333-345.
- [14] G.G. Sezer, O.Z. Yeşilel, M. Arıcı, H. Erer, Polyhedron. 102 (2015) 514–520.
- [15] M. Felloni, A.J. Blake, P. Hubberstey, C. Wilson, M. Schröder, Cryst. Growth Des. 9 (2009) 4685-4699.
- [16] I.M.L. Rosa, M.C.S. Costa, B.S. Vitto, L. Amorim, C.C. Correa, C.B. Pinheiro, A.C. Doriguetto, Cryst. Growth Des. 16 (2016) 1606-1616.
- [17] X. Liu, P. Cen, H. Li, H. Ke, S. Zhang, Q. Wei, G. Xie, S. Chen, S. Gao, *Inorg. Chem.* 53 (2014) 8088–8097.
- [18] A.K. Singh, J.I.v.d. Vlugt, S. Demeshko, S. Dechert, F. Meyer, *Eur. J. Inorg. Chem.* (2009) 3431–3439.
- [19] K. Hassanein, O. Castillo, C.J. Gómez-García, F. Zamora, P. Amo-Ochoa, Cryst. Growth Des. 15 (2015) 5485-5494.
- [20] Y.M. Litvinova, Y.M. Gayfulin, D.G. Samsonenko, A.S. Bogomyakov, W.H. Shon, S.-J. Kim, J.-S. Rhyee, Y.V. Mironov, Polyhedron. 115 (2016) 174–179.

- [21] L. Pan, X. Huang, J. Li, J. Solid State Chem. 152 (2000) 236-246.
- [22] J.-H. Yang, S.-L. Zheng, X.-L. Yu, X.-M. Chen, Cryst. Growth Des. 4 (2004) 831-836.
- [23] P. King, R. Clérac, C.E. Anson, A.K. Powell, *Dalton Trans*. (2004) 852-861.
- [24] J. Zhao, L.-S. Long, R.-B. Huang, L.-S. Zheng, Dalton Trans. (2008) 4714–4716.
- [25] X.-H. Zhou, X.-D. Du, G.-N. Li, J.-L. Zuo, X.-Z. You, *Cryst. Growth Des.* 9 (2009) 4487-4496.
- [26] D. Saha, T. Maity, S. Das, S. Koner, Dalton Trans. 42 (2013) 13912–13922.
- [27] S. Barman, H. Furukawa, O. Blacque, K. Venkatesan, O.M. Yaghi, G.-X. Jin, H. Berke, Chem. Commun. 47 (2011) 11882–11884.
- [28] W.L. Driessen, L. Chang, C. Finazzo, S. Gorter, D. Rehorst, J. Reedijk, M. Lutz, A.L. Spek, Inorg. Chim. Acta. 350 (2003) 25-31.
- [29] C.-Z. Xie, R.-F. Li, L.-Y. Wang, Q.-Q. Zhang, Z. Anorg. Allg. Chem. 636 (2010) 657–661
- [30] P. King, R. Clérac, C.E. Anson, C. Coulon, A.K. Powell, Inorg. Chem. 42 (2003) 3492–3500.
- [31] Q.-Q. Dou, Y.-K. He, L.-T. Zhang, Z.-B. Han, *Acta Cryst*. E63 (2007) m2908–m2909.
- [32] APEX2; Bruker AXS Inc.: Madison, WI. (2014).
- [33] SAINT 4.0 Software Reference Manual; Siemens Analytical X-Ray Systems Inc.: Madison, WI. (2000).
- [34] G.M. Sheldrick, SADABS, Program for Empirical Absorption correction of Area Detector Data; University of Gottingen: Gottingen, Germany. (2000).
- [35] G.M. Sheldrick, Acta Crystallogr., Sect. A. A64 (2008) 112–122.
- [36] A.W. Addison, T.N. Rao, J. Chem. Soc., Dalton Trans. (1984) 1349-1356.
- [37] G.P. Shields, P.R. Raithby, F.H. Allen, W.D.S. Motherwell, *Acta Crystallogr.* B56 (2000) 455-465.
- [38] P. Smoleński, J. Kłak, D.S. Nesterov, A.M. Kirillov, *Cryst. Growth Des.* 12 (2012) 5852–5857.
- [39] J.-L. Tian, S.-P. Yan, D.-Z. Liao, Z.-H. Jiang, P. Cheng, *Inorg. Chem. Commun.* (2003) 1025–1029.
- [40] J. Boonmak, S. Youngme, N. Chaichit, G.A.v. Albada, J. Reedijk, Cryst. Growth Des. 9 (2009) 3318-3326.
- [41] F.-M. Nie, Z.-Y. Dong, F. Lu, G.-X. Li, J. Coord. Chem. 63 (2010) 4259–4270.
- [42] O. Kahn, "Molecular Magnetism", Chapter 10. (1993).
- [43] J.-M. Dominguez-Vera, E. Colacio, J. Ruiz, J.M. Moreno, M.R. Sundberg, Acta Chem. Scand. 46 (1992) 1055-1058.
- [44] J.C. Bayoń, P. Esteban, G. Net, P.G. Ramussen, K.N. Baker, C.W. Hahn, M.M. Gumz, Inorg. Chem. 30 (1991) 2572-2574
- [45] S.-F. Huang, Y.-C. Chou, P. Misra, C.-J. Lee, S. Mohanta, H.-H. Wei, *Inorg. Chim. Acta.* 357 (2004) 1627–1631.
- [46] J.-C. Liu, D.-G. Fu, J.-Z. Zhuang, C.-Y. Duan, X.-Z. You, J. Chem. Soc., Dalton Trans. (1999) 2337–2342.

# **Supporting Information for Part I**

**Table S1**. The selected bond lengths (Å) and angles (°) for compounds 1-4

| Cu1—O1i       1.9619(11)       O1—Cu1—O7       92         Cu1—N1       2.0066(12)       O1i—Cu1—O7       88         Cu1—N1i       2.0066(12)       N1—Cu1—O7       89         Cu1—O7       2.4957(14)       N1i—Cu1—O7       90         Cu1—O7i       2.4957(14)       N2—Cu2—O6       92         Cu2—N2       1.9703(12)       N2—Cu2—O3       82         Cu2—O6       1.9777(12)       O6—Cu2—O3       13         Cu2—O3       1.9992(11)       N2—Cu2—N3       17         Cu2—N3       2.0339(12)       O6—Cu2—N3       87         Cu2—O5       2.1734(15)       O3—Cu2—N3       93         O1—Cu1—O1i       180       N2—Cu2—O5       96         O1—Cu1—N1       82.29(5)       O6—Cu2—O5       12  | 80<br>01.96(5)<br>88.04(5)<br>89.01(5)<br>90.99(5)<br>92.47(5)<br>32.54(5)<br>51.00(6) |
|---|--|
| Cu1—O1i       1.9619(11)       O1—Cu1—O7       9.5         Cu1—N1       2.0066(12)       O1i—Cu1—O7       88         Cu1—N1i       2.0066(12)       N1—Cu1—O7       89         Cu1—O7       2.4957(14)       N1i—Cu1—O7       90         Cu1—O7i       2.4957(14)       N2—Cu2—O6       92         Cu2—N2       1.9703(12)       N2—Cu2—O3       82         Cu2—O6       1.9777(12)       O6—Cu2—O3       13         Cu2—O3       1.9992(11)       N2—Cu2—N3       17         Cu2—N3       2.0339(12)       O6—Cu2—N3       87         Cu2—O5       2.1734(15)       O3—Cu2—N3       93         O1—Cu1—O1i       180       N2—Cu2—O5       96         O1—Cu1—N1       82.29(5)       O6—Cu2—O5       13 | 01.96(5)<br>08.04(5)<br>09.01(5)<br>00.99(5)<br>02.47(5)<br>02.54(5)                   |
| Cu1—N1       2.0066(12)       O1i—Cu1—O7       88         Cu1—N1i       2.0066(12)       N1—Cu1—O7       89         Cu1—O7       2.4957(14)       N1i—Cu1—O7       90         Cu1—O7i       2.4957(14)       N2—Cu2—O6       92         Cu2—N2       1.9703(12)       N2—Cu2—O3       82         Cu2—O6       1.9777(12)       O6—Cu2—O3       12         Cu2—O3       1.9992(11)       N2—Cu2—N3       17         Cu2—N3       2.0339(12)       O6—Cu2—N3       87         Cu2—O5       2.1734(15)       O3—Cu2—N3       93         O1—Cu1—O1i       180       N2—Cu2—O5       96         O1—Cu1—N1       82.29(5)       O6—Cu2—O5       12  | 38.04(5)<br>39.01(5)<br>90.99(5)<br>92.47(5)<br>32.54(5)                               |
| Cu1—N1i       2.0066(12)       N1—Cu1—O7       89         Cu1—O7       2.4957(14)       N1i—Cu1—O7       90         Cu1—O7i       2.4957(14)       N2—Cu2—O6       92         Cu2—N2       1.9703(12)       N2—Cu2—O3       82         Cu2—O6       1.9777(12)       O6—Cu2—O3       13         Cu2—O3       1.9992(11)       N2—Cu2—N3       17         Cu2—N3       2.0339(12)       O6—Cu2—N3       87         Cu2—O5       2.1734(15)       O3—Cu2—N3       93         O1—Cu1—O1i       180       N2—Cu2—O5       96         O1—Cu1—N1       82.29(5)       O6—Cu2—O5       12  | 39.01(5)<br>00.99(5)<br>02.47(5)<br>32.54(5)   |
| Cu1—O7       2.4957(14)       N1i—Cu1—O7       90         Cu1—O7i       2.4957(14)       N2—Cu2—O6       92         Cu2—N2       1.9703(12)       N2—Cu2—O3       82         Cu2—O6       1.9777(12)       O6—Cu2—O3       15         Cu2—O3       1.9992(11)       N2—Cu2—N3       17         Cu2—N3       2.0339(12)       O6—Cu2—N3       87         Cu2—O5       2.1734(15)       O3—Cu2—N3       93         O1—Cu1—O1i       180       N2—Cu2—O5       96         O1—Cu1—N1       82.29(5)       O6—Cu2—O5       12  | 00.99(5)<br>02.47(5)<br>32.54(5)   |
| Cu1—O7i       2.4957(14)       N2—Cu2—O6       92         Cu2—N2       1.9703(12)       N2—Cu2—O3       82         Cu2—O6       1.9777(12)       O6—Cu2—O3       15         Cu2—O3       1.9992(11)       N2—Cu2—N3       17         Cu2—N3       2.0339(12)       O6—Cu2—N3       87         Cu2—O5       2.1734(15)       O3—Cu2—N3       93         O1—Cu1—O1i       180       N2—Cu2—O5       96         O1—Cu1—N1       82.29(5)       O6—Cu2—O5       12  | 92.47(5)<br>32.54(5)   |
| Cu2—N2       1.9703(12)       N2—Cu2—O3       82         Cu2—O6       1.9777(12)       O6—Cu2—O3       12         Cu2—O3       1.9992(11)       N2—Cu2—N3       17         Cu2—N3       2.0339(12)       O6—Cu2—N3       83         Cu2—O5       2.1734(15)       O3—Cu2—N3       93         O1—Cu1—O1i       180       N2—Cu2—O5       96         O1—Cu1—N1       82.29(5)       O6—Cu2—O5       13  | 32.54(5)   |
| Cu2—O6       1.9777(12)       O6—Cu2—O3       15         Cu2—O3       1.9992(11)       N2—Cu2—N3       17         Cu2—N3       2.0339(12)       O6—Cu2—N3       87         Cu2—O5       2.1734(15)       O3—Cu2—N3       93         O1—Cu1—O1 <sup>i</sup> 180       N2—Cu2—O5       96         O1—Cu1—N1       82.29(5)       O6—Cu2—O5       12   |  |
| Cu2—O3       1.9992(11)       N2—Cu2—N3       17         Cu2—N3       2.0339(12)       O6—Cu2—N3       87         Cu2—O5       2.1734(15)       O3—Cu2—N3       93         O1—Cu1—O1 <sup>i</sup> 180       N2—Cu2—O5       96         O1—Cu1—N1       82.29(5)       O6—Cu2—O5       13  | 51.00(6)   |
| Cu2—N3       2.0339(12)       O6—Cu2—N3       87         Cu2—O5       2.1734(15)       O3—Cu2—N3       93         O1—Cu1—O1i       180       N2—Cu2—O5       96         O1—Cu1—N1       82.29(5)       O6—Cu2—O5       12   |  |
| Cu2—O5       2.1734(15)       O3—Cu2—N3       93         O1—Cu1—O1 <sup>i</sup> 180       N2—Cu2—O5       96         O1—Cu1—N1       82.29(5)       O6—Cu2—O5       13  | 70.72(5)   |
| O1—Cu1—O1 <sup>i</sup> 180 N2—Cu2—O5 96<br>O1—Cu1—N1 82.29(5) O6—Cu2—O5 1.  | 37.14(5)   |
| O1—Cu1—N1 82.29(5) O6—Cu2—O5 1  | 93.32(5)   |
|   | 06.02(6)   |
| $O1^{1}$ — $Cu1$ — $N1$ 97.71(5) $O3$ — $Cu2$ — $O5$ 96   | 12.75(7)   |
|   | 06.21(7)   |
|   | 2.67(6)  |
| O1 <sup>i</sup> —Cu1—N1 <sup>i</sup> 82.29(5)   |  |
| Compound $2^b$  |  |
|   | 00.18(12)  |
| Cu1—O1 1.974(2) O1—Cu1—N3 83  | 37.07(11)  |
| Cu1—N1 2.008(3) N1—Cu1—N3 16  | 68.32(12)  |
| Cu1—N3 2.015(3) O5—Cu1—O6 86  | 36.73(12)  |
| Cu1—O6 2.395(3) O1—Cu1—O6 93  | 3.25(11)   |
| Cu1—O9 2.672(3) N1—Cu1—O6 89  | 39.55(11)  |
| Cu2—O3 1.959(3) N3—Cu1—O6 96  | 06.39(12)  |
| $Cu2-O3^{i}$ 1.959(3) $O3-Cu2-O3^{i}$ 18  | .80  |
| Cu2—N2 2.005(3) O3—Cu2—N2 83  | 33.40(11)  |
| Cu2—N2 <sup>i</sup> 2.005(3) O3 <sup>i</sup> —Cu2—N2 96   | 06.60(11)  |
| Cu2—O7 2.515(4) O3—Cu2—N2 <sup>i</sup> 96   | 06.59(11)  |
| Cu2—O7 <sup>i</sup> 2.515(4) O3 <sup>i</sup> —Cu2—N2 <sup>i</sup> 83  | 33.41(11)  |
| O5—Cu1—O1 177.23(10) N2—Cu2—N2 <sup>i</sup> 18  | .80  |
| O5—Cu1—N1 100.23(11) O1—Cu1—N3 8  | 37.07(11)  |
| O1—Cu1—N1 82.54(11)   |  |
| Compound $3^c$  |  |
| Cu1—N1 <sup>i</sup> 1.933(4) N1—Cu1—N2 99   | 9.17(18)   |
| Cu1—N1 1.933(4) O1—Cu1—N2 99  | 9.83(17)   |
| Cu1—O1 2.024(4) O1 <sup>i</sup> —Cu1—N2 99  | 9.83(17)   |
| Cu1—O1 <sup>i</sup> 2.024(4) N3 <sup>ii</sup> —Cu2—N3 18  | .80  |
| Cu1—N2 2.195(6) N3 <sup>ii</sup> —Cu2—O3 <sup>ii</sup> 90   | 0  |
| Cu2—N3 <sup>ii</sup> 2.007(8) N3—Cu2—O3 <sup>ii</sup> 90  | 0  |
| Cu2—N3 2.007(8) N3 <sup>ii</sup> —Cu2—O3 <sup>iii</sup> 90  | 0  |
| Cu2—O3 <sup>ii</sup> 2.201(8) N3—Cu2—O3 <sup>iii</sup> 90   | 00   |
| Cu2—O3 <sup>iii</sup> 2.201(9) O3 <sup>ii</sup> —Cu2—O3 <sup>iii</sup> 86   | 36.1(4)  |
| $Cu2-O3^{iv}$ 2.201(9) $N3^{ii}-Cu2-O3^{iv}$ 90   | 00   |
| Cu2—O3 2.201(9) N3—Cu2—O3 <sup>iv</sup> 90  | 00   |
|   | 3.9(4)   |
| ·   |  |
| N1—Cu1—O1 80.21(17) N3 <sup>ii</sup> —Cu2—O3 90   | .80  |

| N1 <sup>i</sup> —Cu1—O1 <sup>i</sup> | 80.21(17)                      | N3—Cu2—O3                 | 90         |
|--------------------------------------|--------------------------------|---------------------------|------------|
| N1—Cu1—O1 <sup>i</sup>               | 160.47(17)                     | O3 <sup>ii</sup> —Cu2—O3  | 180        |
| O1—Cu1—O1 <sup>i</sup>               | 100.9(2)                       | O3 <sup>iii</sup> —Cu2—O3 | 93.9(4)    |
| N1 <sup>i</sup> —Cu1—N2              | 99.17(18)                      | O3 <sup>iv</sup> —Cu2—O3  | 86.1(4)    |
|                                      |                                |                           |            |
|                                      | Compound <b>4</b> <sup>d</sup> |                           |            |
| Cu1—O10                              | 1.931(4)                       | N1—Cu1—N5                 | 171.65(17) |
| Cu1—O1                               | 1.949(4)                       | O3—Cu2—O5                 | 173.30(17) |
| Cu1—N1                               | 1.989(4)                       | O3—Cu2—N3                 | 96.46(16)  |
| Cu1—N5                               | 2.019(4)                       | O5—Cu2—N3                 | 82.39(16)  |
| Cu1···O4                             | 2.800(3)                       | O3—Cu2—N2                 | 82.21(15)  |
| Cu1—O9                               | 2.472(5)                       | O5—Cu2—N2                 | 98.02(15)  |
| Cu2—O3                               | 1.938(3)                       | N3—Cu2—N2                 | 172.12(18) |
| Cu2—O5                               | 1.945(4)                       | O3—Cu2—O11                | 97.28(16)  |
| Cu2—N3                               | 1.982(4)                       | O5—Cu2—O11                | 89.34(16)  |
| Cu2—N2                               | 1.996(4)                       | N3—Cu2—O11                | 90.73(16)  |
| Cu2—O11                              | 2.346(5)                       | N2—Cu2—O11                | 97.14(16)  |
| Cu3—O12                              | 1.940(4)                       | O12—Cu3—O7                | 166.92(19) |
| Cu3—07                               | 1.960(4)                       | O12—Cu3—N4                | 99.55(17)  |
| Cu3—N4                               | 2.005(4)                       | O7—Cu3—N4                 | 82.66(15)  |
| Cu3—N6 <sup>i</sup>                  | 2.043(4)                       | O12—Cu3—N6 <sup>i</sup>   | 88.70(17)  |
| Cu3—O13                              | 2.199(4)                       | O7—Cu3—N6 <sup>i</sup>    | 86.52(16)  |
| O10—Cu1—O1                           | 175.2(2)                       | N4—Cu3—N6 <sup>i</sup>    | 164.89(18) |
| O10—Cu1—N1                           | 97.74(17)                      | O12—Cu3—O13               | 92.50(19)  |
| O1—Cu1—N1                            | 83.14(15)                      | O7—Cu3—O13                | 100.18(16) |
| O10—Cu1—N5                           | 88.62(18)                      | N4—Cu3—O13                | 100.18(16) |
| O1—Cu1—N5                            | 90.09(16)                      | N6 <sup>i</sup> —Cu3—O13  | 97.44(17)  |

<sup>a</sup>Symmetry codes for **1**: (i) 1-*x*, 2-*y*, 2-*z*. <sup>b</sup>For **2**: (i) 2-*x*, 1-*y*, 1-*z*. <sup>c</sup>For **3**: (i) 1-*x*, *y*, *z*; (ii) 1-*x*, 1-*y*, -*z*; (iii) *x*, 1-*y*, *z*; (iv) 1-*x*, *y*, -*z*. <sup>d</sup>For **4**: (i) *x*, -1+*y*, -1+*z*.

Table S2. Intermolecular hydrogen bond length/Å angles/° in compounds 1-4

|   |            | C 11 <sup>a</sup>              |            |           |
|---|------------|--------------------------------|------------|-----------|
| D II A  | 1/D II)/ Å | Compound <b>1</b> <sup>a</sup> | 1/D 4)/Å   | /DIIA)/0  |
| D-H···A                                       | d(D-H)/Å   | d(H···A)/Å                     | d(D···A)/Å | <(DHA)/°  |
| O5-H1···O8 <sup>i</sup>                       | 0.84       | 1.84                           | 2.635(4)   | 157       |
| O5-H3···O7 <sup>ii</sup>                      | 0.83       | 1.92                           | 2.741(2)   | 170       |
| O6-H5···O4 <sup>iii</sup>                     | 0.84       | 2.00                           | 2.823(2)   | 168       |
| O7-H8···O4 <sup>iv</sup>                      | 0.85       | 1.92                           | 2.7489(2)  | 167       |
| O7-H9···O2 <sup>v</sup>                       | 0.84       | 1.96                           | 2.780(2)   | 169       |
| O8-H10···O2 <sup>iii</sup>                    | 0.85       | 2.21                           | 2.920(5)   | 141       |
| O8-H11···O2 <sup>vi</sup>                     | 0.85       | 2.04                           | 2.785(5)   | 147       |
| C2-H2···O4 <sup>ii</sup>                      | 0.91       | 2.42                           | 3.284(2)   | 160       |
| C6-H6···O8 <sup>vii</sup>                     | 0.93       | 2.44                           | 3.301(5)   | 155       |
|   |            | Compound $2^b$                 |            |           |
| D–H···A                                       | d(D-H)/Å   | d(H···A)/Å                     | d(D···A)/Å | <(DHA)/°  |
| O6-H4···O4 <sup>i</sup>                       | 0.84       | 1.89                           | 2.720(4)   | 168       |
| O6-H5···O10 <sup>ii</sup>                     | 0.85       | 1.92                           | 2.747(4)   | 165       |
| O7–H8···O2 <sup>iii</sup>                     | 0.85       | 1.96                           | 2.796(4)   | 167       |
| O7-H11···O11 <sup>ii</sup>                    | 0.85       | 1.92                           | 2.744(6)   | 162       |
| O9-H14···O1 <sup>iv</sup>                     | 0.85       | 2.07                           | 2.903(4)   | 167       |
| O9-H15···O4 <sup>iii</sup>                    | 0.84       | 2.01                           | 2.839(4)   | 167       |
| O10-H16···O2                                  | 0.84       | 1.88                           | 2.696(4)   | 163       |
| O10-H10···O2                                  | 1.00       | 1.89                           | 2.690(4)   | 135       |
| O10-H17····O3<br>O11-H18····O6 <sup>iii</sup> |            |                                |            |           |
|   | 0.85       | 1.99                           | 2.827(6)   | 168       |
| O11-H19···O8 <sup>v</sup>                     | 0.85       | 2.03                           | 2.884(8)   | 175       |
| C9–H9···O11 <sup>vi</sup>                     | 0.93       | 2.35                           | 3.240(6)   | 159       |
|   | 1/2 / 8    | Compound $3^c$                 |            |           |
| D-H···A                                       | d(D-H)/Å   | d(H···A)/Å                     | d(D···A)/Å | <(DHA)/°  |
| O3-H6···O1                                    | 0.85       | 1.99                           | 2.808(4)   | 161       |
| C4-H4···O2 <sup>i</sup>                       | 0.93       | 2.54                           | 3.179(7)   | 127       |
| O2-H2···O4 <sup>ii</sup>                      | 0.82       | 2.00                           | 2.685(9)   | 141       |
|   |            | Compound $4^d$                 | 0          |           |
| D-H···A                                       | d(D–H) /Å  | d(H···A) /Å                    | d(D···A)/Å | <(DHA) /° |
| O9-H1···O6 <sup>i</sup>                       | 0.86       | 2.03                           | 2.852(6)   | 159       |
| O9–H3···O9 <sup>ii</sup>                      | 0.87       | 2.35                           | 2.856(5)   | 117       |
| O10-H4···O15 <sup>iii</sup>                   | 0.86       | 1.87                           | 2.716(8)   | 170       |
| O11-H6···O8 <sup>i</sup>                      | 0.86       | 1.90                           | 2.744(6)   | 170       |
| N7-H7A···O13 <sup>iv</sup>                    | 0.86       | 2.04                           | 2.829(8)   | 153       |
| N7-H7B···O16 <sup>v</sup>                     | 0.86       | 2.13                           | 2.974(8)   | 165       |
| O12-H10···O16 <sup>vi</sup>                   | 0.86       | 1.91                           | 2.715(7)   | 155       |
| O13-H15···O4 <sup>iii</sup>                   | 0.86       | 1.86                           | 2.718(6)   | 173       |
| O14-H16···O16 <sup>vii</sup>                  | 0.86       | 2.45                           | 2.873(12)  | 111       |
| O14-H17···O11                                 | 0.86       | 2.55                           | 2.996(10)  | 113       |
| O15-H20···O1                                  | 0.86       | 2.37                           | 2.818(7)   | 113       |
| O15-H20···N7 <sup>viii</sup>                  | 0.86       | 2.52                           | 3.089(11)  | 124       |
| O15-H21···O14 <sup>ii</sup>                   | 0.86       | 2.56                           | 3.226(11)  | 135       |
| O16-H22···O7 <sup>ix</sup>                    | 0.87       | 2.13                           | 2.904(6)   | 149       |
| O16-H23···O14 <sup>vii</sup>                  | 0.86       | 2.13                           | 2.873(12)  | 172       |
| C2-H2···O2 <sup>x</sup>                       | 0.93       | 2.02                           | 3.418(6)   | 178       |
| CZ 11ZOZ                                      | 0.33       | ۷.47                           | 3.410(0)   | 1/0       |

<sup>a</sup>Symmetry codes for **1**: (i) 1-*x*, 1-*y*, 1-*z*; (ii) 1-*x*, 1-*y*, 2-*z*; (iii) 1-*x*, 2-*y*, 1-*z*; (iv) *x*, *y*, -1+*z*; (v) -*x*, 2-*y*, 2-*z*; (vi) 1+*x*, -1+*y*, -1+*z*; (vii) 2-*x*, 1-*y*, 1-*z*. <sup>b</sup>For **2**: (i) *x*, 1.5-*y*, 0.5+*z*; (ii) -1+*x*, *y*, *z*; (iii) 1-*x*, 1-*y*, 1-*z*; (iv) 1-*x*, 0.5+*y*, 0.5-*z*; (v) 1-*x*, -*y*, 1-*z*; (vi) 1-*x*, 0.5-*y*, 0.5+*z*. <sup>c</sup>For **3**: (i) 1.5-*x*, 1.5-*y*, *z*; (ii) *x*, *y*, -*z*. <sup>d</sup>For **4**: (i) 1+*x*, *y*, *z*; (ii) 1-*x*, 1-*y*, 2-*z*; (iii) -1+*x*, *y*, *z*; (iv) *x*, -1+*y*, -1+*z*; (v) 1-*x*, 2-*y*, 1-*z*; (vii) *x*, 1+*y*, *z*; (vii) 1-*x*, 1-*y*, 1-*z*; (viii) 1-*x*, 2-*y*, 2-*z*; (ix) 1+*x*, -1+*y*, *z*; (x) -*x*, 1-*y*, 1-*z*.

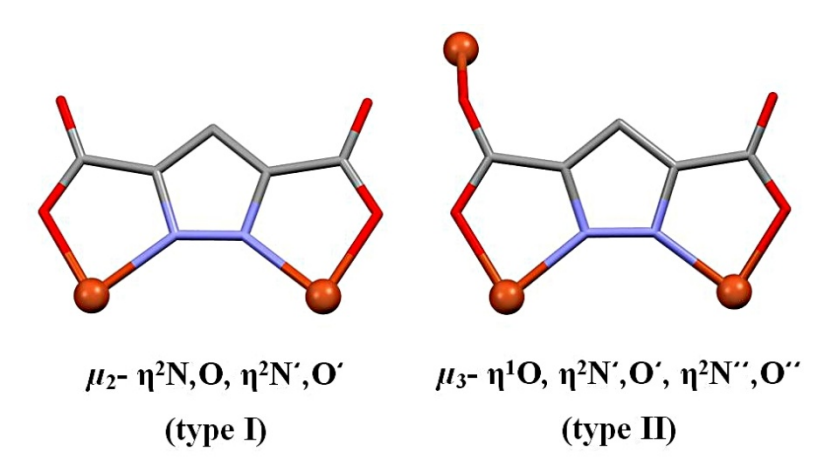
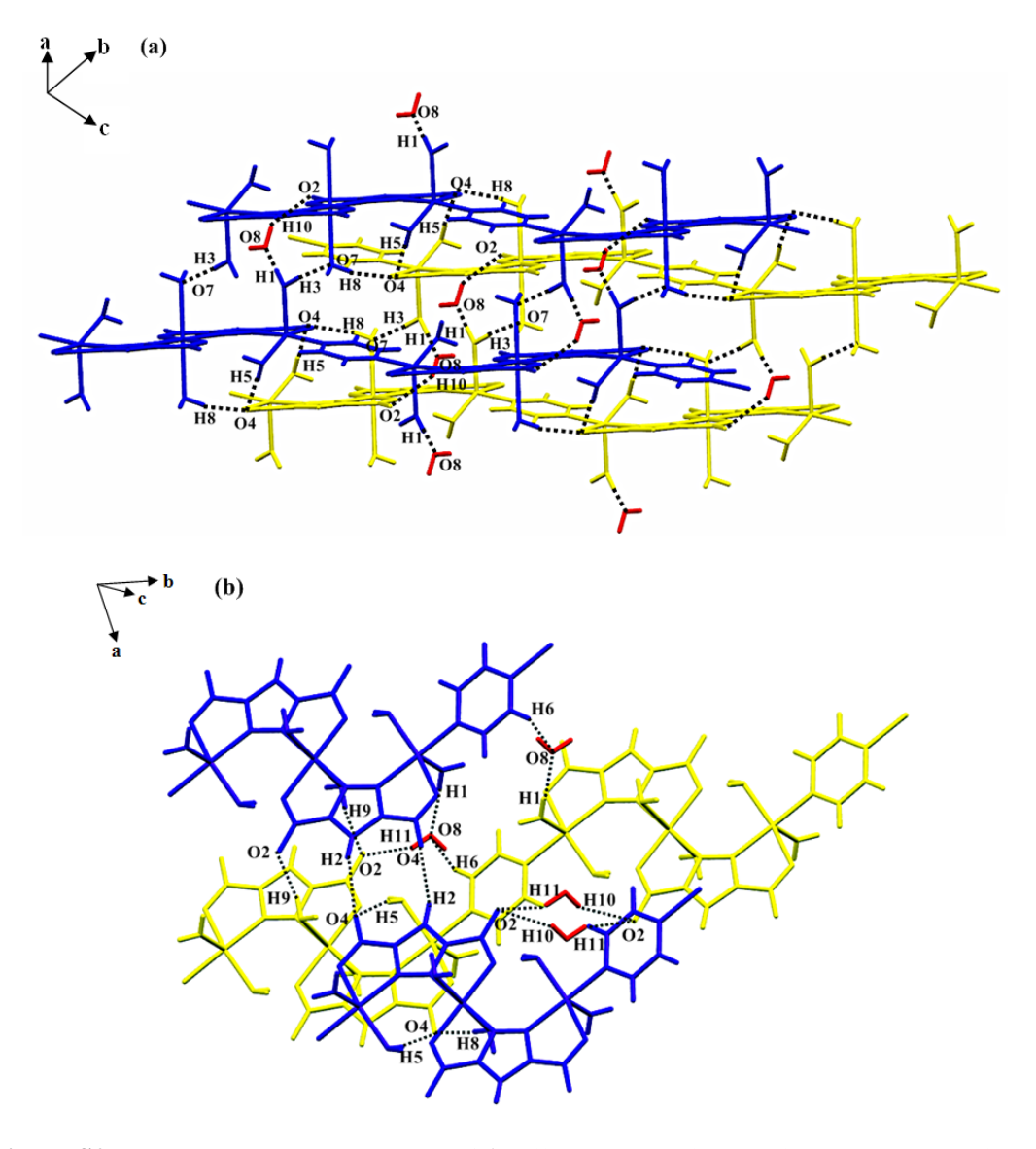
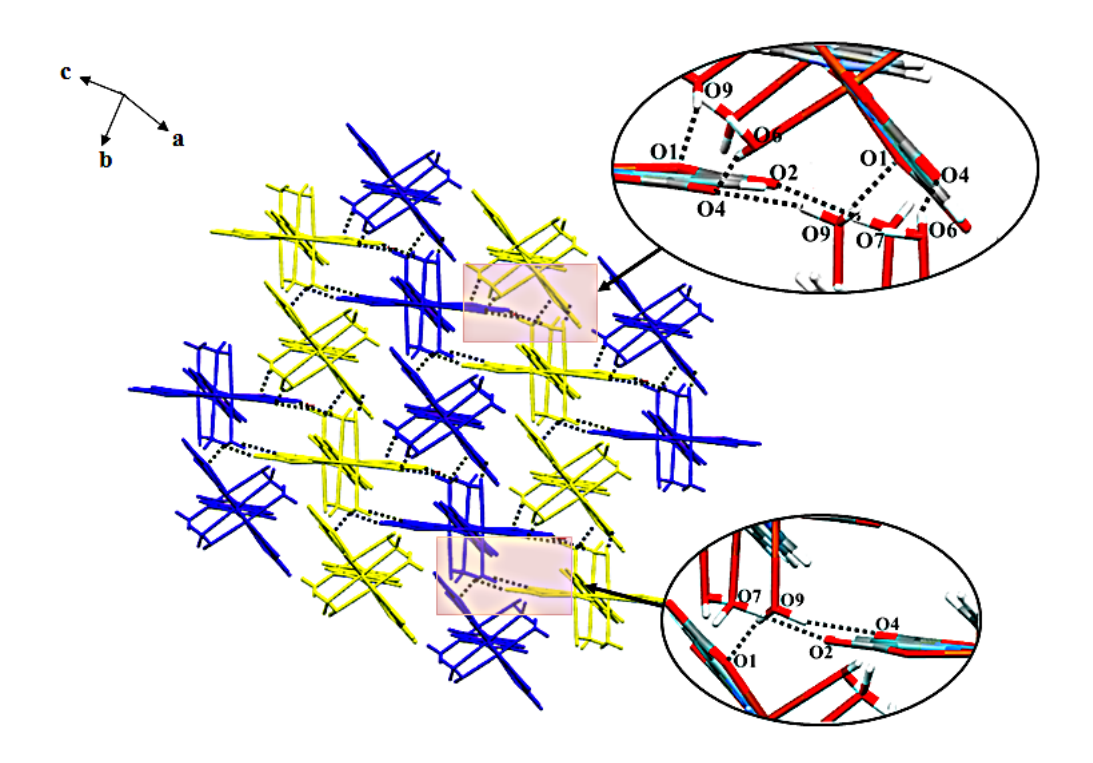


Figure S1. Coordination modes of pyrazole-3,5-dicarboxylate in 1-4.



**Figure S2.** 3D supramolecular structure of **1** built by various interchain hydrogen bonding (dash lines).



**Figure S3.**3D supramolecular network of **2** built by hydrogen bonding interactions.

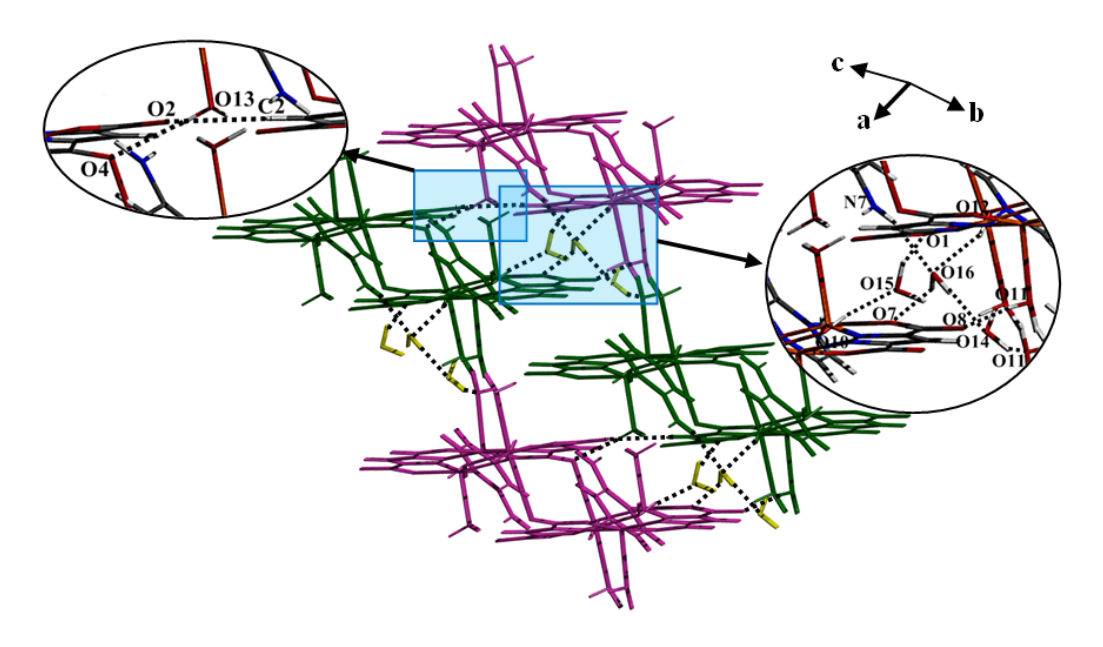


**Figure S4.** 3D packing diagram of **4** formed by various weak interchain hydrogen bonding interactions.

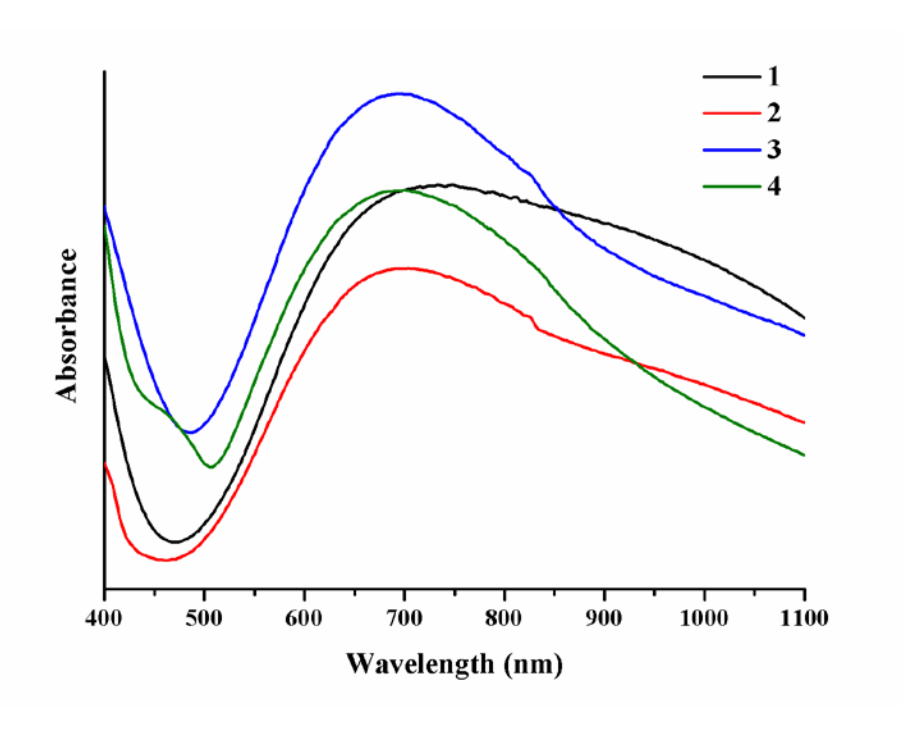
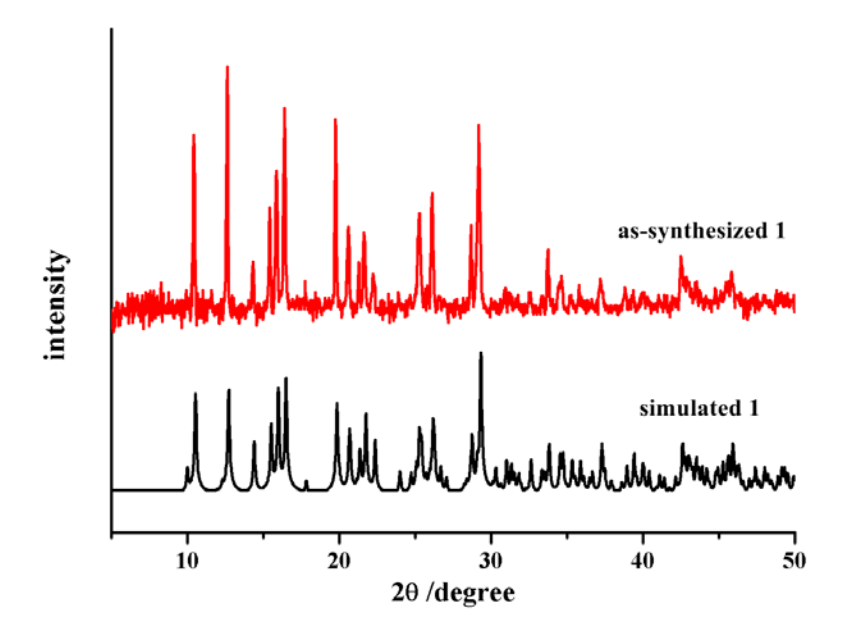
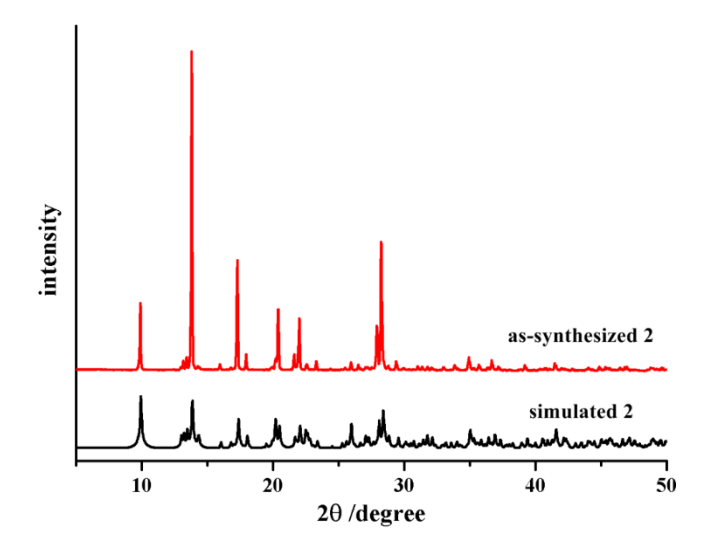


Figure S5. The electronic spectra of 1-4.



**Figure S6.** XRPD patterns of simulated from single-crystal X-ray data and as-synthesized of **1**.



**Figure S7.** XRPD patterns of simulated from single-crystal X-ray data and as-synthesized of **2**.

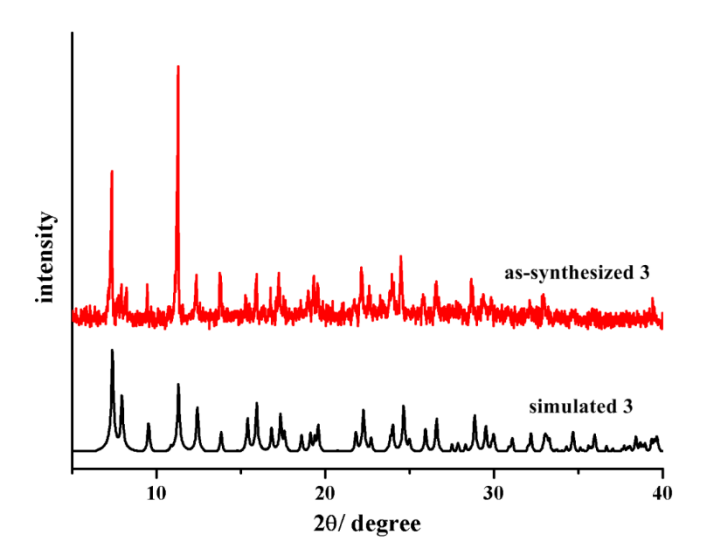


**Figure S8.** XRPD patterns of simulated from single-crystal X-ray data and as-synthesized of **3**.

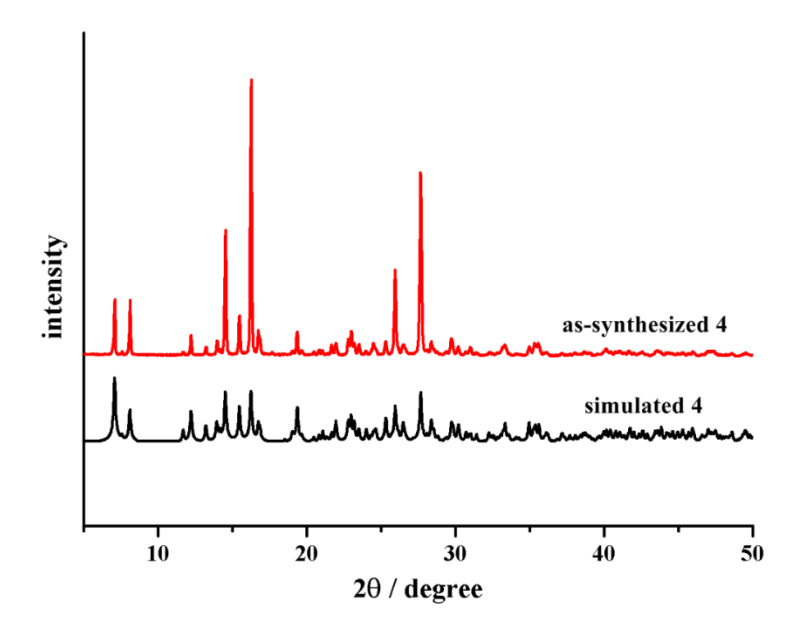


**Figure S9.** XRPD patterns of simulated from single-crystal X-ray data and as-synthesized of **4**.

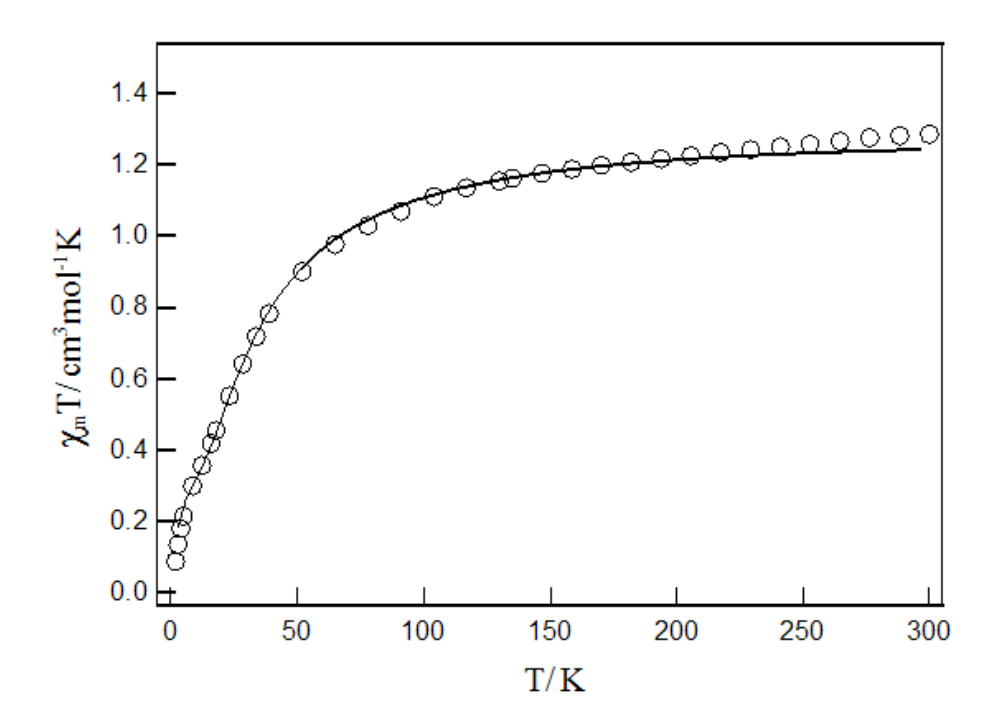


**Figure S10.** Experimental values of  $\chi_{\rm M}T$ , per Cu<sub>3</sub>, (open circles) versus temperature (K) plot for compound **1**. The solid lines is the best fit using the linear  $S = \frac{1}{2}$  trimer model described in the text that includes an inter-trimer term,  $\theta$ . Best-fit parameters: g = 2.19; J = -14.0 cm<sup>-1</sup>;  $\theta = -4.3$  K; N $\alpha = 100$  x  $10^{-6}$  cm<sup>3</sup> mol<sup>-1</sup>.

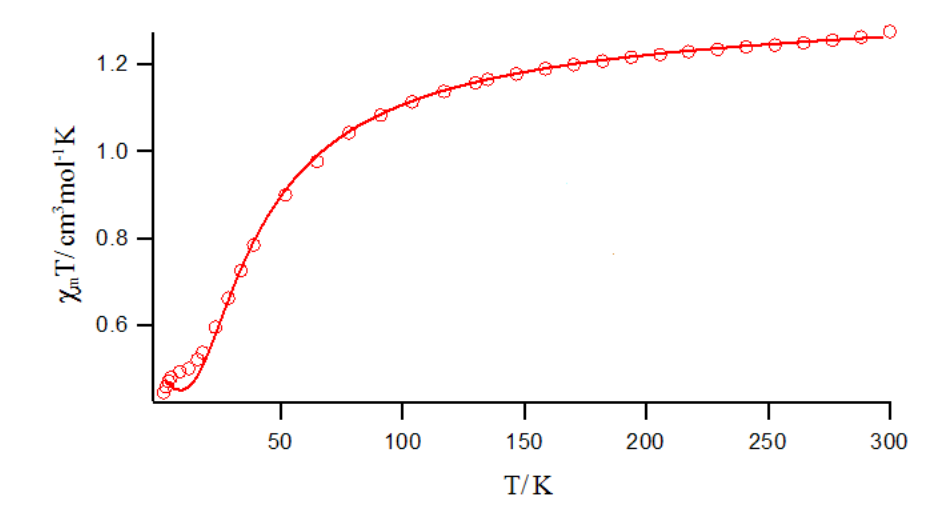


**Figure S11.** Experimental values of  $\chi_{\rm M}T$ , per Cu<sub>3</sub>, (open circles) versus temperature (K) plot for compound **2**. The solid lines is the best fit using the linear  $S = \frac{1}{2}$  trimer model described in the text that includes an inter-trimer term,  $\theta$ . Best-fit parameters: g = 2.16; J = -16.5 cm<sup>-1</sup>;  $\theta = 0.2$  K; N $\alpha = 60$  x  $10^{-6}$  cm<sup>3</sup> mol<sup>-1</sup>.

# **PART II**

# Anion-dependent self-assembly of copper coordination polymers based on pyrazole-3,5-dicarboxylate and 1,2-di(4-pyridyl) ethylene

### Introduction

Self-assembled coordination polymers (CPs) have gained extensive attention for not only their fascinating structural diversities but also their applications in many fields, such gas storage, catalysis, magnetism, luminescence, and ion exchange. The structural assemblies can be influenced by many factors, such as ligand, source of metal ion, counterion, stoichiometry, temperature, and the pH of the solution. Consequently, several architectures of CPs have been remarkably constructed. In the case of the anion, it can act as either coordination ligand or counterion balancing the framework charge depending on its coordination ability. The use of different anions in the reaction may affect the self-assembly of coordination polymers. Notably, the study of cationic host frameworks for anionic guest exchange has become a significant research area because the traditional ion exchange resin has the limitation of its thermal and chemical stability. Nowadays, many porous CPs with anion exchange properties have been widely reported. The anion exchange process in CPs generally involves either a solid-state diffusion mechanism or solvent-mediated exchange process.

The organic bridging ligand is a primary factor that controls and facilitates the formation of CPs. Pyrazole-3,5-dicarboxylic acid ( $H_3pzdc$ ) is a multifunctional ligand which exhibits various coordination ability (Figure S1).  $^{17-19}$   $H_3pzdc$  has potential six coordination sites including four carboxylate oxygen and two pyrazole nitrogen atoms. Thus,  $H_3pzdc$  can coordinate as a mono- to the hexadentate ligand. A variety of complexes based on  $H_3pzdc$  containing transition and lanthanide metal ions have been documented.  $^{20-22}$  The diversified CPs containing Cu(II) ion have been known, in contrast to other transition metals, because Cu(II) center exhibits diverse coordination geometries in one compound owing to Jahn-Teller distortion. The pyrazole-3,5-dicarboxylato Cu(II) complexes frequently provide dinuclear or trinuclear Cu(II) building unit.  $^{18, 23}$  Apart from the  $H_3pzdc$  ligand, the flexible N,N'-ditopic spacer is used as an ancillary ligand for a dimensional extension. They can rotate or bend to adopt the proper conformation and hold the energetic minimum when coordinating to the metal centers, which cause a great structural diversity. In this work, 1,2-di(4-pyridyl)ethylene (dpe) was used as flexible  $N,N\square$ -ditopic co-ligand for increasing dimensionality of Cu(II) pyrazole-3,5-dicarboxylate.

Herein a novel series of pyrazole-3,5-dicarboxylato Cu(II) coordination polymers with 1,2-di(4-pyridyl)ethylene have been synthesized by using various starting copper(II) salts, including  $NO_3$ ,  $ClO_4$ ,  $BF_4$ , SCN,  $SO_4^{2-}$ , and  $PO_4^{3-}$  anions, the structural diversity of all compounds indicates the role of anion on the structural assemblies. The anion exchange properties of **1-4** have been studied. Also, the luminescent properties of **1-6** and exchanged products were investigated.

# **Experimental section**

## Physical measurements

All chemicals and solvents were received from commercial sources and were used without further purification. FT-IR spectra were obtained by using the standard Pike ATR cell on a Bruker Tensor 27 FT-IR spectrophotometer in  $4000-600~\text{cm}^{-1}$  spectral range. Solid-state electronic spectra were measured on a PerkinElmer Lambda2S spectrophotometer (400-1100~nm). Elemental analyses (C, H, N) were carried out with a PerkinElmer PE 2400CHNS analyzer. Thermogravimetric analyses (TGA) were done by using a Hitachi STA7200 thermal analyzer between 35 and 750 °C in  $N_2$  atmosphere with a heating rate of  $10~\text{°C min}^{-1}$ . The X-ray powder di finactional (SERPD): detain temperature by using a PANalytical EMPYREAN with monochromatic CuK $\alpha$ , and the recording speed was 0.5 s/step in the 20~range of  $5-50^\circ$ . The K<sup>+</sup> ion was detected by PerkinElmer atomic absorption spectrometer (AAS). The solid-state fluorescent spectra of ligands  $H_3$ pzdc, dpe, compounds 1-6, 1-4-SCN and 1-4-N<sub>3</sub> were measured by SHIMADZU RF-5301PC Spectrofluoro photometer.

# Preparation of compounds 1-6

{[Cu₂(pzdc)(dpe)₂]NO₃}<sub>n</sub> (1). The mixture solution of Cu(NO₃)₂·3H₂O (0.5 mmol, 0.1208 g), 1,2□-di(4-pyridyl)ethylene (0.5 mmol, 0.0911 g) and pyrazole-3,5-dicarboxylic acid (0.5 mmol, 0.0871 g) in ethanol (2 mL), DMF (2 mL) and H₂O (13 mL) was sealed in a 25 mL glass vial. The mixture was heated at 120 °C for 1 day and then slowly cooled down to room temperature. The blue crystals of 1 were obtained. Yield: 66 mg (37%) based on copper salt Anal. Calcd. for Cu₂C₂9H₂1NγOγ: C, 49.29; H, 3.00; N, 13.88. Found: C, 48.96; H, 3.10; N, 13.55%. ATR-FT-IR peaks ( $\nu$ (cm⁻¹)): 1613s ( $\nu$ (C=N)), 1558s ( $\nu$ (oCO)), 1505s, 1431w, 1395m ( $\nu$ (oCO)), 1338s ( $\nu$ (NO₃⁻)), 1219m, 1114w, 1055m, 1026m, 977m, 832s, 792m. UV-vis (diffuse reflectance, cm⁻¹): 15015.

 $\{[Cu_2(pzdc)(dpe)_2]ClO_4\}_n$  (2). The preparation of **2** was similar to that of **1**, except  $Cu(ClO_4)_2 \cdot nH_2O$  (0.5 mmol, 0.1853 g) replaced  $Cu(NO_3)_2 \cdot 3H_2O$ . The blue crystals of **2** were obtained. Yield: 112 mg (60%) based on copper salt. Anal.Calcd. for  $Cu_2C_{29}Cl\ H_{21}N_6O_8$ : C, 46.81; H, 2.84; N, 11.29. Found: C, 46.74; H, 2.62; N, 11.22%. ATR-FT-IR peaks ( $\nu(cm^{-1})$ ): 1610s ( $\nu(C=N)$ ), 1549s ( $\nu(C=N)$ ), 1501s, 1432m, 1388m ( $\nu(C=N)$ ), 1335s, 1287w, 1206m, 1089s ( $\nu(ClO_4)$ ), 1029m, 972m, 831s, 828w,792m. UV-vis (diffuse reflectance, cm<sup>-1</sup>): 14881.

Caution: Perchlorate salts are highly explosive and must be handled with care.

 $\{[Cu_2(pzdc)(dpe)_2]BF_4\}_n$  (3). The preparation of **3** was similar to that of **1**, except  $Cu(BF_4)_2 \cdot nH_2O$  (0.5 mmol, 0.1186 g) replaced  $Cu(NO_3)_2 \cdot 3H_2O$ . The blue crystals of **3** were obtained. Yield: 33 mg (18%) based on copper salt. Anal.Calcd. for  $Cu_2C_{29}BF_4H_{21}N_6O_4$ : C, 47.62; H, 2.89; N, 11.49. Found: C, 47.38; H, 2.76; N, 11.65%. ATR-FT-IR peaks ( $\nu(cm^{-1})$ ): 1611s ( $\nu(C=N)$ ), 1550s ( $\nu_{as}(OCO)$ ), 1502s, 1432m, 1389m ( $\nu_{s}(OCO)$ ), 1337s, 1289w, 1208m, 1053s ( $\nu(BF_4)$ ), 1026s, 970s, 832s, 790m. UV-vis (diffuse reflectance, cm<sup>-1</sup>): 14970.

 $\{[Cu_2(pzdc)(dpe)_2]SCN\}_n$  (4). The mixture solution of  $CuCl_2 \cdot 2H_2O$  (0.5 mmol, 0.0824 g), 1,2  $\Box$ -di(4-pyridyl)ethylene (0.5 mmol, 0.0911 g), pyrazole-3,5-dicarboxylic acid (0.5 mmol, 0.0871 g) and KSCN (0.5 mmol, 0.0486 g) in ethanol (2 mL), DMF (2 mL) and  $H_2O$  (13 mL) was sealed in a 25 mL glass vial. The mixture was heated at 120 °C for 1 day and then slowly cooled down to room temperature. The blue crystals of 4 were obtained.

Yield: 114 mg (65%) based on copper salt Anal. Calcd. for  $Cu_2C_{30}H_{21}N_7O_4S$ : C, 51.28; H, 3.01; N, 13.95. Found: C, 50.94; H, 3.09; N, 13.97%. ATR-FT-IR peaks ( $\nu$ (cm<sup>-1</sup>)): 2050m ( $\nu$ (SCN<sup>-</sup>)), 1612s ( $\nu$ (C=N)), 1552s ( $\nu$ <sub>as</sub>(OCO)), 1504s, 1430m, 1392m ( $\nu$ <sub>s</sub>(OCO)), 1338s, 1209m, 1112w, 1052m, 1011m, 968m, 829s, 793m. UV-vis (diffuse reflectance, cm<sup>-1</sup>): 15020.

 $\{[Cu_4Cu_4^I(pzdc)_4(dpe)_6](H_2O)_4\}_{2n}$  (5). The preparation of 5 was similar to that of 1, except  $CuSO_4 \cdot 5H_2O$  (0.5 mmol, 0.1248 g) replaced  $Cu(NO_3)_2 \cdot 3H_2O$ . The green crystals of 5 were obtained. Yield: 14 mg (10%) based on copper salt. Anal.Calcd. for  $Cu_8C_{92}H_{72}N_{20}O_{20}$ : C, 48.34; H, 3.17; N, 12.25. Found: C, 48.22; H, 3.28; N, 12.55%. ATR-FT-IR peaks ( $\nu(cm^{-1})$ ): 3274br ( $\nu(OH)$ ), 1595br (( $\nu(C=N)$ ) and  $\nu_{as}(OCO)$ ), 1500w, 1478m, 1413w, 1381m ( $\nu_{s}(OCO)$ ), 1292s, 1230m, 1064m, 1000m, 828s, 768(m). UV-vis (diffuse reflectance, cm<sup>-1</sup>): 14925.

 $\{[Cu_5(HPO_4)_2(pzdc)_2(dpe)_3](H_2O)_5\}_n$  (6). The preparation of **6** was similar to that of **1**, except  $Cu_3(PO_4)_2 \cdot 2H_2O$  (0.5 mmol, 0.2080 g) replaced  $Cu(NO_3)_2 \cdot 3H_2O$ . The purple crystals of **6** were obtained. Yield: 75 mg (52%) based on copper salt. Anal.Calcd. for  $Cu_5C_{46}H_{44}N_{10}O_{21}P_2$ : C, 38.04; H, 3.05; N, 9.64. Found: C, 37.72; H, 2.86; N, 9.70%. ATR-FT-IR peaks  $(\nu(cm^{-1}))$ : 3381br  $(\nu(OH))$ , 1636br  $(\nu(C=N))$ , 1609br  $(\nu_{as}(OCO))$ , 1504m, 1427m, 1393m  $(\nu_s(OCO))$ , 1327m, 1297m, 1208w, 1065br  $(\nu(HPO_4^{-2}))$ , 1000br  $(\nu(HPO_4^{-2}))$ , 921s, 833s, 781s. UV-vis (diffuse reflectance, cm<sup>-1</sup>): 14327.

# X-ray crystallography

The single-crystal X-ray data of 1-6 were collected at 298 K (except 1 was collected at 100 K) by using a Bruker D8 Quest PHOTON100 with graphite-monochromated MoKa radiation with the APEX2 program.<sup>24</sup> The data integration was done by SAINT<sup>25</sup> and the absorption correction was perfored by the SADABS<sup>26</sup>. The structure solution was solved by intrinsic phasing<sup>27</sup> and refined by the least-squares method on  $F^2$  with anisotropic thermal parameters for non-H atoms using the SHELXTL program.<sup>28</sup> The H atoms were assigned in calculated positions and isotropically refined. The disordered counteranions in 1-4 (NO<sub>3</sub> for 1, ClO<sub>4</sub> for 2, BF<sub>4</sub> for 3, and SCN for 4) locate on a crystallographic inversion center, so the occupancies of entire counteranions were refined to 0.5. The highly disordered SCN in 4 was isotropically refined. The disordered lattice water molecules were removed from the diffraction data for compounds 5 and 6 using the SQUEEZE instruction of PLATON software.<sup>29-31</sup> The total electron count removed per unit cell by SQUEEZE was 344 for 5 and 47 for 6. The number of electrons per molecule was 86 (Z' = 2, Z=4) and 47 (Z=1), which were assigned to eight and five water molecules in the formulas, respectively. The actual water molecules in the unit cell are further determined by the elemental analyses and thermogravimetric analyses (TGA). The crystal data, selected bond lengths, and angles for compounds **1–6** are shown in Tables 1 and S1.

Table 1. Crystallographic data for compounds 1-6.

| Compound                                      | 1                              | 2                          | 3   |
|---|--------------------------------|----------------------------|---|
| formula                                       | $Cu_{2}C_{29}H_{21}N_{7}O_{7}$ | $Cu_2C_{29}ClH_{21}N_6O_8$ | Cu <sub>2</sub> BC <sub>29</sub> F <sub>4</sub> H <sub>21</sub> N <sub>6</sub> O <sub>2</sub> |
| molecular weight                              | 706.61                         | 744.05                     | 731.41  |
| T(K)  | 100(2)                         | 298(2)                     | 298(2)  |
| crystal system                                | Orthorhombic                   | orthorhombic               | orthorhombic  |
| space group                                   | P nma                          | P nma                      | P nma   |
| a (Å)   | 12.4115(7)                     | 12.8632(8)                 | 12.7573(6)  |
| b (Å)   | 26.8057(16)                    | 26.6997(18)                | 26.7175(13)   |
| c (Å)   | 8.4121(5)                      | 8.4942(6)                  | 8.4773(3)   |
| $\alpha$ (deg)                                | 90                             | 90                         | 90  |
| $\beta$ (deg)                                 | 90                             | 90                         | 90  |
| γ (deg)                                       | 90                             | 90                         | 90  |
| $V(Å^3)$                                      | 2798.7(3)                      | 2917.3(3)                  | 2889.4(2)   |
| Z   | 4                              | 4                          | 4   |
| $\rho_{\rm cald}$ (g cm <sup>-3</sup> )       | 1.677                          | 1.694                      | 1.681   |
| $\mu$ (Mo K $\alpha$ ) (mm <sup>-1</sup> )    | 1.582                          | 1.613                      | 1.546   |
| data collected                                | 3145                           | 3055                       | 3659  |
| unique data $(R_{int})$                       | 2409(0.0612)                   | 2031(0.0846)               | 2168(0.1181)  |
| $R_1^a / wR_2^b [I > 2\sigma(I)]$             | 0.0511/0.0926                  | 0.0769/0.1887              | 0.0724/0.1431   |
| $R_1^a / wR_2^b$ [all data]                   | 0.0810/0.1004                  | 0.1356/ 0.2085             | 0.1509/0.1683   |
| GOF   | 1.129                          | 1.189                      | 1.050   |
| max/min electron density (e Å <sup>-3</sup> ) | 0.650/-0.755                   | 0.768/ -1.118              | 0.824/-0.950  |

**Table 1.** Crystallographic data for compounds **1-6**. (Cont.)

| Compound   | 4                               | 5                                   | 6  |
|--|---------------------------------|-------------------------------------|--|
| formula  | $Cu_{2}C_{30}H_{21}N_{7}O_{4}S$ | $Cu_{16}C_{184}H_{128}N_{40}O_{40}$ | Cu <sub>5</sub> C <sub>46</sub> H <sub>34</sub> N <sub>10</sub> O <sub>16</sub> P <sub>2</sub> |
| molecular weight                                 | 702.68                          | 4427.90                             | 1362.67  |
| T(K)   | 298(2)                          | 298(2)                              | 298(2)   |
| crystal system                                   | orthorhombic                    | Monoclinic                          | triclinic  |
| space group                                      | P nma                           | P 21/n                              | P -1   |
| a (Å)  | 12.7346(9)                      | 16.3570(7)                          | 9.8788(4)  |
| b (Å)  | 26.731(2)                       | 26.4808(12)                         | 11.1243(4)   |
| c (Å)  | 8.4383(6)                       | 21.4340(9)                          | 13.8420(6)   |
| $\alpha$ (deg)                                   | 90                              | 90                                  | 69.7760(10)  |
| $\beta$ (deg)                                    | 90                              | 93.7730(10)                         | 79.7190(10)  |
| γ (deg)  | 90                              | 90                                  | 64.4060(10)  |
| $V(\mathring{A}^3)$                              | 2872.4(4)                       | 9263.9(7)                           | 1286.56(9)   |
| Z  | 4                               | Z'=2                                | 1  |
| $\rho_{\rm cald}$ (g cm <sup>-3</sup> )          | 1.625                           | 1.587                               | 1.759  |
| $\mu$ (Mo K $\alpha$ ) (mm <sup>-1</sup> )       | 1.604                           | 1.876                               | 2.175  |
| data collected                                   | 2886                            | 18998                               | 5294   |
| unique data $(R_{int})$                          | 1755(0.0905)                    | 10197 (0.1063)                      | 3845(0.0470)   |
| $R_1^a / w R_2^b [I > 2\sigma(I)]$               | 0.0687/0.1630                   | 0.0634/0.1152                       | 0.0416/0.0801  |
| $R_1^a / wR_2^b$ [all data]                      | $0.1394/\ 0.1944$               | 0.1516/0.1417                       | 0.0728/0.0903  |
| GOF  | 1.055                           | 1.002                               | 1.011  |
| max/min electron<br>density (e Å <sup>-3</sup> ) | 1.578/ -0.883                   | 1.513/-0.853                        | 0.711/-0.560   |

# Anion exchange experiments

The anion-exchange experiments were performed with compounds **1–4**. A 20 mg of powder sample was placed into saturated aqueous solution (5 mL) of NaNO<sub>3</sub>, NaClO<sub>4</sub>, NaBF<sub>4</sub>, NaN<sub>3</sub>, or KSCN and constantly stirred at ambient temperature for 1 day. Then, the solid sample was collected by filtration, washed with 50 mL of deionized water, and dried in air for 1 day. The solid product was characterized by IR and UV-Vis spectroscopy, and PXRD. The occurrence of anion exchange was verified by comparison of the characterization data with those of **1-4**. For **1-SCN**, IR (cm<sup>-1</sup>): v(CN) 2105; v(NO<sub>3</sub>) 1338. UV-vis (cm<sup>-1</sup>): 15060. For **2-SCN**, IR (cm<sup>-1</sup>): v(CN) 2102; v(ClO<sub>4</sub>) 1089. UV-vis (cm<sup>-1</sup>): 14970. For **3-SCN**, IR (cm<sup>-1</sup>): v(CN) 2103; v(BF<sub>4</sub>) 1051. UV-vis (cm<sup>-1</sup>): 15015. For **4-SCN**, IR (cm<sup>-1</sup>): v(CN) 2050 and 2106. UV-vis (cm<sup>-1</sup>): 15037. For **1-N<sub>3</sub>**, IR (cm<sup>-1</sup>): v(N<sub>3</sub>): 2069. UV-vis (cm<sup>-1</sup>): 16367 and 13458. For **3-N<sub>3</sub>**, IR (cm<sup>-1</sup>): v(N<sub>3</sub>): 2064. UV-vis (cm<sup>-1</sup>): 16077 and 13123. For **4-N<sub>3</sub>**, IR (cm<sup>-1</sup>): v(N<sub>3</sub>): 2069. UV-vis (cm<sup>-1</sup>): 15870.

#### Results and discussion

## General observations and spectroscopic techniques

Compounds **1-6** were obtained by the solvothermal reactions of  $H_3pzdc$ , dpe and many copper(II) salts under the same conditions. Compounds **1-4** are isostructural and exhibit 3D pillar-layered cationic frameworks, interspersed with lattice monoanions within the channels. Each lattice anions is surrounded by four  $\mu_2$ -dpe pillar-linkers with a variety of torsion angles, depending on a kind of counteranion. Compound **5** shows a neutral mixed-valence Cu(I, II) 2D interpenetrated network without the sulfate anion in the lattice. In contrast, compound **6** shows 3D coordination framework containing coordinated  $\mu_4$ -hydrogenphosphate anion. The different structural frameworks of all compounds indicate the significant role of anions on the self-assembly.

The ATR-IR spectra of **1-6** (Figure S2 and S3) reveal the strong intensity peak around 1610 cm<sup>-1</sup> which can be assigned to the stretching vibrations of the pyridine ring. The peaks around approximately 1600-1400 cm<sup>-1</sup> correspond to the asymmetric and symmetric stretching vibrations of the carboxylate group for the pzdc ligand.<sup>32</sup> The IR spectra of **1-4** show a characteristic strong peak for each counteranion at 1338 cm<sup>-1</sup> ( $\nu$ (NO<sub>3</sub>) in **1**),<sup>13</sup> 1089 cm<sup>-1</sup>( $\nu$ (ClO<sub>4</sub>) in **2**),<sup>14</sup> 1053 cm<sup>-1</sup> ( $\nu$ (BF<sub>4</sub>) in **3**)<sup>33</sup> and 2050 cm<sup>-1</sup> ( $\nu$ (SCN) in **4**)<sup>34</sup>. The IR spectrum of **6** shows medium peaks in the range of 1100-1000 cm<sup>-1</sup> corresponding to the vibration of phosphate anion. The broad peaks around 3600-3200 cm<sup>-1</sup> in **5** and **6** are assigned to  $\nu$ (OH) from the water molecules. The solid-state UV-Vis spectra of **1-6** were studied at room temperature (Figure S5). All compounds exhibit a single broad absorption band around 15200-14300 cm<sup>-1</sup> which correspond to distorted octahedral and square pyramidal geometries for Cu(II).<sup>35, 36</sup>

## **Description of crystal structures**

## Crystal structures of $\{[Cu_2(pzdc)(dpe)_2]X\}_n(X = NO_3^-(1), ClO_4^-(2), BF_4^-(3), SCN^-(4)\}$

Single-crystal analysis revealed that compounds 1-4 are isostructural and they crystallize in the orthorhombic Pnma space group. The crystal structure of 1 is described detail herein. There are two crystallographically independent Cu(II) centers (Cu1 and Cu2) located on a crystallographic mirror plane. The Cu1 ion is five-coordinated, adopting a square pyramidal geometry ( $\tau = 0.01$  for 1,  $\tau = 0.12$  for 2,  $\tau = 0.09$  for 3,  $\tau = 0.08$  for 4, Addison's parameter  $\tau =$ 0 for square pyramid and  $\tau = 1$  for trigonal bipyramid).<sup>37</sup> Each Cu1 center is coordinated by two carboxylate oxygen atoms (O1, O3) from two different pzdc<sup>3</sup>- ligands and two pyridine nitrogen atoms from two  $\mu_2$ -dpe in the equatorial plane. The axial position is occupied by a pyrazole nitrogen atom (N4). The central Cu2 is six-coordinated adopting an elongated octahedral geometry. The basal plane is occupied by one carboxylate oxygen atom from pzdc<sup>3-</sup>, one pyrazole nitrogen atom from another pzdc<sup>3-</sup> and two pyridyl nitrogen atoms from two  $\mu_2$ -dpe. The apical position is located by two carboxylate oxygen atoms from two distinct pzdc<sup>3-</sup> (O1, O2) (Figure 1). The Cu-N and Cu-O distances are in the range of 1.949(4)-2.173(4) Å, while the elongated axial Cu2-O distances are 2.305(4) and 2.425(4) Å, indicating the presence of a common Jahn-Teller effect in the Cu(II) ion. 20, 38 The Cu1N<sub>2</sub>O<sub>2</sub> plane is not totally planar with tetrahedral distortion between the planes of 20.71° (26.88° for **2**, 25.62° for **3**, 24.94° for **4**). The Cu1 is shifted by 0.259(1) Å (0.324(2) Å for 2, 0.316(2) Å for 3, 0.306(2) Å for 4) from the mean equatorial plane toward the axial position. Pzdc<sup>3</sup>-

connects the Cu1 and Cu2 ions in a  $\mu_5$ - $\eta^1$ O,  $\eta^2$ N',O',  $\eta^2$ N'',O'',  $\eta^1$ O''' coordination mode (Figure S1) to form two-dimensional (2D) cationic Cu(II) layered coordination polymer in ac crystallographic plane. The layer consists of 13-membered macrocycle enclosed by three Cu(II) ions and four pzdc<sup>3-</sup> with the closest Cu···Cu distance of 3.914 (1) Å (Figure 2). Also, the  $\mu_2$ -dpe spacers connect adjacent layers along b crystallographic axis constructing a 3D cationic pillar-layer coordination framework (Figure 4). The two pyridine rings of bipyridyl moieties are not coplanar with the dihedral angle between the two planar pyridine rings of 5.06° (3.20° for 2, 2.23° for 3, 2.00° for 4). The C-CH=CH-C torsion angle of  $\mu_2$ dpe is 178.25-179.62° for **1-4**. The Cu···Cu separation via  $\mu_2$ -dpe is 13.418(1) Å for **1** (13.388) (1) Å for **2**, 13.391(1) Å for **3**, and 13.400(1) Å for **4**). The 3D cationic framework of **1** contains a 1D open-channel along c axis which is occupied by disordered  $NO_3$  lattice anion (Figure 3). The dimension of the channel in ab plane is about 3.95 x 13.42  $\text{Å}^2$  (4.65 x 13.39  $\text{Å}^2$ for 2, 4.49 x 13.39 Å<sup>2</sup> for 3, and 4.45 x 13.40 Å<sup>2</sup> for 4). Besides electrostatic interaction between the cationic framework and anionic guest, the weak intermolecular hydrogen bonds involving C-H of  $\mu_2$ -dpe linker and lattice anion also stabilize an entire supramolecular frameworks of 1-3 (Figure 4, Table S2).

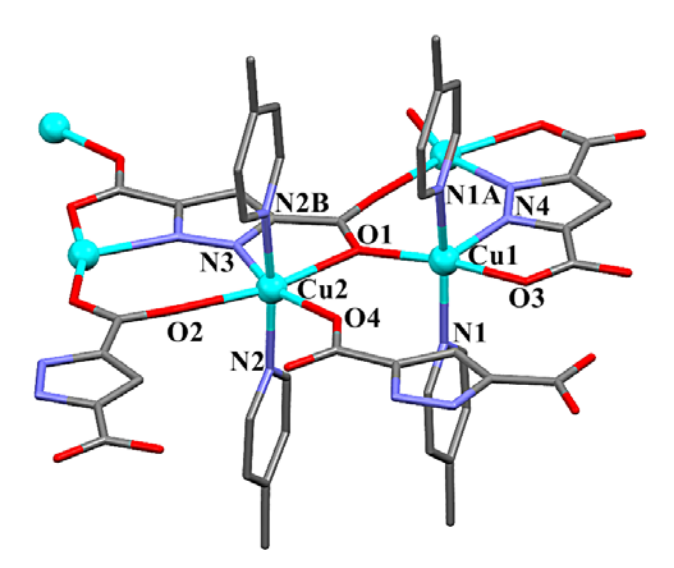


**Figure 1.** Crystal structure and atom labeling scheme of **1**. All hydrogen atoms and lattice nitrate anion are omitted for clarity (symmetry code: A = x, 0.5-y, z; B = 1-x, -0.5+y, 1-z).

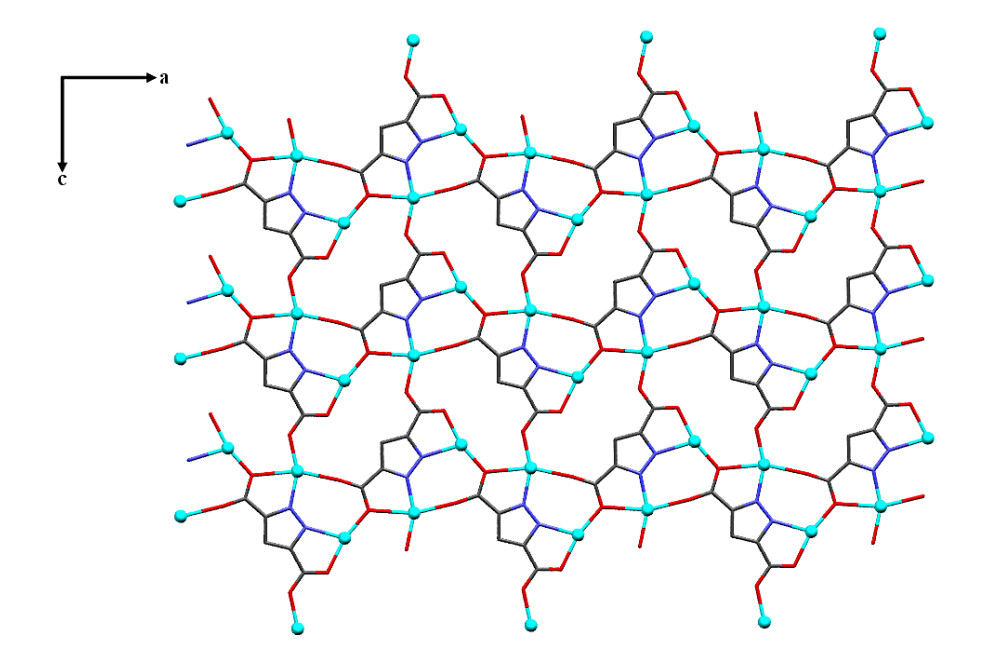


**Figure 2.** The 2D layer of 1 in the ac plane constructed by Cu(II) ions and  $\mu_5$ -pzdc<sup>3</sup>.

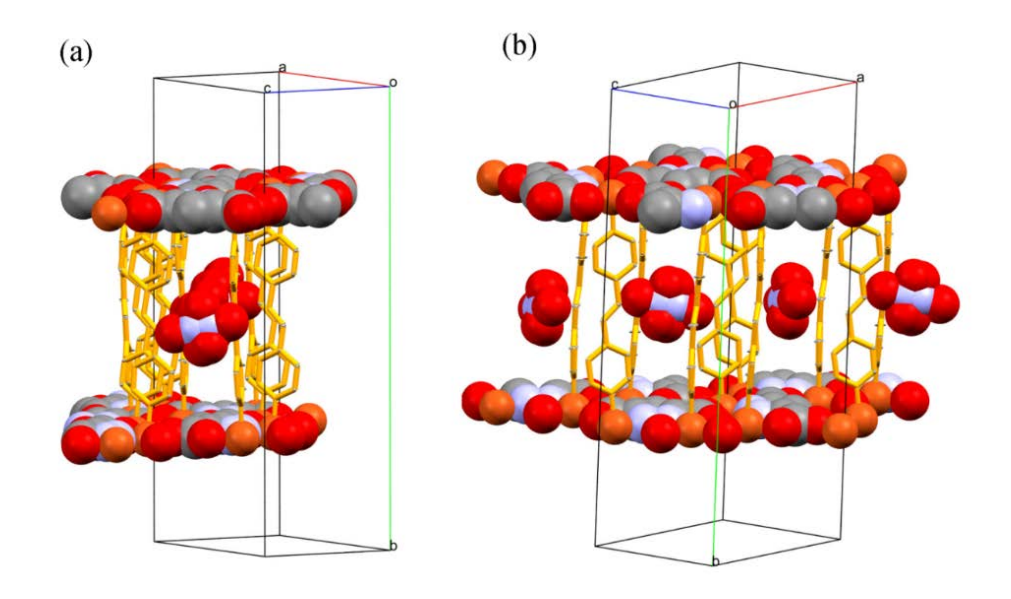


**Figure 3.** The space-filling model of disordered NO<sub>3</sub> anions incorporated into the 1D open-channel of the 3D cationic framework of **1** in different views.

## Crystal structure of $\{[Cu_4(I)Cu(II)_4(pzdc)_4(dpe)_6](H_2O)_4\}_{2n}$ (5)

Single-crystal analysis revealed that compound **5** crystallizes in the monoclinic,  $P2_1/n$  space group. The asymmetric unit of **5** contains four Cu(II) ions (Cu1-Cu4), four Cu(I) ions (Cu5-Cu8), four pzdc<sup>3-</sup>, six dpe ligands and four lattice water molecules. All monovalent copper atoms are three-coordination completed by one carboxylate oxygen atom from pzdc<sup>3-</sup> and two pyridyl nitrogen atoms from two different  $\mu_2$ -dpe. The Cu(I)–N and Cu(I)–O

distances are in the ordinary range among 1.901(4)-2.345(4) Å. 39, 40 While all divalent copper atoms display square pyramidal geometry ( $\tau = 0.02-0.05$ ) which are coordinated by two carboxylate oxygen atoms and two pyrazoyl nitrogen atoms from two pzdc3- in the basal plane, the axial position is occupied by one nitrogen atom from  $\mu_2$ -dpe. The Cu(II)–N and Cu(II)-O distances are in the range of 1.921(4)- 2.264(4) Å. <sup>20, 38</sup> The CuN<sub>2</sub>O<sub>2</sub> square base is not totally planar with tetrahedral twist between the planes of 23.29°, 22.83°, 24.77°, and 23.60° for Cu1-Cu4, respectively. The Cu(II) is shifted by 0.306(1) Å, 0.298(1) Å, 0.324(1) Å, and 0.310(1) Å from the mean equatorial plane toward the axial site for Cu1-Cu4, respectively. The calculation of the bond valence sum (BVS) for copper centers in 5 was also performed using the Cu-X bond constants derived previously (see the Supporting Information). 41-43 The BVS analysis resulted in the values of 2.10, 2.14, 2.11, 2.11 for Cu1-Cu4, respectively, and 0.93, 0.94, 0.94, and 0.93 for Cu5-Cu8, respectively, thus confirming the formal oxidation states of +2 for Cu1-Cu4 and +1 for Cu5-Cu8 ions. Two pzdc<sup>3-</sup> ligands bind two Cu(II) ions, giving dinuclear Cu(II) unit with Cu···Cu separations of 3.957(1) and 3.950(1) Å. Each dinuclear Cu(II) unit is connected via double  $\mu_2$ -dpe spacers with Cu···Cu separation of 13.876(1) and 13.891(1) Å, forming tetranuclear Cu(II) unit. Each tetranuclear Cu(II) unit consists of two [Cu(II)<sub>2</sub>(pzdc)<sub>2</sub>]<sup>2-</sup> conformations as A and B forms (Figure 5). In the case of A form, the dinuclear Cu(II) unit adopts cis-conformation for two carboxylate bridges which are connected to two Cu(I) centers in  $\mu_3$ - $\eta^2$ N,O,  $\eta^2$ N',O',  $\eta^1$ O''-pzdc<sup>3-</sup> bridging mode (Figure S1). For B form, the dinuclear Cu(II) unit adopts trans-conformation for two carboxylate bridges which is linked two Cu(I) centers through two pzdc<sup>3-</sup> in  $\mu_3$ - $\eta^2$ N,O,  $\eta^2 N', O', \eta^1 O''$  and  $\mu_3 - \eta^2 N, O, \eta^2 N', O', \eta^1 O'$  modes (Figure S1). Moreover, each 3-connected Cu(I) center links with two neighboring Cu(I) centers via two  $\mu_2$ -dpe and also connects with a tetranuclear Cu(II) unit giving rise to mixed-valence Cu(I)-Cu(II) two-dimensional coordination layer (Figure 6a). The C-CH=CH-C torsion angle of  $\mu_2$ -dpe spacers is in the range of 176.29-179.30°. Furthermore, two adjacent layers are interpenetrated to form a twofold  $2D \rightarrow 2D$  parallel interpenetrating network as shown in Figure 6b.

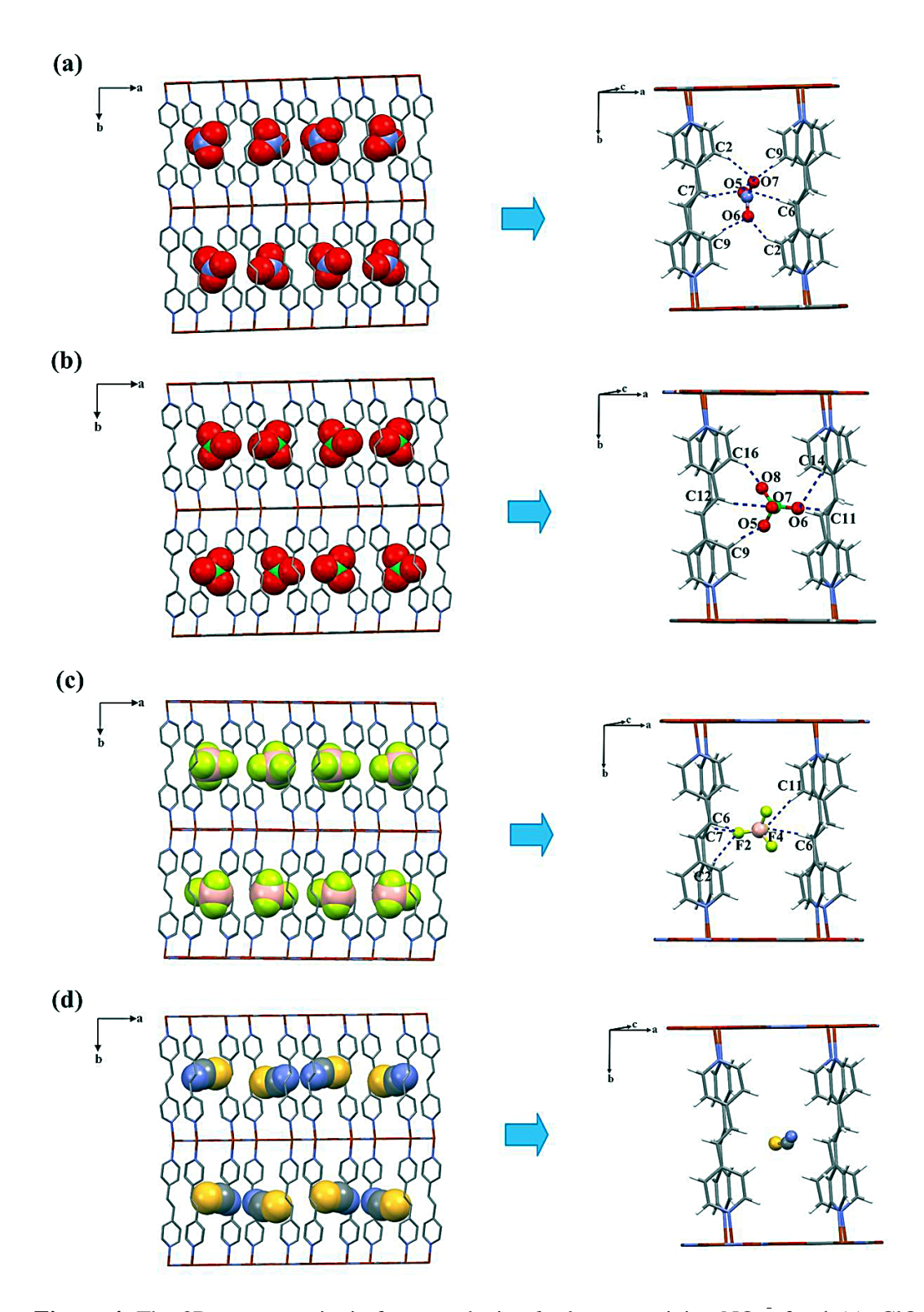


**Figure 4.** The 3D porous cationic frameworks in ab plane containing  $NO_3$  for **1** (a),  $ClO_4$  for **2** (b),  $BF_4$  for **3** (c), and SCN for **4** (d) in the pores. The insets present the weak hydrogen bonds between C–H of dpe linker and lattice anions. The disordered positions of all anions are omitted for clarity.

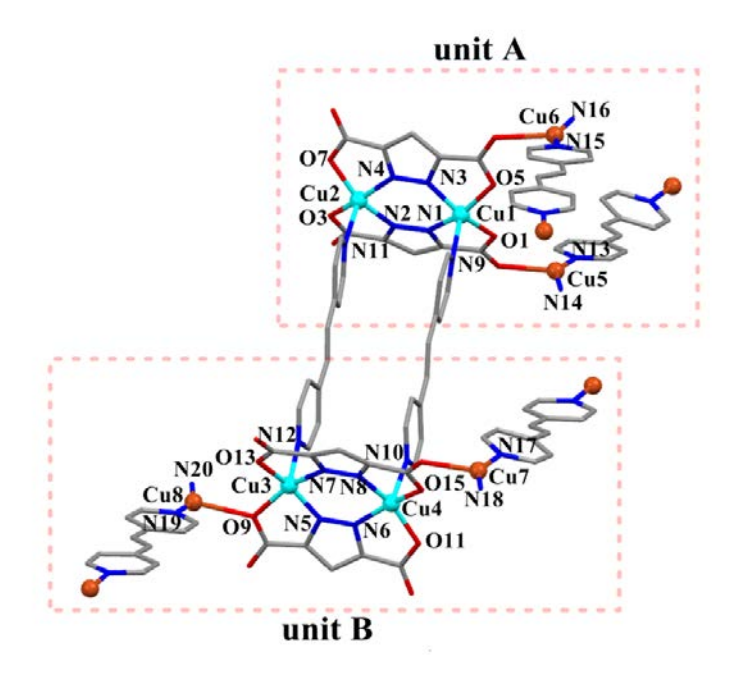


**Figure 5.** View of the coordination environments of Cu(I) and Cu(II) ions in **5** with atom labels. All hydrogen atoms are omitted for clarity.

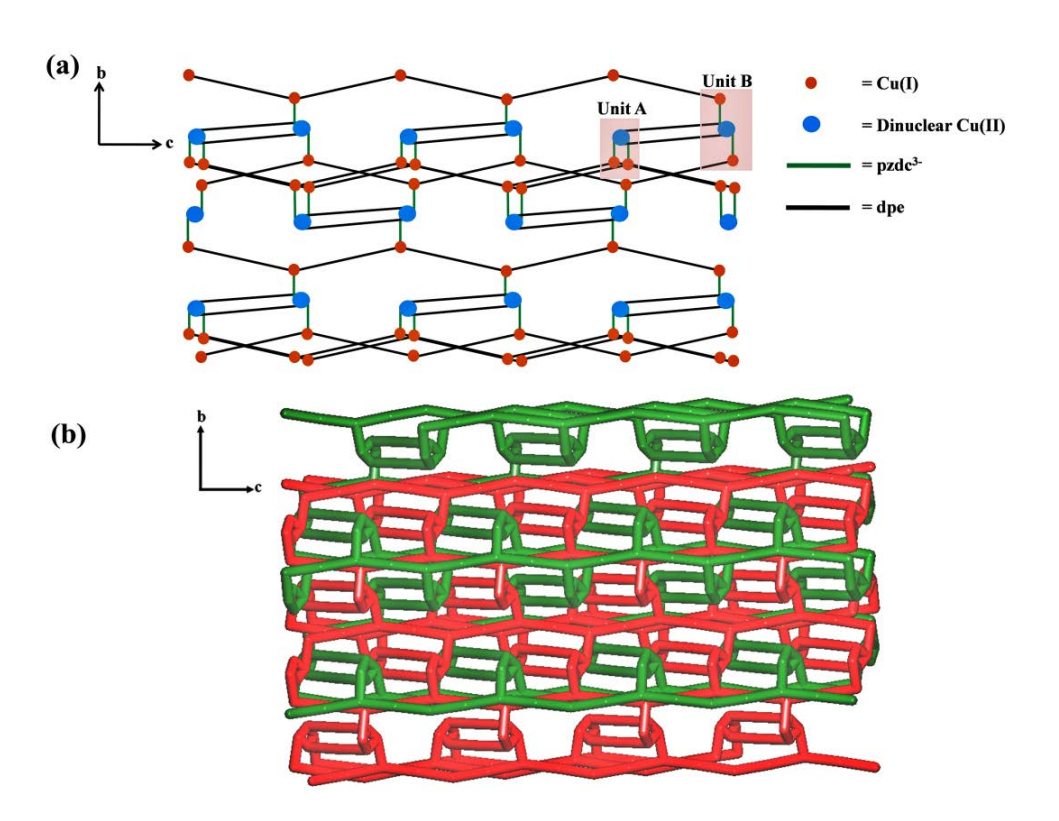


**Figure 6.** (a) The mixed-valence Cu(I, II) 2D coordination polymer of **5** in bc plane. (b) The two-fold 2D  $\rightarrow$  2D parallel interpenetrated network of **5**.

## Crystal structure of $\{[Cu_5(HPO_4)_2(pzdc)_2(dpe)_3](H_2O)_5\}_n$ (6)

Compound 6 crystallizes in the triclinic P-1 space group. The asymmetric unit contains three crystallographically independent Cu(II) ions, one Hpzdc<sup>2</sup>-, one-half of dpe ligands, one hydrogenphosphate, five lattice water molecules. The coordination environment of Cu(II) centers is shown in Figure 7. The Cu1 center exhibits a square pyramidal geometry  $(\tau = 0.15)$ , coordinated by one carboxylate oxygen, one pyrazoly nitrogen atom from pzdc<sup>3</sup>-, one hydrogenphosphate oxygen (O5), and one pyridyl nitrogen from  $\mu_2$ -dpe in a basal position. The axial site is occupied by an oxygen from another HPO<sub>4</sub><sup>2</sup>. The Cu1N<sub>2</sub>O<sub>2</sub> square plane is not totally planar with tetrahedral distortion between the planes of 9.87°. The Cu1 is shifted by 0.010(1) Å from the mean equatorial plane toward the axial position. The Cu2 is four-coordinated with a square planar geometry ( $\tau_4 = 0.20$ , four-coordinate geometry index  $\tau_4$ = 0 for a perfect square planar and  $\tau_4$  = 1 for a perfect tetrahedron). <sup>44, 45</sup> The copper(II) center is completed by one carboxylate oxygen and one pyrozoly nitrogen atom from pzdc<sup>3</sup>-, oxygen from  $HPO_4^{2-}$  and one pyridyl nitrogen from  $\mu_2$ -dpe. The  $Cu2N_2O_2$  square base is not completely planar with tetrahedral distortion between the planes of 16.69°. The Cu3 center lies on a crystallographic inversion center and adopts perfect square planar geometry which is bonded with two pyridyl nitrogen from  $\mu_2$ -dpe and two oxygen atoms from two different HPO<sub>4</sub><sup>2-</sup>. The Cu–N and Cu–O distances are in the range of 1.890(3)-2.382(2) Å. The Cu1 and Cu2 ions are connected by  $\mu_2$ - $\eta^2$ N,O,  $\eta^2$ N',O'-pzdc<sup>3-</sup> (Figure S1) forming a Cu(II) dimer with Cu···Cu separation of 4.315(1) Å. Then, two hydrogenphosphate anions connect two adjacent dinuclear Cu(II) units and two Cu3 centers generating a 1D chain of Cu3-HPO<sub>4</sub>-[Cu1Cu2]<sub>2</sub>-HPO<sub>4</sub> along crystallographic b axis (Figure 8a). Moreover, each 1D chain of 6 is linked together by six  $\mu_2$ -dpe spacers in a different direction to generate 3D framework as shown in Figure 8b (Figure S4).

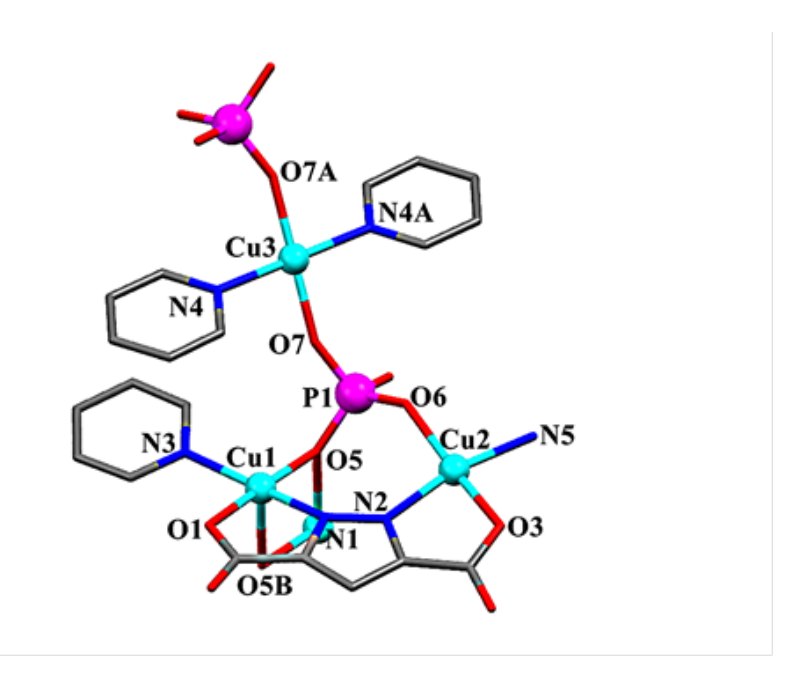


**Figure 7.** The coordination environments of Cu(II) ions in **6**. All hydrogen atoms are omitted for clarity (symmetry code: A = -x, 1-y, 1-z; B = -x, 2-y, 1-z).

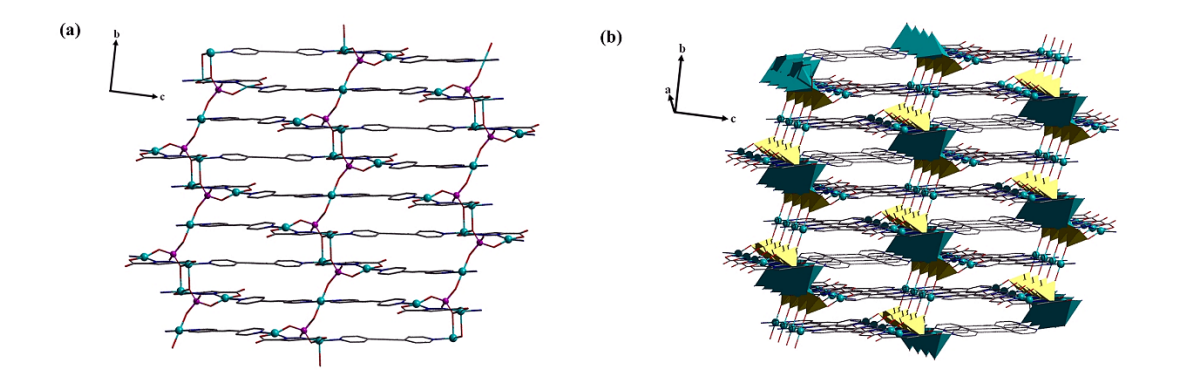


**Figure 8.** (a) View of a 2D layer of **6** in bc plane. (b) The 3D framework of **6.** The yellow and blue polygons represent HPO<sub>4</sub><sup>2-</sup> and Cu(II) centers, respectively.

## Thermal analyses

Thermogravimetric analysis (TGA) of all compounds except compound **2** were performed in the  $N_2$  atmosphere from 30-750 °C. Compound **2** contains perchlorate anion which may be the potential for an explosion at high temperature. The isostructures of **1-4** are stable up to about 300 °C. Then the structures are collapsed. Compounds **5** shows a gradual weight loss of 3.2% from 30-260 °C corresponding to the escape of eight water molecules (calcd. 3.2%). Then the structure is decomposed. Compound **6** reveals gradual weight loss of 6.0% in the range of 30-280 °C corresponding to the release of five water molecules (calcd. 6.2%). Then the structures decompose to  $[Cu_3(PO_4)_2]_2$  (found, 54.0%, calcd. 52.4%) (Figure S6).

## Anion exchange studies and SCN sorption of 1-4

As demonstrated by the X-ray structures, the counteranions (NO<sub>3</sub> (1), ClO<sub>4</sub> (2), BF<sub>4</sub> (3) and SCN (4)) are occupied within the 1D channel of the 3D pillar-layered cationic frameworks of 1-4. In addition, compounds 1-4 are insoluble in common organic solvents and water. Consequently, these metal organic frameworks are potentially expected to exhibit anion exchange properties. The anion exchange of 1-4 were verified by IR and UV-Vis reflectance spectra and X-ray powder diffraction (PXRD). When a suspension of crystalline powder of 1 in a saturated aqueous solution of KSCN was stirred continuously for 1 day at room temperature, the blue color of crystalline solid was changed to greenish blue. The IR spectrum of 1-SCN (Figure 9) shows the identical intensity and position of original v(NO<sub>3</sub><sup>-</sup>) at 1338 cm<sup>-1</sup> along with increasing peak intensity at 2105 cm<sup>-1</sup>, that is an indication of v(CN)of thiocyanate. The UV-Vis reflectance spectrum of 1-SCN shows broad absorption band around 15060 cm<sup>-1</sup> which is slightly blue-shifted in comparison to those of 1 implying that the coordination environment around Cu(II) ions are varied (Figure S8). The PXRD pattern of 1-**SCN** (Figure 10) is identical to that of 1 which could be evidence for nonstructural transformation during the exchange process. In contrast, the NO<sub>3</sub> in 1 could not be exchanged by ClO<sub>4</sub> and BF<sub>4</sub> anions that were confirmed by IR spectra.

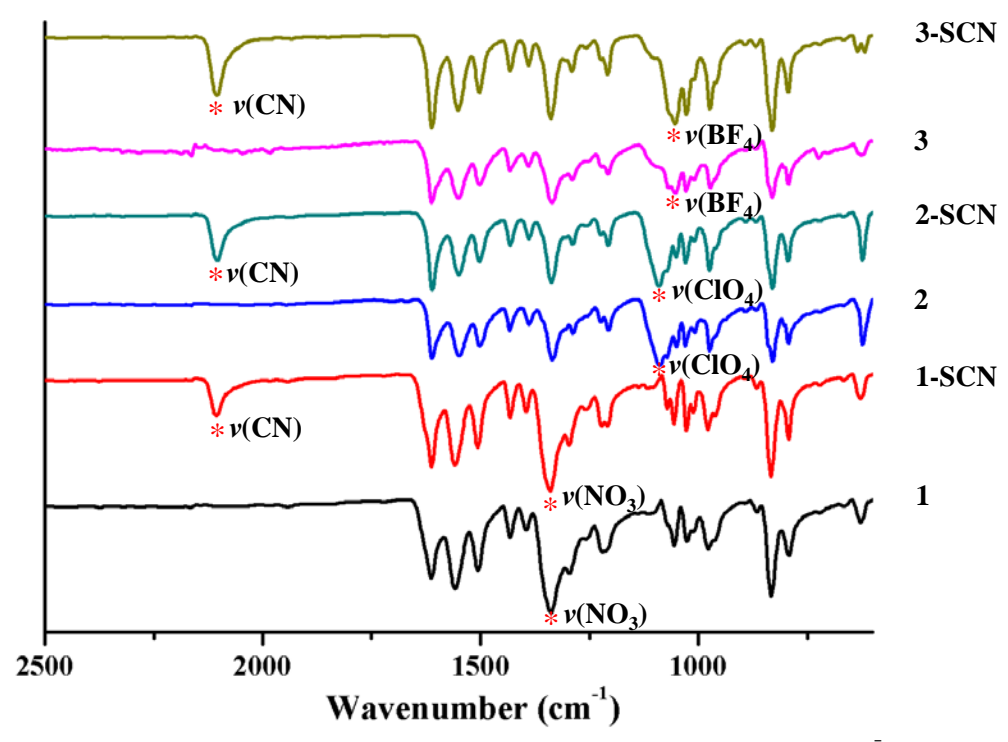


**Figure 9.** IR spectra of the anion exchange products with SCN anion.

The above anion exchange procedure can be extended to other anions. When the blue crystalline solids of 2-3 were continuously stirred in a saturated aqueous solution of KSCN for 1 day, their colors of were also changed to greenish blue. The IR spectra (Figure 9) for the products of exchange also show the original peaks of v(ClO<sub>4</sub>) at 1089 cm<sup>-1</sup> for 2, and v(BF<sub>4</sub>) at 1051 cm<sup>-1</sup> for 3 and the appearance of new peaks at 2100 cm<sup>-1</sup>, being as same as 1-SCN. The UV-Vis reflectance spectra of 2-3-SCN exhibit blue-shifted absorption bands around 14970-15015 cm<sup>-1</sup> (Figure S8). The PXRD patterns of 2-3-SCN confirm that their crystallinities are still the same as original crystalline phase during anion exchange process (Figure 10). In contrast, the ClO<sub>4</sub> in 2 is not exchanged by both NO<sub>3</sub> and BF<sub>4</sub> anions, as well as the BF<sub>4</sub> in 3 is not exchanged by NO<sub>3</sub> and ClO<sub>4</sub>. Inversely, crystalline solids 1-3-SCN, and compound 4 cannot be replaced by other anions. According to the IR spectroscopic data that is used widely to monitor anion exchange, they reveal that the intensity of the vibrational peak of original counteranion within the framework is not decreased after anion exchange process, but the new peak of v(CN) around 2100 cm<sup>-1</sup> appears. It indicates that isostructures 1-3 exhibit the sorption properties of SCN anion without any anion exchange process. To confirm the sorption of thiocyanate anion in these isostructural series, compound 4 which contains lattice SCN within the porous, was constantly stirred in a saturated aqueous solution of KSCN under the same condition. Interestingly, the IR spectrum of 4-SCN exhibits two characteristic peaks of v(CN). The new one appears at 2100 cm<sup>-1</sup> and the original one is at 2053 cm<sup>-1</sup> (Figure S7). The first peak of v(CN) that is identically found in those of 1-3-SCN indicates Cu-SCN, thiocyanato complexes (2100-2120 cm<sup>-1</sup>)<sup>46, 47</sup> whereas those peaks of lattice SCN anions exhibit v(CN) at 2053 cm<sup>-1</sup>. 34, 47 The crystalline phase of **4-SCN** is identical to that of 4 which is verified by PXRD. The above results imply that isostructures 1-4 display chemisorption of thiocyanate without destruction of their crystalline framework. Moreover, to balance the charge of overall frameworks during chemisorption of thiocyanate

anion, we used the atomic absorption spectroscopy (AAS) for detection of K<sup>+</sup> ions in **1-4-SCN**. The observed K<sup>+</sup> amount in analytes is 0.13-0.16 mol K<sup>+</sup> per mol **1-4**. The observed small amount of K<sup>+</sup> in **1-4-SCN** suggests that the chemisorption of SCN may occur on the surface of 3D frameworks of **1-4** which agree with no observed solvent accessible voids for **1-4**, calculated by PLATON program. The chemisorption of SCN may be attributed to the unsaturated 5-coordination Cu(II) center in **1-4** may play a crucial role on chemisorption of SCN without the collapse of their crystalline frameworks.

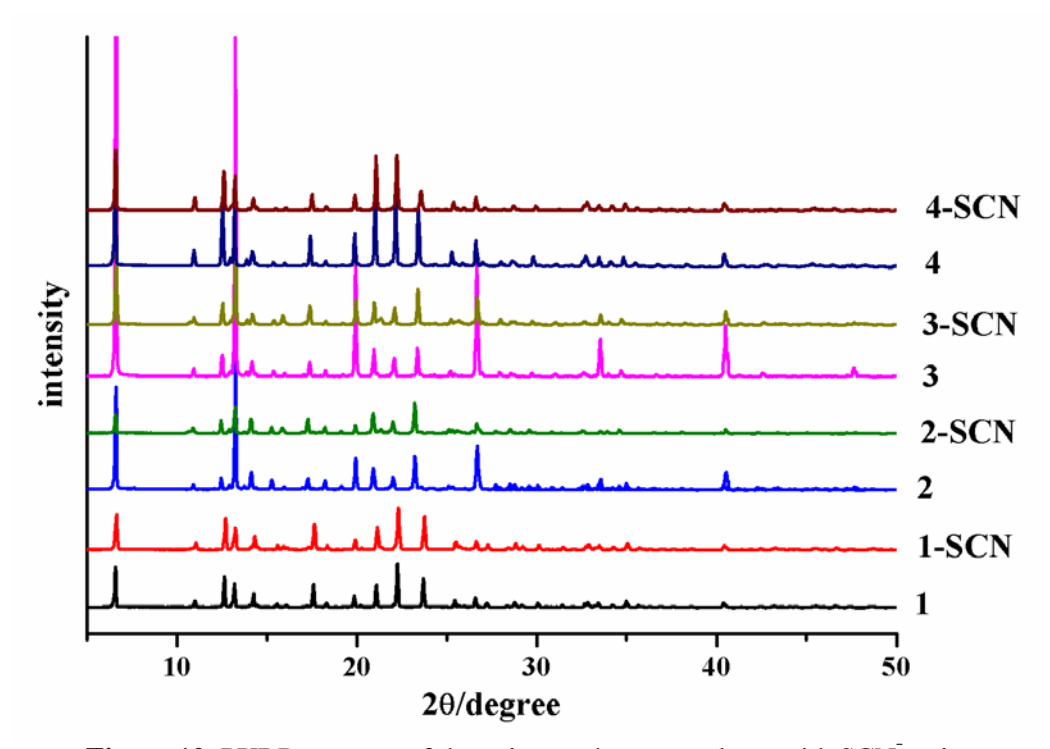


**Figure 10.** PXRD patterns of the anion exchange products with SCN anion.

To further study the effect of the stronger coordinating ability of the anion, the  $N_3$ was used to examine anion exchange properties in 1-4. The IR spectra for 1-4-N<sub>3</sub> show the disappearance of an intense peaks of  $v(NO_3)$ ,  $v(ClO_4)$ ,  $v(BF_4)$  and v(CN) for 1-4, respectively, and exhibit the growth of a new  $N_3$  peak at 2070 cm<sup>-1</sup> (Figure S9). <sup>12,48</sup> The UV-Vis reflectance spectra of 1-4-N<sub>3</sub> show blue-shifted absorption bands around 16367-15870 cm<sup>-1</sup> which is agreement with the alteration of color from blue to green (Figure S10). Moreover, none of 1-4-N<sub>3</sub> contains any number of Na<sup>+</sup> ions that was verified by AAS, confirming that the exchange process undergoes in the samples. The PXRD patterns of 1-4- $N_3$  are different to those of the original 1-4 implying the anion-induced structural transformation (Figure S11). The resulting IR spectra and PXRD of exchanged products differ significantly from that of the original compounds, suggesting that it is not only the original ions quantitatively displaced by the N<sub>3</sub> but also the solid-state topology fully changes. It seems that the variation of their structures upon anion exchange may be related to the coordinating ability of the different anions. Therefore, the exchange of lattice anion by strong coordinating anion can produce the structural change. Notably, both the sorption of SCN and anion-exchange of N<sub>3</sub> mentioned above are an irreversible process which may involve the dissociation of Cu(II)-SCN or Cu(II)-N<sub>3</sub> bonds. Therefore, they cannot be easily exchanged by other weak coordinating anions.

## Fluorescent properties

The solid-state emission spectra at room temperature of compounds 1-6, chemisorption samples 1-4-SCN, exchanged samples 1-4-N<sub>3</sub>, H<sub>3</sub>pzdc, and dpe ligands have been investigated. The free ligand dpe displays the strong emission peak at 368 nm and the small one at 509 nm ( $\lambda_{ex} = 320$  nm) whereas the H<sub>3</sub>pzdc displays two insignificant emission peaks at 368 and 472 nm ( $\lambda_{ex} = 285$  nm) (Figure S12). The emission behavior of the ligands can be assigned to  $\pi^* \to \pi$  and  $\pi^* \to n$  transitions. Upon excitation of solid samples 1-6 and 1-4-SCN at 320 nm, they exhibit two emission bands with the main peak at 468 nm and the minor peak at about 362-370 nm (Figure S12). In comparison with the dpe ligand, the emission intensity of all compounds shows quenching phenomena at 368 nm. However, the enhancement of the intensity around 468 nm was observed. The luminescent behavior may probably ascribe to the ligand-to-ligand charge transfer (LLCT) and/or ligand-to-metal charge transfer (LMCT). 49-54 Some differences in the emission intensity in 1-6 may relate to the distinct structures, coordination environments, and the counteranions. The emission intensity of chemisorption samples 1-4-SCN are slightly increased comparing with 1-4 (Figure S13), that may be attributed from the distinct copper(II) geometry and the adsorption of KSCN. In contrast to the emission spectra of exchanged samples 1-4-N<sub>3</sub>, they exhibited slightly shifted and quenching emission peaks which also confirm the structural transformation when exchanging by an azide anion.

## **Conclusions**

By the solvothermal reaction of different starting Cu(II) salts, H<sub>3</sub>pzdc and dpe coligands, three unique distinct structures of ternary coordination networks were obtained. In the case of monoanion, 1-4 are isostructural and exhibit 3D porous pillarlayered cationic coordination framework stabilizing by counteranions within their channels. The various sizes and shapes of anions somewhat affect the torsion angles of  $\mu_2$ -dpe spacer and the channel's dimension. When using sulfate dianion, compound 5 shows mixed-valence Cu(I, II) 2D+2D  $\rightarrow$  2D parallel interpenetrated layer without the incorporation of  $SO_4^{2-}$  in the structure. At vigorous reaction temperature, the species arising from  $SO_4^{2-}$  may play a key role in the reduction of Cu(II) ion. Finally, compound 6 exhibits 3D coordination framework including coordinated HPO<sub>4</sub><sup>2</sup>- bridge which is generated by starting PO<sub>4</sub><sup>3-</sup>. The distinct coordination modes of pzdc<sup>3-</sup> also play a fundamental role on structural assemblies of these CPs. The anion exchange between weak coordinating anions, NO<sub>3</sub>, ClO<sub>4</sub> and BF<sub>4</sub> were not observed, but the chemisorption of SCN on frameworks 1-4 balancing by K+ with color change was found instead. The unsaturated 5-coordination Cu(II) center in 1-4 may play a crucial role on chemisorption of SCN without the collapse of their crystalline frameworks. In addition, the anion-induced structural transformation was observed when exchanging by a powerful coordinating ability of  $N_3$ .

#### References

- 1. S. K. Elsaidi, M. H. Mohamed, J. S. Loring, B. P. McGrail and P. K. Thallapally, *Appl. Mater. Interfaces*, 2016, **8**, 28424–28427.
- 2. K. Sarkar and P. Dastidar, *Chem. Eur. J.*, 2016, **22**, 1 13.
- 3. S. Suckert, M. Rams, M. Böhme, L. S. Germann, R. E. Dinnebier, W. Plass, J. Werner and C. Näther, *Dalton Trans.*, 2016, **45**, 18190–18201.
- 4. N. M. Khatri, M. H. Pablico-Lansigan, W. L. Boncher, J. E. Mertzman, A. C. Labatete, L. M. Grande, D. Wunder, M. J. Prushan, W. Zhang, P. S. Halasyamani, J. H. S. K. Monteiro, A. d. Bettencourt-Dias and S. L. Stoll, *Inorg. Chem.*, 2016, 55, 11408–11417.
- 5. S. Roy, H. M. Titi, B. K. Tripuramallu, N. Bhunia, R. Verma and I. Goldberg, *Cryst. Growth Des.*, 2016, **16**, 2814–2825.
- 6. Z.-X. Wang, L.-F. Wu, H.-P. Xiao, X.-H. Luo and M.-X. Li, *Cryst. Growth Des.*, 2016, **16**, 5184–5193.
- 7. F.-Y. Cui, K.-L. Huang, Y.-Q. Xu, Z.-G. Han, X. Liu, Y.-N. Chi and C.-W. Hu, *CrystEngComm*, 2009, **11**, 2757–2769.
- 8. P. Kang, S. Jung, J. Lee, H. J. Kang, H. Lee and M.-G. Choi, *Dalton Trans.*, 2016, **45**, 11949-11952.
- 9. Y.-Y. Jia, G.-J. Ren, A.-L. Li, L.-Z. Zhang, R. Feng, Y.-H. Zhang and X.-H. Bu, *Cryst. Growth Des.*, 2016, **16**, 5593–5597.
- 10. N. P. Martin, C. m. Falaise, C. Volkringer, N. Henry, P. Farger, C. Falk, E. Delahaye, P. Rabu and T. Loiseau, *Inorg. Chem.*, 2016, **55**, 8697–8705.
- 11. Z. Zhang, Y. Yang, H. Sun and R. Cao, *Inorg. Chim. Acta*, 2015, **434**, 158–171.
- 12. Y. Ma, A.-L. Cheng, B. Tang and E.-Q. Gao, *Dalton Trans.*, 2014, **43**, 13957-13964.
- 13. R. A. Agarwal and P. K. Bharadwaj, *Cryst. Growth Des.*, 2014, **14**, 6115–6121.
- 14. C.-P. Li, J. Guo and M. Du, *Inorg. Chem. Commun.*, 2013, **38**, 70–73.
- 15. S. Hou, Q.-K. Liu, J.-P. Ma and Y.-B. Dong, *Inorg. Chem.*, 2013, **52**, 3225–3235.
- 16. H. Lü, Y. Mu, J. Li, D. Wu, H. Hou and Y. Fan, *Inorg. Chim. Acta*, 2012, **387**, 450–454.
- 17. L. Pan, X. Huang and J. Li, *J. Solid State Chem.*, 2000, **152**, 236-246.
- 18. P. King, R. Clérac, C. E. Anson and A. K. Powell, *Dalton Trans.*, 2004, 852-861.
- 19. J.-H. Yang, S.-L. Zheng, X.-L. Yu and X.-M. Chen, *Cryst. Growth Des.*, 2004, **4**, 831-836.
- 20. P. King, R. Clérac, C. E. Anson, C. Coulon and A. K. Powell, *Inorg. Chem.*, 2003, 42, 3492-3500.
- 21. J. Xia, B. Zhao, H.-S. Wang, W. Shi, Y. Ma, H.-B. Song, P. Cheng, D.-Z. Liao and S.-P. Yan, *Inorg. Chem.*, 2007, **46**, 3450-3458.
- 22. C.-B. Liu, L. Liu, S.-S. Wang, X.-Y. Li, G.-B. Che, H. Zhao and Z.-L. Xu, *J. Inorg. Organomet. Polym.*, 2012, **22**, 1370–1376.
- 23. S. Barman, H. Furukawa, O. Blacque, K. Venkatesan, O. M. Yaghi, G.-X. Jinc and H. Berke, *Chem. Commun.*, 2011, **47**, 11882–11884.
- 24. APEX2; Bruker AXS Inc.: Madison, WI., 2014.
- 25. SAINT 4.0 Software Reference Manual; Siemens Analytical X-Ray Systems Inc.: Madison, WI,, 2000.
- 26. Sheldrick, G. M. SADABS, Program for Empirical Absorption correction of Area Detector Data; University of Go□ttingen: Go□ttingen, Germany, 2000.
- 27. G. M. Sheldrick, *Acta Cryst.*, 2015, **A71**, 3-8.
- 28. G. M. Sheldrick, Acta Crystallogr., 2008, A64, 112–122.

- 29. A. L. Spek, J. Appl. Cryst., 2003, **36**, 7-13.
- 30. A. L. Spek, Acta Cryst., 2015, C71, 9–18.
- 31. A. L. Spek, *Acta Cryst.*, 2009, **D65**, 148–155.
- 32. M. Pait, E. Colacio and D. Ray, *Polyhedron*, 2015, **88**, 90–100.
- 33. S. Y. Moon, M. W. Park, T. H. Noh and O.-S. Jung, *J. Mol. Struct.*, 2013, **1054**–**1055**, 326–330.
- 34. E. Melnic, E. B. Coropceanu, A. Forni, E. Cariati, O. V. Kulikova, A. V. Siminel, V. C. Kravtsov and M. S. Fonari, *Cryst. Growth Des.*, 2016, **16**, 6275–6285.
- 35. P. Suvanvapee, J. Boonmak, F. Klongdee, C. Pakawatchai, B. Moubaraki, K. S. Murray and S. Youngme, *Cryst. Growth Des.*, 2015, **15**, 3804–3812.
- 36. J. Boonmak, S. Youngme, N. Chaichit, G. A. v. Albada and J. Reedijk, *Cryst. Growth Des.*, 2009, **9**, 3318–3326.
- 37. A. W. Addison and T. N. Rao, J. Chem. Soc. Dalton Trans., 1984, 1349-1356.
- 38. W. L. Driessen, L. Chang, C. Finazzo, S. Gorter, D. Rehorst, J. Reedijk, M. Lutz and A. L. Spek, *Inorg. Chim. Acta*, 2003, **350**, 25-31.
- 39. G. Kang, Y. Jeon, K. Y. Lee, J. Kim and T. H. Kim, *Cryst. Growth Des.*, 2015, **15**, 5183–5187.
- 40. J. Troyano, J. Perles, P. Amo-Ochoa, F. Zamora and S. Delgado, *CrystEngComm*, 2016, **18**, 1809-1817.
- 41. G. P. Shields, P. R. Raithby, F. H. Allen and W. D. S. Motherwell, *Acta Crystallogr.*, 2000, **B56**, 455-465.
- 42. P. Smoleński, J. Kłak, D. S. Nesterov and A. M. Kirillov, *Cryst. Growth Des.*, 2012, **12**, 5852–5857.
- 43. H.-Z. Zhang, Y.-M. Chen, Y.-H. Yu, G.-F. Hou and J.-S. Gao, *Polyhedron*, 2016, **110**, 93-99.
- 44. L. Yang, D. R. Powell and R. P. Houser, *Dalton Trans.*, 2007, 955–964.
- 45. L. K. Das, C. Diaz and A. Ghosh, *Cryst. Growth Des.*, 2015, **15**, 3939–3949.
- 46. L. Song, C. Jiang, C. Ling, Y.-R. Yao, Q.-H. Wang and D. Chen, *J. Inorg. Organomet. Polym.*, 2016, **26**, 320–325.
- 47. K. Nakamoto, John Wiley & Sons, Inc., 2008.
- 48. X.-M. Zhang, Y.-Q. Wang, Y. Song and E.-Q. Gao, *Inorg. Chem.*, 2011, **50**, 7284–7294.
- 49. A. Vogler and H. Kunkely, *Coord. Chem. Rev.*, 2007, **251**, 577–583.
- 50. M. Du, X.-J. Jiang and X.-J. Zhao, *Inorg. Chem.*, 2006, **45**, 3998-4006.
- 51. X.-L. Wang, F.-F. Sui, H.-Y. Lin and G.-C. Liu, *Aust. J. Chem.*, 2015, **68**, 1076–1083.
- 52. X. Cao, B. Mu and R. Huang, *CrystEngComm.*, 2014, **16**, 5093–5102.
- 53. G. Liang, Y. Liu, X. Zhang and Z. Yi, *CrystEngComm.*, 2014, **16**, 9896–9906.
- 54. Y. Feng, D.-B. Wang, B. Wan, X.-H. Li and Q. Shi, *Inorg. Chim. Acta*, 2014, **413**, 187–193.

## **Supporting Information for Part II**

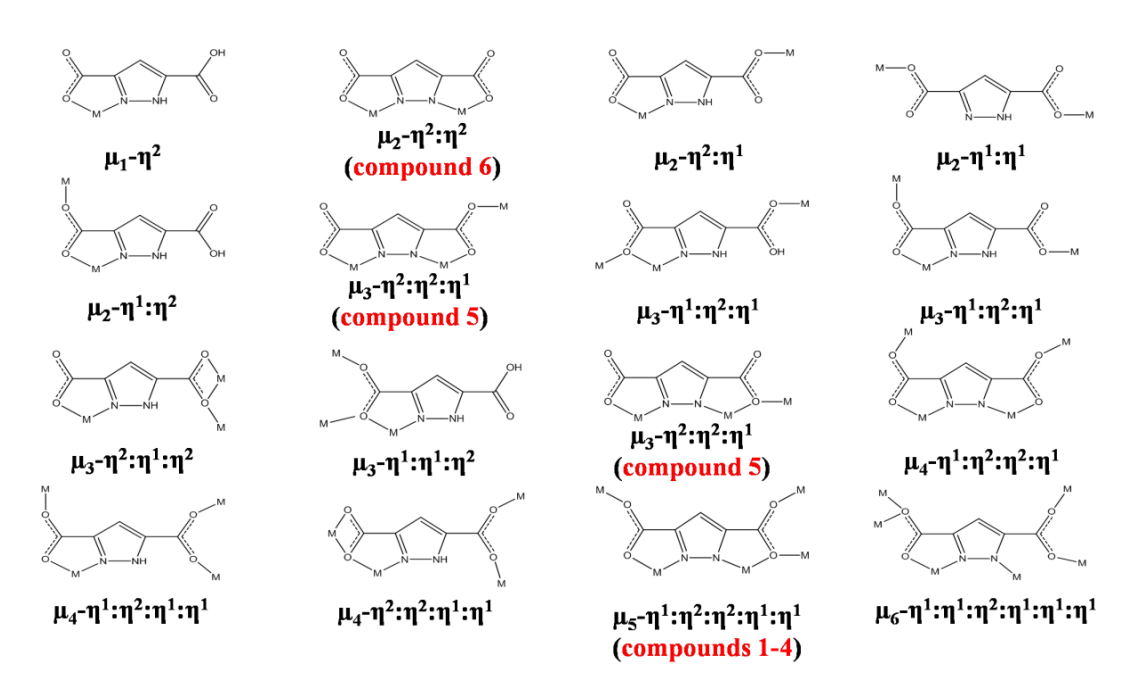


Figure S1. Diverse coordination modes of pyrazole-3,5-dicarboxylate.

**Table S1**. The selected bond lengths (Å) and angles (°) for compounds **1-6**.

| Table S1. The selected                  |                   | les (°) for compounds <b>1-6</b> .       |                        |
|---|-------------------|--|------------------------|
|   | Compound $1^a$ (1 | 00 K)                                    |                        |
| Cu1—O1                                  | 1.949(4)          | N1 <sup>i</sup> —Cu1—N4 <sup>ii</sup>    | 96.71(9)               |
| Cu1—N1 <sup>i</sup>                     | 2.019(3)          | N1—Cu1—N4 <sup>ii</sup>                  | 96.71(9)               |
| Cu1—N1                                  | 2.019(3)          | O3 <sup>ii</sup> —Cu1—N4 <sup>ii</sup>   | 79.75(15)              |
| Cu1—O3 <sup>ii</sup>                    | 2.043(4)          | N3—Cu2—O4 <sup>iii</sup>                 | 156.89(15)             |
| Cu1—O5                                  |                   | N3—Cu2—O4<br>N3—Cu2—N2 <sup>iv</sup>     |                        |
| Cu1—N4 <sup>ii</sup>                    | 2.173(4)          |  | 92.44(9)               |
| Cu2—N3                                  | 1.981(5)          | O4 <sup>iii</sup> —Cu2—N2 <sup>iv</sup>  | 89.23(9)               |
| Cu2—O4 <sup>iii</sup>                   | 1.990(4)          | N3Cu2N2 <sup>v</sup>                     | 92.44(9)               |
| Cu2—N2 <sup>iv</sup>                    | 2.025(3)          | O4 <sup>iii</sup> —Cu2—N2 <sup>v</sup>   | 89.23(9)               |
| Cu2—N2 <sup>v</sup>                     | 2.025(3)          | N2 <sup>iv</sup> —Cu2—N2 <sup>v</sup>    | 171.00(18)             |
| Cu2—O2 <sup>vi</sup>                    | 2.305(4)          | N3—Cu2—O2 <sup>vi</sup>                  | 88.30(16)              |
| Cu2—O1                                  | 2.425(4)          | O4 <sup>iii</sup> —Cu2—O2 <sup>vi</sup>  | 114.81(14)             |
| O1—Cu1—N1 <sup>i</sup>                  | 90.44(9)          | N2 <sup>iv</sup> —Cu2—O2 <sup>vi</sup>   | 86.30(9)               |
| 01—Cu1—N1                               | 90.44(9)          | N2 <sup>v</sup> —Cu2—O2 <sup>vi</sup>    | 86.30(9)               |
| N1 <sup>i</sup> —Cu1—N1                 | 164.79(18)        | N3—Cu2—O1                                | 74.38(15)              |
| O1—Cu1—O3 <sup>ii</sup>                 |                   | O4 <sup>iii</sup> —Cu2—O1                |                        |
|   | 165.54(14)        |  | 82.51(13)              |
| N1 <sup>i</sup> —Cu1—O3 <sup>ii</sup>   | 87.68(9)          | N2 <sup>iv</sup> —Cu2—O1                 | 94.30(9)               |
| N1—Cu1—O3 <sup>ii</sup>                 | 87.68(9)          | N2 <sup>v</sup> —Cu2—O1                  | 94.30(9)               |
| O1—Cu1—N4 <sup>ii</sup>                 | 114.71(16)        | O2 <sup>vi</sup> —Cu2—O1                 | 162.68(14)             |
|   | Compound          | $2^b$                                    |                        |
| Cu1—O1                                  | 1.957(7)          | N4 <sup>i</sup> —Cu1—N2 <sup>iii</sup>   | 96.7(2)                |
| Cu1—N4 <sup>i</sup>                     | 2.003(6)          | N4 <sup>ii</sup> —Cu1—N2 <sup>iii</sup>  | 96.7(2)                |
| Cu1—N4 <sup>ii</sup>                    | 2.003(6)          | O3 <sup>iii</sup> —Cu1—N2 <sup>iii</sup> | 78.7(3)                |
| Cu1—O3 <sup>iii</sup>                   | 2.121(8)          | N1—Cu2—N3                                | 93.87(19)              |
| Cu1—N2 <sup>iii</sup>                   | 2.157(9)          | N1—Cu2—N3 <sup>iv</sup>                  | 93.87(19)              |
| Cu2—N1                                  |                   | N3—Cu2—N3 <sup>iv</sup>                  |                        |
|   | 2.008(8)          |  | 165.9(4)               |
| Cu2—N3                                  | 2.008(6)          | N1—Cu2—O4 <sup>v</sup>                   | 156.4(3)               |
| Cu2—N3 <sup>iv</sup>                    | 2.008(6)          | N3—Cu2—O4 <sup>v</sup>                   | 88.79(19)              |
| Cu2—O1                                  | 2.492(8)          | N3 <sup>iv</sup> —Cu2—O4 <sup>v</sup>    | 88.79(19)              |
| Cu2—O2                                  | 2.504(8)          | N3 <sup>iv</sup> —Cu2—O2                 | 84.29(19)              |
| Cu2—O4 <sup>v</sup>                     | 2.030(8)          | N3—Cu2—O2                                | 84.29(19)              |
| O1—Cu1—N4 <sup>i</sup>                  | 89.2(2)           | N3 <sup>iv</sup> —Cu2—O1                 | 96.74(18)              |
| O1—Cu1—N4 <sup>ii</sup>                 | 89.2(2)           | N3—Cu2—O1                                | 96.74(18)              |
| N4 <sup>i</sup> —Cu1—N4 <sup>ii</sup>   | 164.8(4)          | O1—Cu2—O2                                | 160.76(26)             |
| O1—Cu1—O3 <sup>iii</sup>                | 157.6(3)          | O1—Cu2—N1                                | 72.83(28)              |
| N4 <sup>i</sup> —Cu1—O3 <sup>iii</sup>  | 87.9(2)           | O2—Cu2—N1                                | 87.93(30)              |
| N4 <sup>ii</sup> —Cu1—O3 <sup>iii</sup> | 87.9(2)           | O1—Cu2—O4 <sup>v</sup>                   | 83.61(27)              |
| O1—Cu1—N2 <sup>iii</sup>                | 123.7(3)          | O2—Cu2—O4 <sup>v</sup>                   | 115.63(29)             |
| OI—CuI—N2                               | Compound          |  | 113.03(29)             |
| C 1 01                                  |                   |  | 06.02(15)              |
| Cu1—O1                                  | 1.954(5)          | N1—Cu1—N4 <sup>ii</sup>                  | 96.82(15)              |
| Cu1—N1                                  | 2.008(4)          | N1 <sup>i</sup> —Cu1—N4 <sup>ii</sup>    | 96.82(15)              |
| Cu1—N1 <sup>i</sup>                     | 2.008(4)          | O4 <sup>ii</sup> —Cu1—N4 <sup>ii</sup>   | 78.9(2)                |
| Cu1—O4 <sup>ii</sup>                    | 2.094(5)          | N3 <sup>iii</sup> —Cu2—N2 <sup>iv</sup>  | 93.64(13)              |
| Cu1—N4 <sup>ii</sup>                    | 2.167(6)          | N3 <sup>iii</sup> —Cu2—N2 <sup>v</sup>   | 93.64(13)              |
| Cu2—N3 <sup>iii</sup>                   | 1.996(6)          | N2 <sup>iv</sup> —Cu2—N2 <sup>v</sup>    | 167.4(3)               |
| Cu2—N2 <sup>iv</sup>                    | 2.014(4)          | N3 <sup>iii</sup> —Cu2—O3                | 156.6(2)               |
| Cu2—N2 <sup>v</sup>                     | 2.014(4)          | N2 <sup>iv</sup> —Cu2—O3                 | 88.70(13)              |
| Cu2—O1                                  | 2.473(5)          | N2 <sup>v</sup> —Cu2—O3                  | 88.70(13)              |
| Cu2—O2                                  | 2.464(5)          | N2 <sup>v</sup> —Cu2—O1                  | 95.95(15)              |
| Cu2—O3                                  | 2.027(5)          | N2 <sup>iv</sup> —Cu2—O1                 | 95.95(15)              |
| Cu2—03<br>O1—Cu1—N1                     | 89.32(14)         | N2 —Cu2—O1<br>N2 <sup>v</sup> —Cu2—O2    | 93.93(13)<br>84.99(14) |
|   |                   | N2 —Cu2—O2<br>N2 <sup>iv</sup> —Cu2—O2   |                        |
| O1—Cu1—N1 <sup>i</sup>                  | 89.32(14)         |  | 84.99(14)              |
| N1—Cu1—N1 <sup>i</sup>                  | 164.7(3)          | N3 <sup>iii</sup> —Cu2—O1                | 73.24(19)              |
| O1—Cu1—O4 <sup>ii</sup>                 | 159.2(2)          | N3 <sup>iii</sup> —Cu2—O2                | 88.31(20)              |
| N1—Cu1—O4 <sup>ii</sup>                 | 87.93(14)         | O1—Cu2—O3                                | 83.32(19)              |
| N1 <sup>i</sup> —Cu1—O4 <sup>ii</sup>   | 87.93(14)         | O2—Cu2—O3                                | 115.12(20)             |
| N1 <sup>i</sup> —Cu1—N2                 | 99.13(15)         | O1—Cu2—O2                                | 161.55(17)             |
| O1—Cu1—N4 <sup>ii</sup>                 | 121.9(2)          |  |                        |
| -                                       | * *               |  |                        |

Table S1. The selected bond lengths (Å) and angles (°) for compounds 1-6. (Cont.)

| C 1 01                                |            | Compound 4 <sup>d</sup>                 | 06.00(10)  |
|---------------------------------------|------------|---|------------|
| Cu1—O1                                | 1.959(6)   | N1 <sup>i</sup> —Cu1—N4 <sup>ii</sup>   | 96.80(18)  |
| Cu1—N1 <sup>i</sup>                   | 2.002(5)   | N1—Cu1—N4 <sup>ii</sup>                 | 96.80(18)  |
| Cu1—N1                                | 2.002(5)   | O4 <sup>ii</sup> —Cu1—N4 <sup>ii</sup>  | 78.6(3)    |
| Cu1—O4 <sup>ii</sup>                  | 2.073(7)   | O3—Cu2—N3 <sup>iii</sup>                | 157.6(3)   |
| Cu1—N4 <sup>ii</sup>                  | 2.163(8)   | O3Cu2N2 <sup>iv</sup>                   | 88.55(16)  |
| Cu2—O1                                | 2.462(6)   | N3 <sup>iii</sup> —Cu2—N2 <sup>iv</sup> | 93.42(16)  |
| Cu2—O2                                | 2.452(6)   | O3—Cu2—N2 <sup>v</sup>                  | 88.55(16)  |
| Cu2—O3                                | 1.984(6)   | N3 <sup>iii</sup> —Cu2—N2 <sup>v</sup>  | 93.42(16)  |
| Cu2—N3 <sup>iii</sup>                 | 2.003(7)   | N2 <sup>iv</sup> —Cu2—N2 <sup>v</sup>   | 168.7(3)   |
| Cu2—N2 <sup>iv</sup>                  | 2.017(5)   | O1—Cu2—N2 <sup>iv</sup>                 | 95.27(18)  |
| Cu2—N2 <sup>v</sup>                   | 2.017(5)   | O1—Cu2—N2 <sup>v</sup>                  | 95.27(18)  |
| O1—Cu1—N1 <sup>i</sup>                | 89.32(17)  | O2—Cu2—N2 <sup>iv</sup>                 | 85.60(18)  |
| O1—Cu1—N1                             | 89.32(17)  | O2—Cu2—N2 <sup>v</sup>                  | 85.60(18)  |
| N1 <sup>i</sup> —Cu1—N1               | 164.8(4)   | O1—Cu2—O2                               | 162.22(22) |
| O1—Cu1—O4 <sup>ii</sup>               | 159.9(3)   | O1—Cu2— N3 <sup>iii</sup>               | 73.45(26)  |
| N1 <sup>i</sup> —Cu1—O4 <sup>ii</sup> | 88.05(17)  | O2—Cu2— N3 <sup>iii</sup>               | 88.77(28)  |
| N1—Cu1—O4 <sup>ii</sup>               | 88.05(17)  | O1—Cu2—O3                               | 84.11(23)  |
| O1—Cu1—N4 <sup>ii</sup>               | 121.4(3)   | O2—Cu2—O3                               | 113.67(25) |
| 01—cu1—11 <del>4</del>                |            | Compound $5^e$                          | 113.07(23) |
| Cu1—N1                                | 1.929(4)   | N1—Cu1—O5                               | 162.55(16) |
| Cu1—N1<br>Cu1—N3                      | 1.921(4)   | O1—Cu1—O5                               | 101.38(15) |
| Cu1—N3<br>Cu1—N9                      |            |   |            |
|                                       | 2.250(4)   | N3—Cu1—N9                               | 97.46(16)  |
| Cu1—O1                                | 2.010(3)   | N1—Cu1—N9                               | 96.56(17)  |
| Cu1—O5                                | 2.030(3)   | O1—Cu1—N9                               | 100.99(15) |
| Cu2—N2                                | 1.934(4)   | O5—Cu1—N9                               | 100.32(15) |
| Cu2—N4                                | 1.931(4)   | N2—Cu2—N4                               | 93.22(18)  |
| Cu2—N11                               | 2.264(4)   | N2—Cu2—O3                               | 80.03(16)  |
| Cu2—O3                                | 1.997(3)   | N4—Cu2—O3                               | 163.56(16) |
| Cu2—O7                                | 2.012(4)   | N2—Cu2—O7                               | 160.62(16) |
| Cu3—N5                                | 1.923(4)   | N4—Cu2—O7                               | 79.80(17)  |
| Cu3—N7                                | 1.938(4)   | O3—Cu2—O7                               | 101.69(15) |
| Cu3—N12                               | 2.246(4)   | N2—Cu2—N11                              | 95.72(17)  |
| Cu3—O9                                | 2.048(4)   | N4—Cu2—N11                              | 97.09(17)  |
| Cu3—O13                               | 1.974(4)   | O3—Cu2—N11                              | 98.48(15)  |
| Cu4—N6                                | 1.934(4)   | O7—Cu2—N11                              | 103.04(16) |
| Cu4—N8                                | 1.931(4)   | N5—Cu3—N7                               | 93.37(19)  |
| Cu4—N10                               | 2.246(4)   | N5—Cu3—O13                              | 161.58(16) |
| Cu4—O11                               | 2.006(4)   | N7—Cu3—O13                              | 80.59(17)  |
| Cu4—O15                               | 2.016(4)   | N5—Cu3—O9                               | 79.57(17)  |
| Cu5—N13                               | 1.930(4)   | N7—Cu3—O9                               | 159.98(15) |
| Cu5—N14 <sup>i</sup>                  | 1.926(4)   | O13—Cu3—O9                              | 100.23(15) |
| Cu5—O2                                | 2.227(4)   | N5—Cu3—N12                              | 96.49(17)  |
| Cu6-N15                               | 1.912(4)   | N7—Cu3—N12                              | 96.80(17)  |
| Cu6—N16 <sup>ii</sup>                 | 1.911(4)   | O13—Cu3—N12                             | 101.48(16) |
| Cu6—O6                                | 2.293(4)   | O9—Cu3—N12                              | 102.57(15) |
| Cu7—N17                               | 1.923(4)   | N8—Cu4—N6                               | 93.29(19)  |
| Cu7—N18 <sup>i</sup>                  | 1.935(4)   | N8—Cu4—O11                              | 161.98(16) |
| Cu7—O16                               | 2.201(4)   | N6—Cu4—O11                              | 80.08(17)  |
| Cu8—N19                               | 1.905(4)   | N8—Cu4—O15                              | 79.55(16)  |
| Cu8—N20 <sup>iii</sup>                | 1.903(4)   | N6—Cu4—O15<br>N6—Cu4—O15                | 160.97(16) |
| Cu8—09                                | 2.345(4)   | O11—Cu4—O15                             |            |
|                                       |            |   | 101.36(15) |
| N3—Cu1—N1                             | 93.62(18)  | N8—Cu4—N10                              | 97.52(17)  |
| N3—Cu1—O1                             | 160.93(16) | N6—Cu4—N10                              | 98.42(17)  |
| N1—Cu1—O1                             | 79.56(16)  | O11—Cu4—N10                             | 100.01(16) |
| N3—Cu1—O5                             | 79.87(16)  | O15—Cu4—N10                             | 99.98(15)  |

**Table S1**. The selected bond lengths (Å) and angles (°) for compounds **1-6**. (Cont.)

|                           | Compou     | nd 5 <sup>e</sup>                      |            |
|---------------------------|------------|--|------------|
| N14 <sup>i</sup> —Cu5—N13 | 150.46(19) | N17—Cu7—N18 <sup>i</sup>               | 150.51(19) |
| N14 <sup>i</sup> —Cu5—O2  | 106.54(16) | N17—Cu7—O16                            | 106.83(16) |
| N13—Cu5—O2                | 102.73(17) | N18 <sup>i</sup> —Cu7—O16              | 102.36(16) |
| N15—Cu6—N16 <sup>ii</sup> | 155.1(2)   | N20 <sup>iii</sup> —Cu8—N19            | 156.7(2)   |
| N15—Cu6—O6                | 99.57(17)  | N20 <sup>iii</sup> —Cu8—O9             | 99.66(16)  |
| N16 <sup>ii</sup> —Cu6—O6 | 104.70(17) | N19—Cu8—O9                             | 103.40(16) |
|                           | Compou     | and <b>6</b> <sup>f</sup>              |            |
| Cu1—O5                    | 1.957(2)   | O1—Cu1—N3                              | 88.78(12)  |
| Cu1—N1                    | 1.968(3)   | O5—Cu1—O5 <sup>i</sup>                 | 79.52(10)  |
| Cu1—O1                    | 1.991(3)   | N1—Cu1—O5 <sup>i</sup>                 | 101.82(11) |
| Cu1—N3                    | 2.010(3)   | O1—Cu1—O5 <sup>i</sup>                 | 103.29(11) |
| Cu1—O5 <sup>i</sup>       | 2.382(2)   | N3—Cu1—O5 <sup>i</sup>                 | 89.64(11)  |
| Cu2—O6                    | 1.898(3)   | O6—Cu2—O3                              | 164.58(12) |
| Cu2—O3                    | 1.944(3)   | O6—Cu2—N2                              | 95.87(12)  |
| Cu2—N2                    | 1.948(3)   | O3—Cu2—N2                              | 82.49(12)  |
| Cu2—N5                    | 2.011(3)   | O6—Cu2—N5                              | 94.75(15)  |
| Cu3—O7 <sup>ii</sup>      | 1.890(3)   | O3—Cu2—N5                              | 88.87(15)  |
| Cu3—O7                    | 1.890(3)   | N2—Cu2—N5                              | 167.75(15) |
| Cu3—N4                    | 2.029(3)   | O7 <sup>ii</sup> —Cu3—O7               | 180        |
| Cu3—N4 <sup>ii</sup>      | 2.029(3)   | O7 <sup>ii</sup> —Cu3—N4               | 92.79(12)  |
| O5—Cu1—N1                 | 95.01(10)  | O7—Cu3—N4                              | 87.21(12)  |
| O5—Cu1—O1                 | 175.05(11) | O7 <sup>ii</sup> —Cu3—N4 <sup>ii</sup> | 87.21(12)  |
| N1—Cu1—O1                 | 80.46(11)  | O7—Cu3—N4 <sup>ii</sup>                | 92.79(12)  |
| O5—Cu1—N3                 | 95.35(12)  | N4—Cu3—N4 <sup>ii</sup>                | 180        |
| N1—Cu1—N3                 | 165.77(12) |  |            |

<sup>a</sup>Symmetry codes for **1**: (i) x, 0.5-y, z; (ii) -0.5+x, y, 0.5-z; (iii) x, y, 1+z; (iv) 1-x, 1-y, 1-z; (v) 1-x, -0.5+y, 1-z; (vi) 0.5+x, y, 0.5-z. <sup>b</sup>For **2**: (i) 1-x, -0.5+y, -z; (ii) 1-x, 1-y, -z; (iii) -0.5+x, y, 0.5-z; (iv) x, 0.5-y, z; (v) x, y, -1+z. <sup>c</sup>For **3**: (i) x, 1.5-y, z; (ii) 0.5+x, y, 0.5-z; (iii) x, y, 1+z; (iv) 1-x, 1-y, 1-z; (v) 1-x, 0.5+y, 1-z. <sup>d</sup>For **4**: (i) x, 0.5-y, z; (ii) -0.5+x, y, 1.5-z; (iii) x, y, 1+z; (iv) 2-x, 1-y, 2-x; (v) 2-x, -0.5+y, 2-x. <sup>e</sup>For **5**: (i) -0.5+x, 0.5-y, -0.5+x; (ii) 0.5+x, 0.5-y, 0.5+x; (iii) 0.5+x, 1.5-y, 0.5+x. <sup>f</sup>For **6**: (i) -x, 2-y, 1-x; (ii) -x, 1-y, 1-x.

**Table S2**. Intermolecular hydrogen bond length/Å angles/° in compounds 1-4.

|                            |          | Compound 1 <sup>a</sup>     |                             |          |  |
|----------------------------|----------|-----------------------------|-----------------------------|----------|--|
| D-H···A                    | d(D-H)/Å | $d(H\cdots A)/\mathring{A}$ | $d(D\cdots A)/\mathring{A}$ | <(DHA)/° |  |
| C2-H2···O6                 | 0.95     | 2.56                        | 3.279(16)                   | 133      |  |
| C2-H2···O7 <sup>i</sup>    | 0.95     | 2.59                        | 3.406(17)                   | 144      |  |
| C6-H6···O5                 | 0.95     | 2.30                        | 3.241(9)                    | 169      |  |
| C7-H7···O5 <sup>ii</sup>   | 0.95     | 2.35                        | 2.943(9)                    | 120      |  |
| C9-H9···O5                 | 0.95     | 2.44                        | 3.383(10)                   | 173      |  |
| C9-H9···O6 <sup>i</sup>    | 0.95     | 2.49                        | 3.269(16)                   | 140      |  |
|                            |          | Compound $2^b$              |                             |          |  |
| D-H···A                    | d(D-H)/Å | d(H···A)/Å                  | $d(D\cdots A)/\mathring{A}$ | <(DHA)/° |  |
| C9-H9···O5 <sup>i</sup>    | 0.93     | 2.49                        | 3.22(4)                     | 135      |  |
| C11-H11···O6 <sup>ii</sup> | 0.93     | 2.04                        | 2.93(2)                     | 160      |  |
| C12-H12···O7 <sup>i</sup>  | 0.93     | 2.33                        | 3.25(2)                     | 169      |  |
| C14-H14···O6 <sup>ii</sup> | 0.93     | 2.53                        | 3.35(4)                     | 147      |  |
| C16-H16···O8i              | 0.93     | 2.55                        | 3.26(4)                     | 133      |  |
| Compound 3 <sup>c</sup>    |          |                             |                             |          |  |
| D-H···A                    | d(D-H)/Å | d(H···A)/Å                  | $d(D\cdots A)/\mathring{A}$ | <(DHA)/° |  |
| C2-H2···F2 <sup>i</sup>    | 0.93     | 2.52                        | 3.364(18)                   | 151      |  |
| C6-H6···F4                 | 0.93     | 2.22                        | 3.134(14)                   | 169      |  |
| C6-H6···F2 <sup>ii</sup>   | 0.93     | 2.38                        | 2.846(14)                   | 111      |  |
| C7-H7···F2 <sup>iii</sup>  | 0.93     | 2.12                        | 3.009(15)                   | 159      |  |
| C11-H11···F4               | 0.93     | 2.50                        | 3.421(14)                   | 169      |  |
|                            |          | Compound $4^d$              |                             |          |  |
| D–H···A                    | d(D-H)/Å | d(H···A)/Å                  | $d(D\cdots A)/\mathring{A}$ | <(DHA)/° |  |
| C6-H6···S1                 | 0.93     | 2.78                        | 3.610(19)                   | 150      |  |

<sup>a</sup>Symmetry codes for **1**: (i) 1-x, 1-y, 2-z; (ii) -0.5+x, y, 1.5-z. <sup>b</sup>For **2**: (i) 1-x, 1-y, 1-z; (ii) 1.5-x, 1-y, -0.5+z. <sup>c</sup>For **3**: (i) 0.5+x, y, 0.5-z; (ii) 1-x, 1-y, -z; (iii) 0.5+x, y, 0.5-z.

## Bond Valence Sum (BVS) Studies.

The BVS analysis was performed according to the following equations:

BVS = 
$$\sum_{i=1}^{n} s_i$$
  
 $s_i = \exp[(r_0 - r)/0.37]$ 

Where r is the experimentally derived bond length for ligand, i and  $r_0$  is a parameter characteristic of the bond, which is a calculated value depending on the geometry and coordination number of the complex. The  $r_0$  values were taken from the literature. The values used for  $r_0$  include the Cu(I)–N = 1.571, Cu(I)–O = 1.567, Cu(II)–N = 1.713, and Cu(II)–O = 1.655 Å.

- 1. I. D. Brown and D. Altermatt, *Acta Cryst.*, 1985, **B41**, 244-247.
- 2. I. D. Brown, Acta Cryst., 1992, **B48**, 553-572.
- 3. G. P. Shields, P. R. Raithby, F. H. Allen and W. D. S. Motherwell, *Acta Crystallogr.*, 2000, **B56**, 455-465.

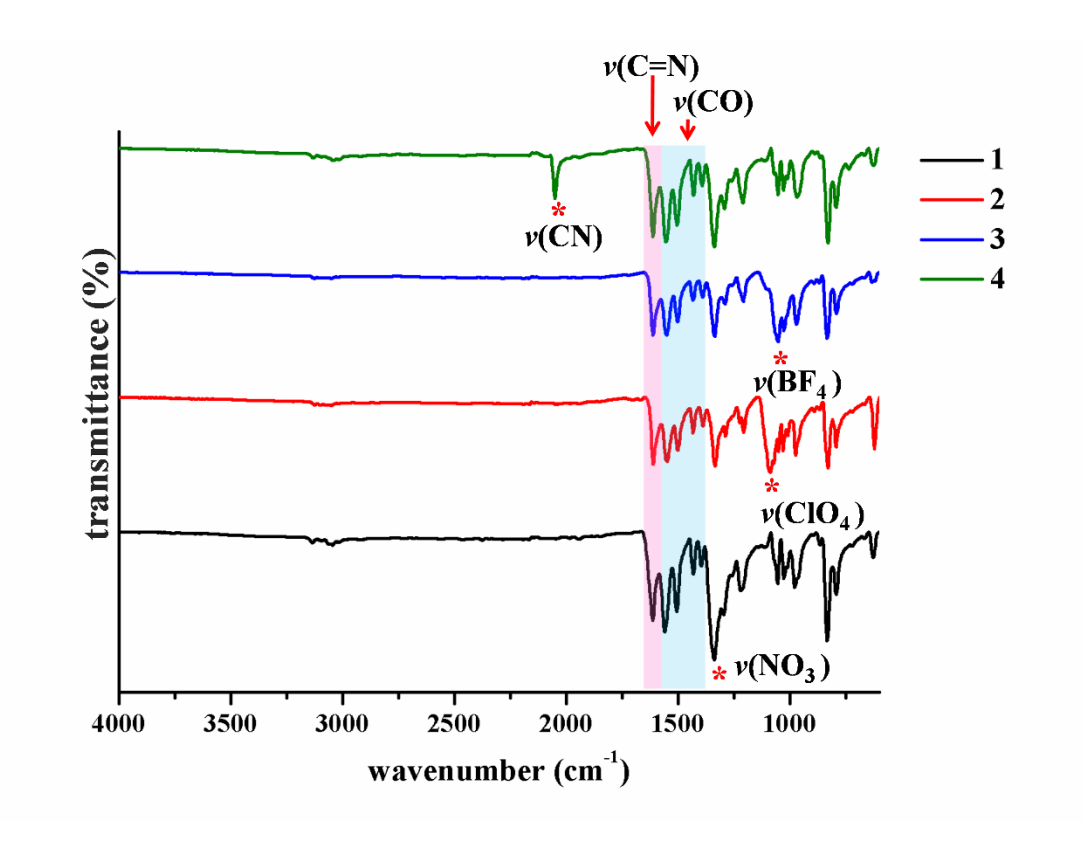


Figure S2. IR spectra of compounds 1-4.

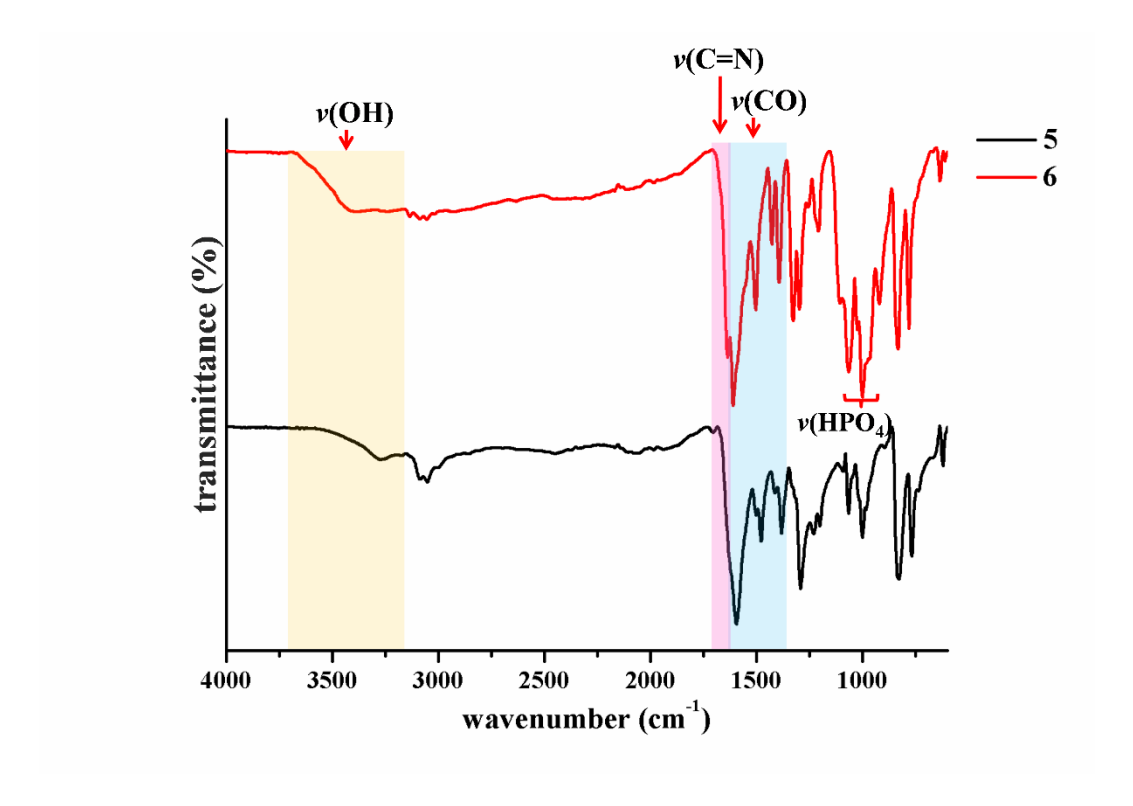


Figure S3. IR spectra of 5 and 6.

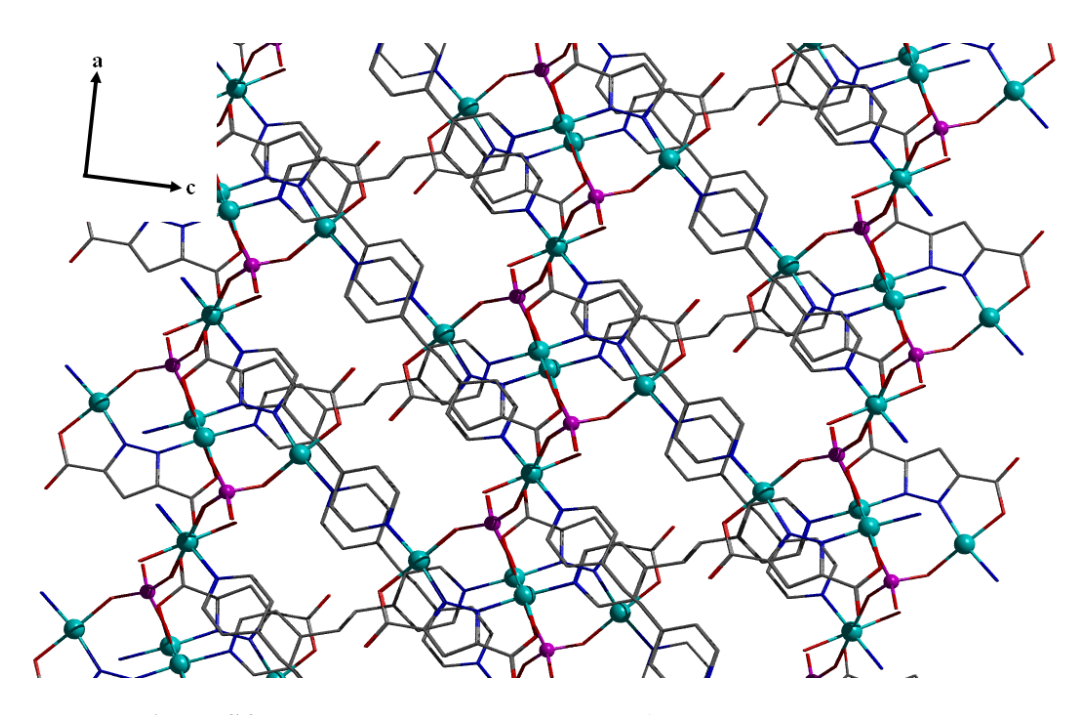


Figure S4. 3D coordination framework of 6 in ac crystallographic plane.

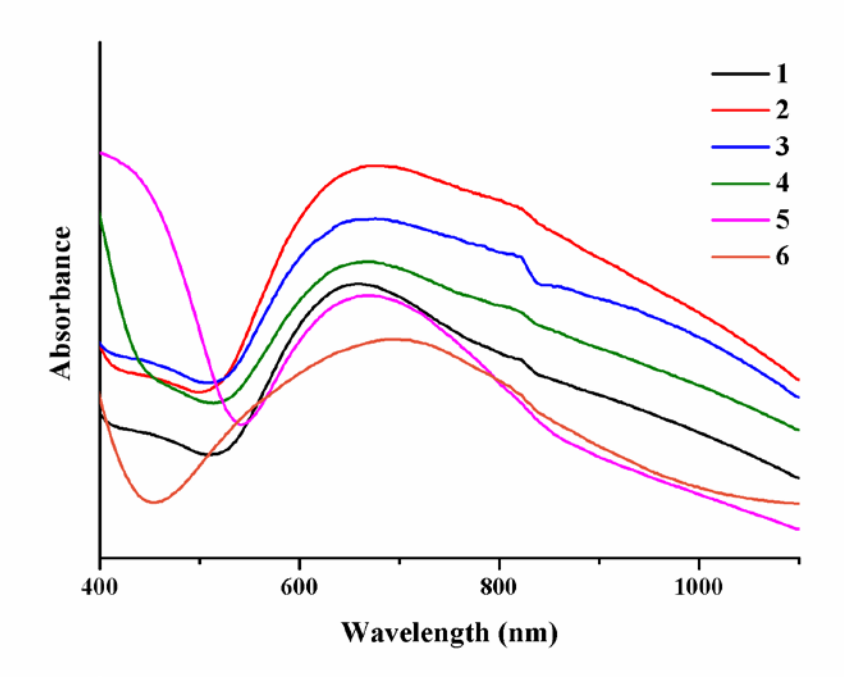


Figure S5. The electronic spectra of 1-6.

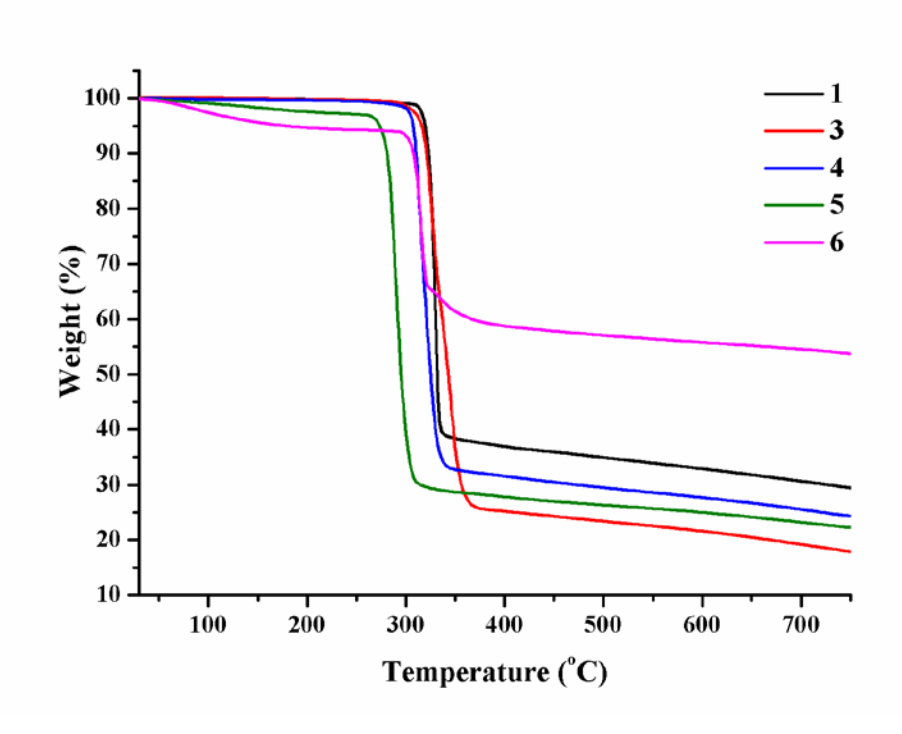
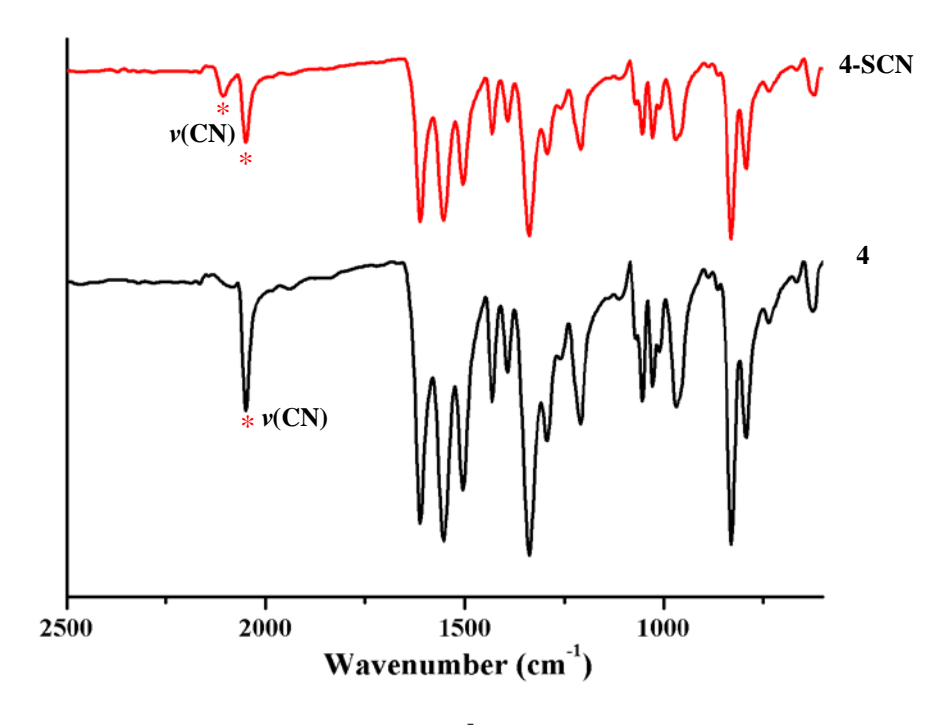
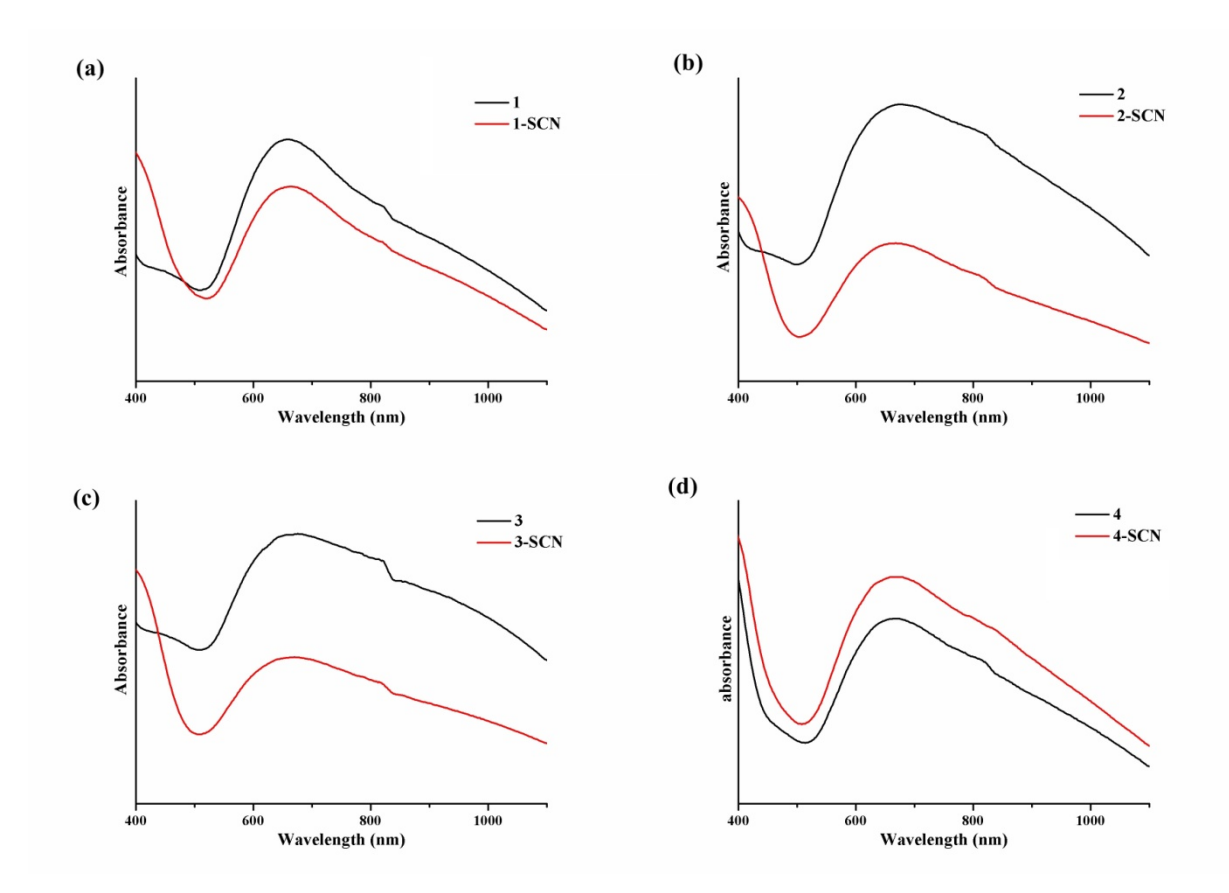


Figure S6. TGA curves of compounds 1 and 3-6.



**Figure S7.** IR spectra of SCN chemisorption of compound **4**.



**Figure S8.** UV-Vis spectra of the anion exchange products with SCN anion.

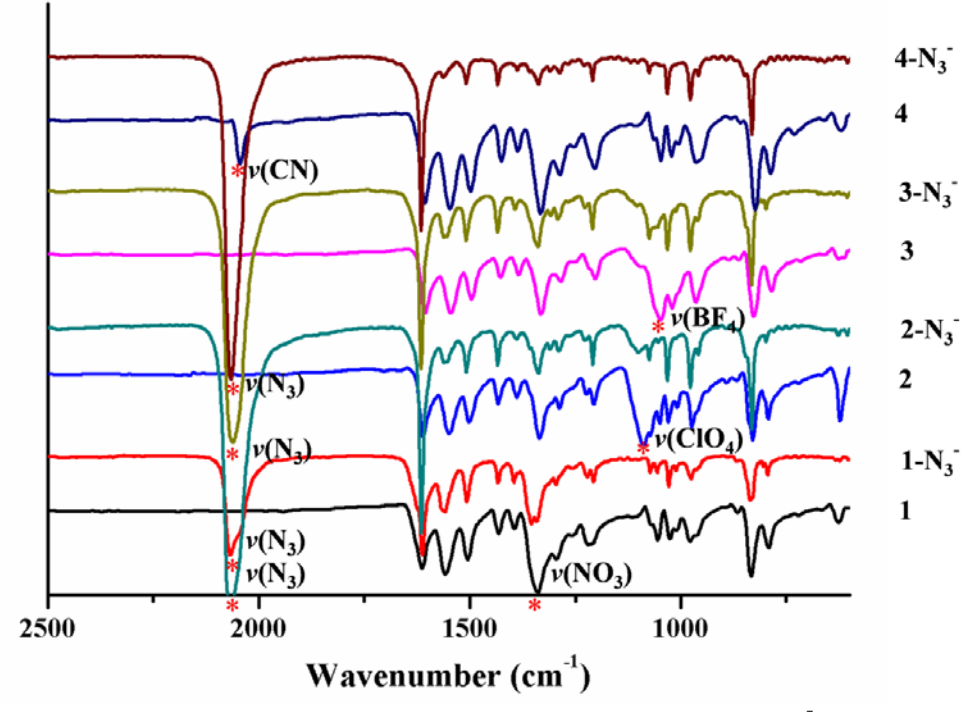


**Figure S9.** IR spectra of the anion exchange product with  $N_3^-$  anion.

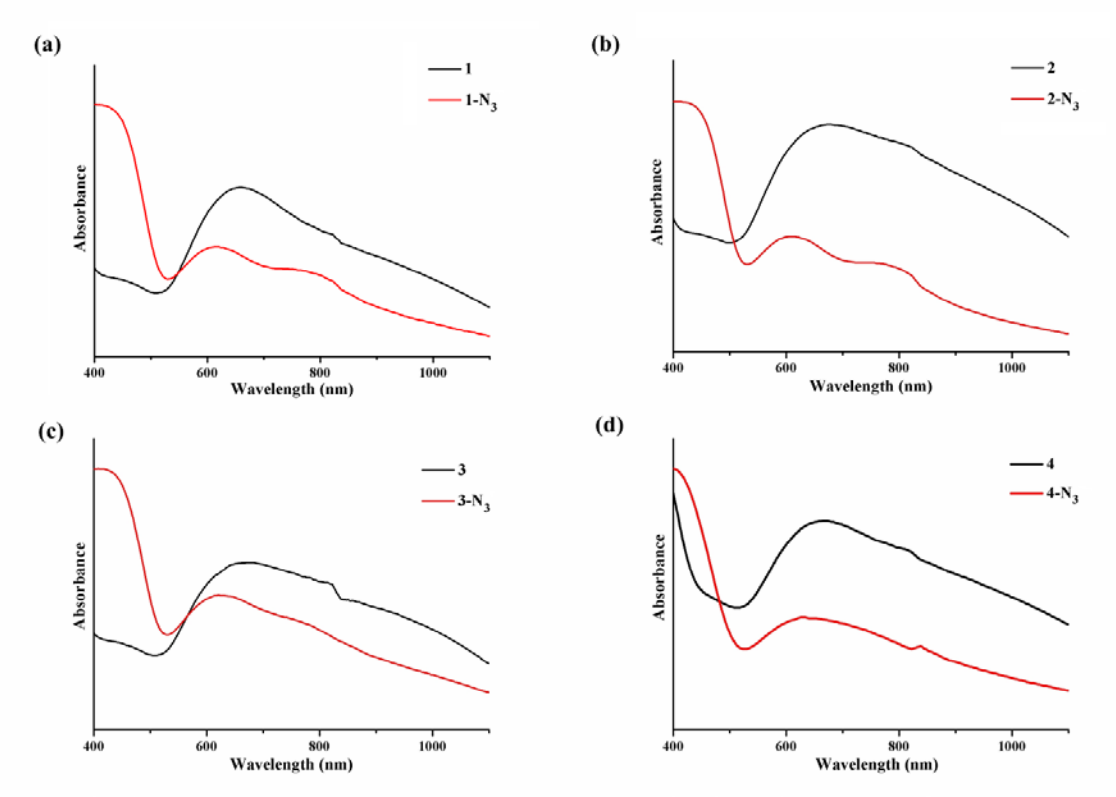


**Figure S10.** UV-Vis spectra of the anion exchange products with  $N_3^-$  anion.

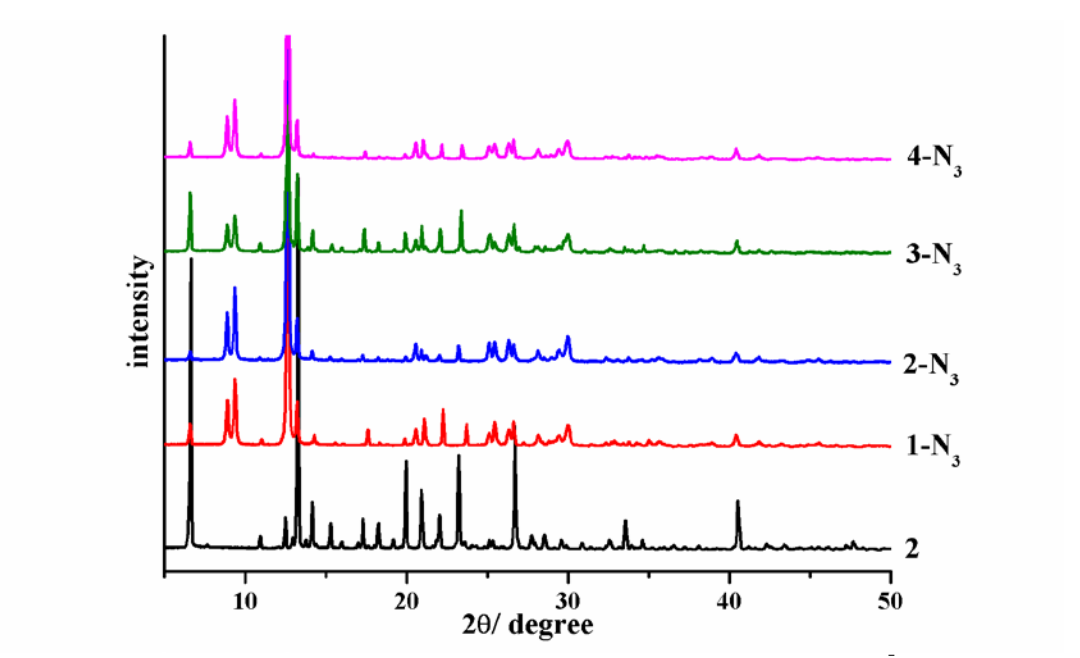
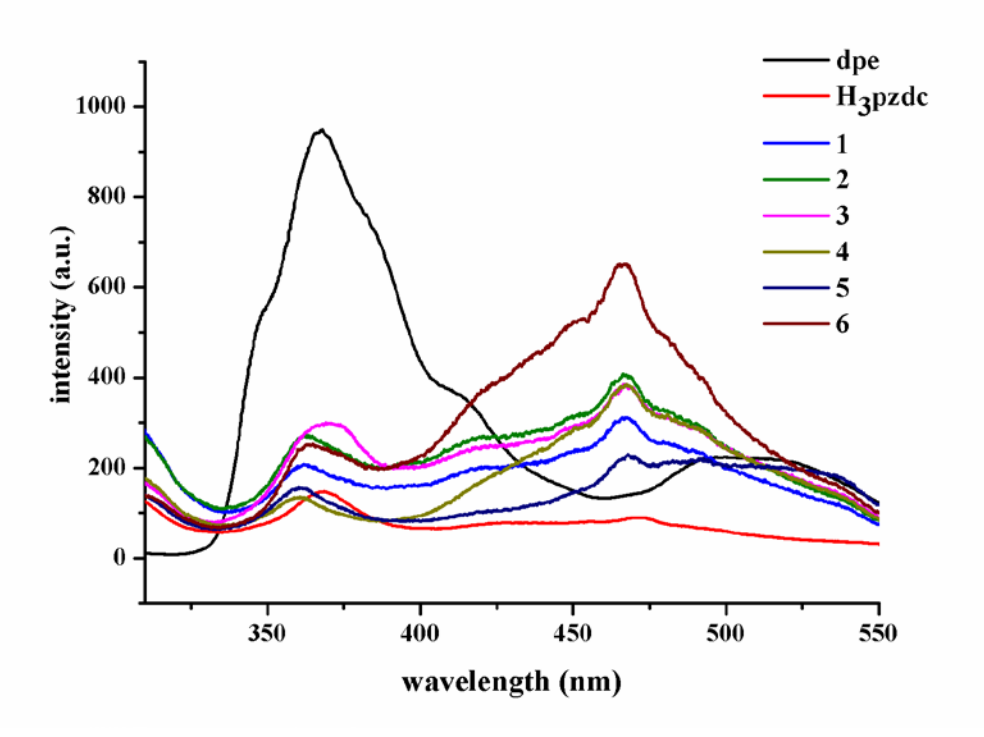


Figure S11. PXRD patterns of the anion exchange products with  $N_3^{\top}$  anion.



**Figure S12.** The emission spectra of compounds **1-6**, H<sub>3</sub>pzdc, and dpe ligands.

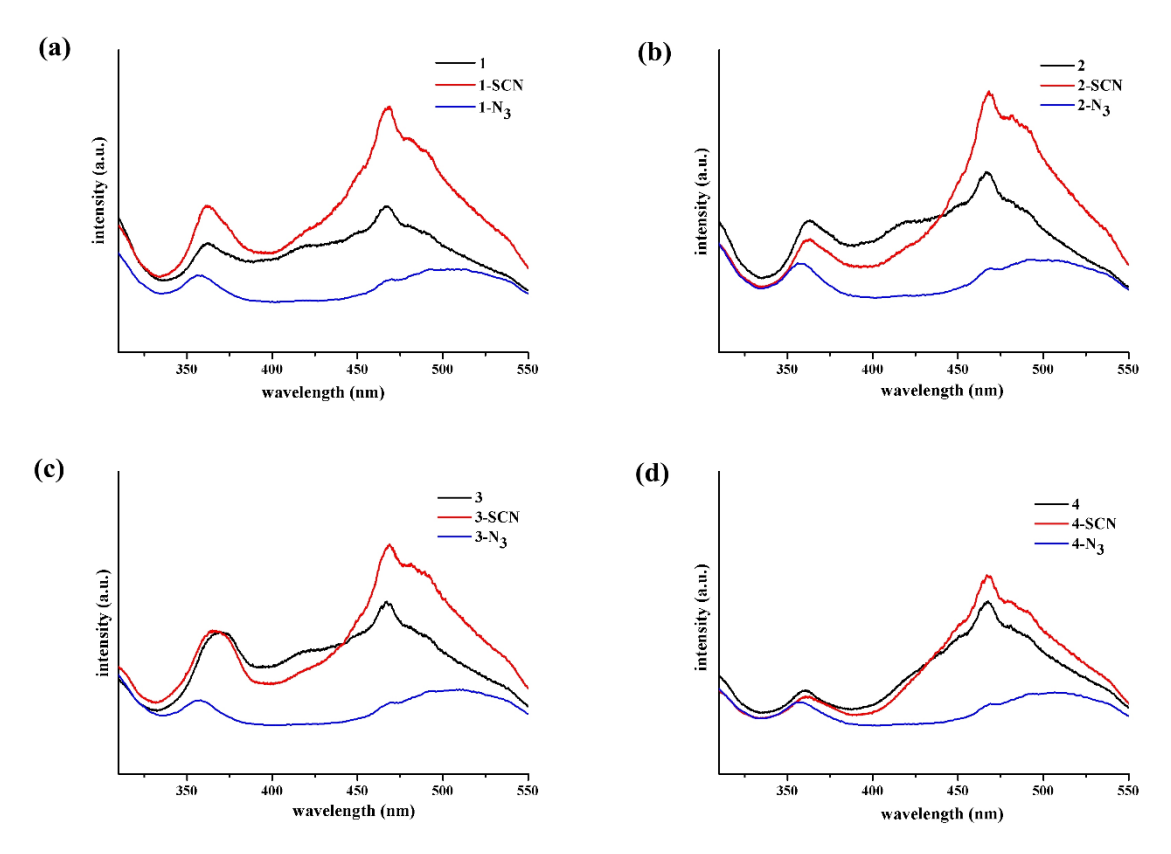


Figure S13. The emission spectra of compounds 1-4, 1-4-SCN, and  $1-4-N_3$ .

## **OUTPUT OF THE RESEARCH**

## **Publication papers:**

- 1) F. Klongdee, <u>J. Boonmak</u>\*, S. Youngme, Anion-dependent self-assembly of copper coordination polymers based on pyrazole3,5-dicarboxylate and 1,2-di(4-pyridyl)ethylene, *Dalton Transactions*, **2017**, 46, 4806-4815. (IF 2016 = 4.029, Q1)
- 2) F. Klongdee, <u>J. Boonmak</u>\*, B. Moubaraki, K. S. Murray, S. Youngme, Copper(II) coordination polymers containing neutral trinuclear or anionic dinuclear building units based on pyrazole-3,5-dicarboxylate: Synthesis, structures and magnetic properties, *Polyhedron*, **2017**, 126, 8-16. (IF 2016 = 1.926, Q2)

## **Presentations:**

- 1) <u>J. Boonmak\*</u>, "Copper coordination polymers based on pyrazole-3,5-dicarboxylate with various N,N' ditopic spacers" *Invited speaker* (special session: crystallography) at The 43<sup>rd</sup> Congress on Science and Technology of Thailand, Chamchuri 10, Chulalongkorn University, Bangkok, Thailand, October 17-19, 2017.
- 2) F. Klongdee, <u>J. Boonmak</u>\*, S. Youngme, Anion-dependent self-assembly of copper coordination polymers based on pyrazole-3,5-dicarboxylate and 1,2-di (4-pyridyl)ethylene, *Poster presented* at 43<sup>rd</sup> Congress on Science and Technology of Thailand, Chamchuri 10, Chulalongkorn University, Bangkok, Thailand, October 17-19, 2017.
- 3) F. Klongdee, <u>J. Boonmak</u>\*, S. Youngme, 3D pillar-layered copper(II) coordination polymers based on pyrazole-dicarboxylate: solvothermal synthesis, structures and anion exchange studies, *Poster presented* at *PERCH-CIC Congress IX: 2016 International Congress for Innovation in Chemistry*, Jomtien Palm Beach Hotel & Resort, Pattaya, Chonburi, Thailand, June 26-29, 2016.
- 4) F. Klongdee, <u>J. Boonmak</u>\*, S. Youngme, Anions as templates in the synthesis of copper coordination polymers containing pyrazole-3,5-dicarboxylate and 1,2-di(4-pyridyl)ethylene, *Poster presented* at *Pure and Applied Chemistry International Conference 2016 Thailand*, BITEC, Bangkok, Thailand, February 9-11, 2016.

## M.Sc. Student:

1) Miss Fatima Klongdee (2017): "Series of Pyrazole-3,5-dicarboxylato Copper Coordination Polymers: Structural Diversity, Anion-dependent Structural Assembly, Magnetic and Anion Exchange Studies" Master of Science in Chemistry, Graduate School, Khon Kaen University.

## **APPENDICES**

## **Publication papers:**

## Part I:

F. Klongdee, <u>J. Boonmak</u>\*, B. Moubaraki, K. S. Murray, S. Youngme, Copper(II) coordination polymers containing neutral trinuclear or anionic dinuclear building units based on pyrazole-3,5-dicarboxylate: Synthesis, structures and magnetic properties, *Polyhedron*, 2017, 126, 8-16. (IF 2016 = 1.926, Q2)

## Part II:

F. Klongdee, <u>J. Boonmak</u>\*, S. Youngme, Anion-dependent self-assembly of copper coordination polymers based on pyrazole3,5-dicarboxylate and 1,2-di(4-pyridyl) ethylene, *Dalton Transactions*, 2017, 46, 4806-4815.

(IF 2016 = 4.029, Q1)

# Dalton Transactions



## **PAPER**



**Cite this:** *Dalton Trans.*, 2017, **46**, 4806

# Anion-dependent self-assembly of copper coordination polymers based on pyrazole-3,5-dicarboxylate and 1,2-di(4-pyridyl)ethylene†

Fatima Klongdee, Jaursup Boonmak \*\* and Sujittra Youngme

By utilizing a pyrazole-3,5-dicarboxylic acid ( $H_3pzdc$ ) and flexible 1,2-di(4-pyridyl)ethylene (dpe) with various copper(II) salts under the same solvothermal synthetic conditions, six novel coordination polymers, namely, {[ $Cu_2(pzdc)(dpe)_2|X$ }<sub>n</sub> ( $X = NO_3^-$  (1),  $ClO_4^-$  (2),  $BF_4^-$  (3),  $SCN^-$  (4)), {[ $Cu(II)_4Cu(I)_4(pzdc)_4(dpe)_6](H_2O)_4$ }<sub>2n</sub> (5), and {[ $Cu_5(HPO_4)_2$  (pzdc)<sub>2</sub>(dpe)<sub>3</sub>]( $H_2O)_5$ }<sub>n</sub> (6) were obtained. The structural diversity of compounds 1–6 depends on the starting Cu(II) salts. Compounds 1–4 are isostructural and exhibit a 3D porous cationic pillar-layered coordination framework with lattice monoanions incorporated into the channels of the framework. When using copper(III) sulfate as a reagent, a neutral mixed-valence Cu(III) 2D + 2D  $\rightarrow$  2D parallel interpenetrated layer of 5 was obtained. In the case of a phosphate trianion, compound 6 shows a 3D coordination framework which contains  $\mu_4$ -HPO<sub>4</sub><sup>2-</sup> linking between Cu(III) centers. The anion-exchange properties of 1–4 were studied. Interestingly, compounds 1–4 exhibit the irreversible chemisorption of the thiocyanate anion instead of anion exchange without the destruction of their structural framework as confirmed by PXRD, IR, UV-Vis, and AA spectroscopy. Moreover, the anion-induced structural transformation of 1–4 was observed when exchanging with an azide anion. The luminescent properties of 1–6 and exchanged products were also investigated.

Received 2nd February 2017, Accepted 15th March 2017 DOI: 10.1039/c7dt00406k

rsc.li/dalton

## Introduction

Self-assembled coordination polymers (CPs) have gained extensive attention for not only their fascinating structural diversities but also their applications in many fields, such as gas storage, catalysis, magnetism, luminescence, and ion exchange. The structural assemblies can be influenced by many factors, such as the ligand, source of metal ion, counterion, stoichiometry, temperature, and the pH of the solution. Consequently, several architectures of CPs have been remarkably constructed. In the case of an anion, it can act as either a coordination ligand or counterion balancing the framework charge depending on its coordination ability. The use of different anions in the reaction may affect the self-assembly of coordination polymers. Notably, the study of cationic host frameworks for anionic guest exchange has become

a significant research area because the traditional ion exchange resin has the limitation of its thermal and chemical stability. Nowadays, many porous CPs with anion exchange properties have been widely reported. The anion exchange process in CPs generally involves either a solid-state diffusion mechanism or solvent-mediated exchange process. 15,16

The organic bridging ligand is a primary factor that controls and facilitates the formation of CPs. Pyrazole-3,5-dicarboxylic acid (H3pzdc) is a multifunctional ligand which exhibits various coordination abilities (Fig. S1†). 17-19 H<sub>3</sub>pzdc has six potential coordination sites including four carboxylate oxygen and two pyrazole nitrogen atoms. Thus, H<sub>3</sub>pzdc can coordinate as a mono- to hexadentate ligand. A variety of complexes based on H<sub>3</sub>pzdc containing transition and lanthanide metal ions have been documented.<sup>20-22</sup> The diversified CPs containing the Cu(II) ion have been known, in contrast to other transition metals, because the Cu(II) center exhibits diverse coordination geometries in one compound owing to Jahn-Teller distortion. The pyrazole-3,5-dicarboxylato Cu(II) complexes frequently provide a dinuclear or trinuclear Cu(II) building unit. 18,23 Apart from the H<sub>3</sub>pzdc ligand, the flexible N,N'ditopic spacer is used as an ancillary ligand for a dimensional extension. They can rotate or bend to adopt the appropriate conformation and hold the energetic minimum when coordinating to the metal centers, which causes a great structural

Materials Chemistry Research Center, Department of Chemistry and Center of Excellence for Innovation in Chemistry, Faculty of Science, Khon Kaen University, Khon Kaen, 40002, Thailand. E-mail: Jaursup@kku.ac.th

† Electronic supplementary information (ESI) available: X-ray crystallographic data 1–6 in CIF format. Figures for the diffuse-reflectance absorption spectra, PXRD patterns, packing structures, FTIR spectra, and tables for X-ray data collection. CCDC 1522622–1522627 for 1–6. For ESI and crystallographic data in CIF or other electronic format see DOI: 10.1039/c7dt00406k

Dalton Transactions Paper

diversity. In this work, 1,2-di(4-pyridyl)ethylene (dpe) was used as a flexible N,N'-ditopic co-ligand for increasing the dimensionality of Cu( $\pi$ ) pyrazole-3,5-dicarboxylate.

Herein a novel series of pyrazole-3,5-dicarboxylato  $Cu(\pi)$  coordination polymers with 1,2-di(4-pyridyl)ethylene have been synthesized by using various starting copper( $\pi$ ) salts, including  $NO_3^-$ ,  $ClO_4^-$ ,  $BF_4^-$ ,  $SCN^-$ ,  $SO_4^{2-}$ , and  $PO_4^{3-}$  anions; the structural diversity of all compounds indicates the role of the anion in the structural assemblies. The anion exchange properties of 1–4 have been studied. Also, the luminescent properties of 1–6 and exchanged products were investigated.

## **Experimental section**

#### Physical measurements

All chemicals and solvents were received from commercial sources and were used without further purification. FT-IR spectra were obtained by using the standard Pike ATR cell on a Bruker Tensor 27 FT-IR spectrophotometer in the 4000-600 cm<sup>-1</sup> spectral range. Solid-state electronic spectra were measured on a PerkinElmer Lambda2S spectrophotometer (400-1100 nm). Elemental analyses (C, H, N) were carried out with a PerkinElmer PE 2400CHNS analyzer. Thermogravimetric analyses (TGA) were done by using a Hitachi STA7200 thermal analyzer between 35 and 750 °C under an  $N_2$  atmosphere with a heating rate of 10 °C min<sup>-1</sup>. The X-ray powder diffraction (XRPD) data were collected at room temperature by using a PANalytical EMPYREAN with monochromatic CuKα, and the recording speed was 0.5 s per step in the  $2\theta$  range of 5–50°. The K<sup>+</sup> ion was detected by a PerkinElmer atomic absorption spectrometer (AAS). The solidstate fluorescent spectra of ligands H<sub>3</sub>pzdc, dpe, compounds 1-6, 1-4-SCN and 1-4-N<sub>3</sub> were measured using a SHIMADZU RF-5301PC Spectrofluorophotometer.

## Preparation of compounds 1-6

{[Cu<sub>2</sub>(pzdc)(dpe)<sub>2</sub>]NO<sub>3</sub>}<sub>n</sub> (1). The mixture solution of Cu(NO<sub>3</sub>)<sub>2</sub>·3H<sub>2</sub>O (0.5 mmol, 0.1208 g), 1,2'-di(4-pyridyl)ethylene (0.5 mmol, 0.0911 g) and pyrazole-3,5-dicarboxylic acid (0.5 mmol, 0.0871 g) in ethanol (2 mL), DMF (2 mL) and H<sub>2</sub>O (13 mL) was sealed in a 25 mL glass vial. The mixture solution was heated at 120 °C for 1 day and then slowly cooled down to room temperature. Blue crystals of 1 were obtained. Yield: 66 mg (37%) based on copper salt. Anal. Calcd for Cu<sub>2</sub>C<sub>29</sub>H<sub>21</sub>N<sub>7</sub>O<sub>7</sub>: C, 49.29; H, 3.00; N, 13.88. Found: C, 48.96; H, 3.10; N, 13.55%. ATR-FT-IR peaks ( $\nu$ (cm<sup>-1</sup>)): 1613s ( $\nu$ (C=N)), 1558s ( $\nu$ <sub>as</sub>(OCO)), 1505s, 1431w, 1395m ( $\nu$ <sub>s</sub>(OCO)), 1338s ( $\nu$ (NO<sub>3</sub><sup>-</sup>)), 1219m, 1114w, 1055m, 1026m, 977m, 832s, 792m. UV-vis (diffuse reflectance, cm<sup>-1</sup>): 15 015.

 $\{[Cu_2(pzdc)(dpe)_2]ClO_4\}_n$  (2). The preparation of 2 was similar to that of 1, except that  $Cu(ClO_4)_2 \cdot 6H_2O$  (0.5 mmol, 0.1853 g) replaced  $Cu(NO_3)_2 \cdot 3H_2O$ . Blue crystals of 2 were obtained. Yield: 112 mg (60%) based on copper salt. Anal. Calcd for  $Cu_2C_{29}ClH_{21}N_6O_8$ : C, 46.81; H, 2.84; N, 11.29. Found: C, 46.74; H, 2.62; N, 11.22%. ATR-FT-IR peaks ( $\nu(cm^{-1})$ ): 1610s

 $(\nu(C=N))$ , 1549s  $(\nu_{as}(OCO))$ , 1501s, 1432m, 1388m  $(\nu_{s}(OCO))$ , 1335s, 1287w, 1206m, 1089s  $(\nu(ClO_4^-))$ , 1029m, 972m, 831s, 828w, 792m. UV-vis (diffuse reflectance, cm<sup>-1</sup>): 14 881.

Caution: Perchlorate salts are highly explosive and must be handled with care.

{[Cu<sub>2</sub>(pzdc)(dpe)<sub>2</sub>]BF<sub>4</sub>}<sub>n</sub> (3). The preparation of 3 was similar to that of 1, except that Cu(BF<sub>4</sub>)<sub>2</sub>·nH<sub>2</sub>O (0.5 mmol, 0.1186 g) replaced Cu(NO<sub>3</sub>)<sub>2</sub>·3H<sub>2</sub>O. Blue crystals of 3 were obtained. Yield: 33 mg (18%) based on copper salt. Anal. Calcd for Cu<sub>2</sub>C<sub>29</sub>BF<sub>4</sub>H<sub>21</sub>N<sub>6</sub>O<sub>4</sub>: C, 47.62; H, 2.89; N, 11.49. Found: C, 47.38; H, 2.76; N, 11.65%. ATR-FT-IR peaks ( $\nu$ (cm<sup>-1</sup>)): 1611s ( $\nu$ (C=N)), 1550s ( $\nu$ <sub>as</sub>(OCO)), 1502s, 1432m, 1389m ( $\nu$ <sub>s</sub>(OCO)), 1337s, 1289w, 1208m, 1053s ( $\nu$ (BF<sub>4</sub><sup>-</sup>)), 1026s, 970s, 832s, 790m. UV-vis (diffuse reflectance, cm<sup>-1</sup>): 14 970.

{[Cu<sub>2</sub>(pzdc)(dpe)<sub>2</sub>]SCN}<sub>n</sub> (4). The mixture solution of CuCl<sub>2</sub>·2H<sub>2</sub>O (0.5 mmol, 0.0824 g), 1,2'-di(4-pyridyl)ethylene (0.5 mmol, 0.0911 g), pyrazole-3,5-dicarboxylic acid (0.5 mmol, 0.0871 g) and KSCN (0.5 mmol, 0.0486 g) in ethanol (2 mL), DMF (2 mL) and H<sub>2</sub>O (13 mL) was sealed in a 25 mL glass vial. The mixture solution was heated at 120 °C for 1 day and then slowly cooled down to room temperature. Blue crystals of 4 were obtained. Yield: 114 mg (65%) based on copper salt. Anal. Calcd for Cu<sub>2</sub>C<sub>30</sub>H<sub>21</sub>N<sub>7</sub>O<sub>4</sub>S: C, 51.28; H, 3.01; N, 13.95. Found: C, 50.94; H, 3.09; N, 13.97%. ATR-FT-IR peaks (ν(cm<sup>-1</sup>)): 2050m (ν(SCN<sup>-</sup>)), 1612s (ν(C=N)), 1552s (ν<sub>as</sub>(OCO)), 1504s, 1430m, 1392m (ν<sub>s</sub>(OCO)), 1338s, 1209m, 1112w, 1052m, 1011m, 968m, 829s, 793m. UV-vis (diffuse reflectance, cm<sup>-1</sup>): 15 020.

{[Cu<sub>4</sub>Cu<sub>4</sub><sup>I</sup>(pzdc)<sub>4</sub>(dpe)<sub>6</sub>](H<sub>2</sub>O)<sub>4</sub>}<sub>2n</sub> (5). The preparation of 5 was similar to that of 1, except that CuSO<sub>4</sub>·5H<sub>2</sub>O (0.5 mmol, 0.1248 g) replaced Cu(NO<sub>3</sub>)<sub>2</sub>·3H<sub>2</sub>O. Green crystals of 5 were obtained. Yield: 14 mg (10%) based on copper salt. Anal. Calcd for Cu<sub>8</sub>C<sub>92</sub>H<sub>72</sub>N<sub>20</sub>O<sub>20</sub>: C, 48.34; H, 3.17; N, 12.25. Found: C, 48.22; H, 3.28; N, 12.55%. ATR-FT-IR peaks (ν(cm<sup>-1</sup>)): 3274br (ν(OH)), 1595br ((ν(C=N)) and ν<sub>as</sub>(OCO)), 1500w, 1478m, 1413w, 1381m (ν<sub>s</sub>(OCO)), 1292s, 1230m, 1064m, 1000m, 828s, 768(m). UV-vis (diffuse reflectance, cm<sup>-1</sup>): 14 925.

{[Cu<sub>5</sub>(HPO<sub>4</sub>)<sub>2</sub>(pzdc)<sub>2</sub>(dpe)<sub>3</sub>](H<sub>2</sub>O)<sub>5</sub>}<sub>n</sub> (6). The preparation of 6 was similar to that of 1, except that Cu<sub>3</sub>(PO<sub>4</sub>)<sub>2</sub>·2H<sub>2</sub>O (0.5 mmol, 0.2080 g) replaced Cu(NO<sub>3</sub>)<sub>2</sub>·3H<sub>2</sub>O. Purple crystals of 6 were obtained. Yield: 75 mg (52%) based on copper salt. Anal. Calcd for Cu<sub>5</sub>C<sub>46</sub>H<sub>44</sub>N<sub>10</sub>O<sub>21</sub>P<sub>2</sub>: C, 38.04; H, 3.05; N, 9.64. Found: C, 37.72; H, 2.86; N, 9.70%. ATR-FT-IR peaks (ν(cm<sup>-1</sup>)): 3381br (ν(OH)), 1636br (ν(C=N)), 1609br (ν<sub>as</sub>(OCO)), 1504m, 1427m, 1393m (ν<sub>s</sub>(OCO)), 1327m, 1297m, 1208w, 1065br (ν(HPO<sub>4</sub><sup>2-</sup>)), 1000br (ν(HPO<sub>4</sub><sup>2-</sup>)), 921s, 833s, 781s. UV-vis (diffuse reflectance, cm<sup>-1</sup>): 14 327.

## X-ray crystallography

The single-crystal X-ray data of **1–6** were collected at 298 K (except for 1 which was collected at 100 K) by using a Bruker D8 Quest PHOTON100 with graphite-monochromated MoK $\alpha$  radiation using the APEX2 program. Data integration was done by SAINT<sup>25</sup> and absorption correction was perfomed by SADABS. The structure solution was solved by intrinsic

Paper Dalton Transactions

phasing<sup>27</sup> and refined by the least-squares method on  $F^2$  with anisotropic thermal parameters for non-H atoms using the SHELXTL program.<sup>28</sup> The H atoms were assigned to the calculated positions and isotropically refined. The disordered counteranions in 1-4 (NO<sub>3</sub><sup>-</sup> for 1, ClO<sub>4</sub><sup>-</sup> for 2, BF<sub>4</sub><sup>-</sup> for 3, and SCN<sup>-</sup> for 4) locate on a crystallographic inversion center, so the occupancies of all counteranions were refined to 0.5. The highly disordered SCN<sup>-</sup> in 4 was isotropically refined. The disordered lattice water molecules were removed from the diffraction data for compounds 5 and 6 using the SQUEEZE instruction of PLATON software. 29-31 The total electron count removed per unit cell by SQUEEZE was 344 for 5 and 47 for 6. The number of electrons per molecule was 86 (Z' = 2, Z = 4) and 47 (Z = 1), which were assigned to eight and five water molecules in the formulas, respectively. The actual water molecules in the unit cell are further determined by the elemental analyses and thermogravimetric analyses (TGA). The crystal data, selected bond lengths, and angles for compounds 1-6 are shown in Tables 1 and S1.†

#### Anion exchange experiments

The anion-exchange experiments were performed with compounds 1–4. 20 mg of the powder sample was added into a saturated aqueous solution (5 mL) of NaNO<sub>3</sub>, NaClO<sub>4</sub>, NaBF<sub>4</sub>, NaN<sub>3</sub>, or KSCN and constantly stirred at ambient temperature for 1 day. Then, the solid sample was collected by filtration, washed with 50 mL of deionized water, and dried in air for 1 day. The solid product was characterized by IR and UV-Vis spectroscopy, and PXRD. The occurrence of anion exchange was verified by comparison of the characterization data with those for 1–4. For 1-SCN, IR (cm<sup>-1</sup>):  $\nu$ (CN) 2105;  $\nu$ (NO<sub>3</sub>) 1338. UV-vis (cm<sup>-1</sup>): 15 060. For 2-SCN, IR (cm<sup>-1</sup>):  $\nu$ (CN) 2102;

 $\nu({\rm ClO_4})$  1089. UV-vis (cm<sup>-1</sup>): 14 970. For 3-SCN, IR (cm<sup>-1</sup>):  $\nu({\rm CN})$  2103;  $\nu({\rm BF_4})$  1051. UV-vis (cm<sup>-1</sup>): 15 015. For 4-SCN, IR (cm<sup>-1</sup>):  $\nu({\rm CN})$  2050 and 2106. UV-vis (cm<sup>-1</sup>): 15 037. For 1-N<sub>3</sub>, IR (cm<sup>-1</sup>):  $\nu({\rm N_3})$ : 2069. UV-vis (cm<sup>-1</sup>): 16 260 and 13 072. For 2-N<sub>3</sub>, IR (cm<sup>-1</sup>):  $\nu({\rm N_3})$ : 2069. UV-vis (cm<sup>-1</sup>): 16 367 and 13 458. For 3-N<sub>3</sub>, IR (cm<sup>-1</sup>):  $\nu({\rm N_3})$ : 2064. UV-vis (cm<sup>-1</sup>): 16 077 and 13 123. For 4-N<sub>3</sub>, IR (cm<sup>-1</sup>):  $\nu({\rm N_3})$ : 2069. UV-vis (cm<sup>-1</sup>): 15 870.

## Results and discussion

## General observations and spectroscopic techniques

Compounds 1–6 were obtained by the solvothermal reactions of  $H_3pzdc$ , dpe and many copper(II) salts under the same conditions. Compounds 1–4 are isostructural and exhibit 3D pillar-layered cationic frameworks, interspersed with lattice monoanions within the channels. Each lattice anion is surrounded by four  $\mu_2$ -dpe pillar-linkers with a variety of torsion angles, depending on the kind of counteranion. Compound 5 shows a neutral mixed-valence  $Cu(\iota,II)$  2D interpenetrated network without the sulfate anion in the lattice. In contrast, compound 6 shows a 3D coordination framework containing a coordinated  $\mu_4$ -hydrogen phosphate anion. The different structural frameworks of all compounds indicate the significant role of anions in the self-assembly.

The ATR-IR spectra of **1–6** (Fig. S2 and S3†) reveal the strong intensity peak around 1610 cm<sup>-1</sup> which can be assigned to the stretching vibrations of the pyridine ring. The peaks around approximately 1600–1400 cm<sup>-1</sup> correspond to the asymmetric and symmetric stretching vibrations of the carboxylate group for the pzdc ligand.<sup>32</sup> The IR spectra of **1–4** show a characteristic strong peak for each counteranion at 1338 cm<sup>-1</sup> ( $\nu$ (NO<sub>3</sub><sup>-</sup>) in **1**),<sup>13</sup> 1089 cm<sup>-1</sup> ( $\nu$ (ClO<sub>4</sub><sup>-</sup>) in **2**),<sup>14</sup> 1053 cm<sup>-1</sup>

Table 1 Crystallographic data for compounds 1-6

| Compound   | 1   | 2   | 3   | 4   | 5  | 6  |
|--|---|---|---|---|--|--|
| Formula  | Cu <sub>2</sub> C <sub>29</sub> H <sub>21</sub> N <sub>7</sub> O <sub>7</sub> | Cu <sub>2</sub> C <sub>29</sub> ClH <sub>21</sub> N <sub>6</sub> O <sub>8</sub> | Cu <sub>2</sub> BC <sub>29</sub> F <sub>4</sub> H <sub>21</sub> N <sub>6</sub> O <sub>4</sub> | Cu <sub>2</sub> C <sub>30</sub> H <sub>21</sub> N <sub>7</sub> O <sub>4</sub> S | Cu <sub>16</sub> C <sub>184</sub> H <sub>128</sub> N <sub>40</sub> O <sub>40</sub> | Cu <sub>5</sub> C <sub>46</sub> H <sub>34</sub> N <sub>10</sub> O <sub>16</sub> P <sub>2</sub> |
| Molecular weight                                 | 706.61  | 744.05  | 731.41  | 702.68  | 4427.90  | 1362.67  |
| T(K)   | 100(2)  | 298(2)  | 298(2)  | 298(2)  | 298(2)   | 298(2)   |
| Crystal system                                   | Orthorhombic  | Orthorhombic  | Orthorhombic  | Orthorhombic  | Monoclinic   | Triclinic  |
| Space group                                      | Pnma  | Pnma  | Pnma  | Pnma  | P21/n  | $P\bar{1}$   |
| a (Å)  | 12.4115(7)  | 12.8632(8)  | 12.7573(6)  | 12.7346(9)  | 16.3570(7)   | 9.8788(4)  |
| a (Å)<br>b (Å)                                   | 26.8057(16)   | 26.6997(18)   | 26.7175(13)   | 26.731(2)   | 26.4808(12)  | 11.1243(4)   |
| $c(\mathring{A})$                                | 8.4121(5)   | 8.4942(6)   | 8.4773(3)   | 8.4383(6)   | 21.4340(9)   | 13.8420(6)   |
| $\alpha (\circ)$                                 | 90  | 90  | 90  | 90  | 90   | 69.7760(10)  |
| $\beta$ ( $\circ$ )                              | 90  | 90  | 90  | 90  | 93.7730(10)  | 79.7190(10)  |
| γ (°)  | 90  | 90  | 90  | 90  | 90   | 64.4060(10)  |
| $V(\mathring{A}^3)$                              | 2798.7(3)   | 2917.3(3)   | 2889.4(2)   | 2872.4(4)   | 9263.9(7)  | 1286.56(9)   |
| Z  | 4   | 4   | 4   | 4   | Z'=2   | 1  |
| $\rho_{\rm cald}  ({\rm g  cm}^{-3})$            | 1.677   | 1.694   | 1.681   | 1.625   | 1.587  | 1.759  |
| $\mu \text{ (Mo K}\alpha) \text{ (mm}^{-1})$     | 1.582   | 1.613   | 1.546   | 1.604   | 1.876  | 2.175  |
| Data collected                                   | 3145  | 3055  | 3659  | 2886  | 18 998   | 5294   |
| Unique data $(R_{int})$                          | 2409(0.0612)  | 2031(0.0846)  | 2168(0.1181)  | 1755(0.0905)  | 10 197 (0.1063)  | 3845(0.0470)   |
| $R_1^a/WR_2^b$ $[I > 2\sigma(I)]$                | 0.0511/0.0926   | 0.0769/0.1887   | 0.0724/0.1431   | 0.0687/0.1630   | 0.0634/0.1152  | 0.0416/0.0801  |
| $R_1^a/wR_2^b$ [all data]                        | 0.0810/0.1004   | 0.1356/0.2085   | 0.1509/0.1683   | 0.1394/0.1944   | 0.1516/0.1417  | 0.0728/0.0903  |
| GOF  | 1.129   | 1.189   | 1.050   | 1.055   | 1.002  | 1.011  |
| Max/min electron<br>density (e Å <sup>-3</sup> ) | 0.650/-0.755  | 0.768/-1.118  | 0.824/-0.950  | 1.578/-0.883  | 1.513/-0.853   | 0.711/-0.560   |

 $<sup>^{</sup>a}R = \sum ||F_{o}| - |F_{c}||/\sum |F_{o}|$ .  $^{b}R_{w} = \{\sum [w(|F_{o}| - |F_{c}|)]^{2}/\sum [w|F_{o}|^{2}]\}^{1/2}$ .

Dalton Transactions Paper

 $(\nu(\mathrm{BF_4}^-)~\mathrm{in}~3)^{33}$  and 2050 cm $^{-1}~(\nu(\mathrm{SCN}^-)~\mathrm{in}~4).^{34}$  The IR spectrum of 6 shows medium peaks in the range of 1100–1000 cm $^{-1}$  corresponding to the vibration of the phosphate anion. The broad peaks around 3600–3200 cm $^{-1}~\mathrm{in}~5$  and 6 are assigned to  $\nu(\mathrm{OH})$  from the water molecules. The solid-state UV-Vis spectra of 1–6 were studied at room temperature (Fig. S5†). All compounds exhibit a single broad absorption band around 15 200–14 300 cm $^{-1}$  which corresponds to distorted octahedral and square pyramidal geometries for Cu(II).  $^{35,36}$ 

#### **Description of crystal structures**

Crystal structures of  $\{[Cu_2(pzdc)(dpe)_2]X\}_n$  (X = NO<sub>3</sub><sup>-</sup> (1), ClO<sub>4</sub><sup>-</sup> (2), BF<sub>4</sub><sup>-</sup> (3), SCN<sup>-</sup> (4)). Single-crystal analysis revealed that compounds 1-4 are isostructural and they crystallize in the orthorhombic *Pnma* space group. The crystal structure of 1 is described in detail herein. There are two crystallographically independent Cu(II) centers (Cu1 and Cu2) located on a crystallographic mirror plane. The Cu1 ion is five-coordinated, adopting a square pyramidal geometry ( $\tau = 0.01$  for 1,  $\tau = 0.12$  for 2,  $\tau = 0.09$  for 3,  $\tau = 0.08$  for 4, Addison's parameter  $\tau = 0$  for square pyramid and  $\tau = 1$  for trigonal bipyramid).<sup>37</sup> Each Cu1 center is coordinated by two carboxylate oxygen atoms (O1, O3) from two different pzdc<sup>3-</sup> ligands and two pyridine nitrogen atoms from two  $\mu_2$ -dpe in the equatorial plane. The axial position is occupied by a pyrazole nitrogen atom (N4). The central Cu2 is six-coordinated adopting an elongated octahedral geometry. The basal plane is occupied by one carboxylate oxygen atom from pzdc3-, one pyrazole nitrogen atom from another pzdc<sup>3-</sup> and two pyridyl nitrogen atoms from two  $\mu_2$ -dpe. The apical position is located by two carboxylate oxygen atoms from two distinct pzdc<sup>3-</sup> (O1, O2) (Fig. 1). The Cu-N and Cu-O distances are in the range of 1.949(4)-2.173(4) Å, while the elongated axial Cu2-O distances are 2.305(4) and 2.425(4) Å, indicating the presence of a common Jahn-Teller effect in the  $Cu(\pi)$  ion. <sup>20,38</sup> The  $Cu1N_2O_2$  plane is not totally

planar with tetrahedral distortion between the planes of 20.71° (26.88° for 2, 25.62° for 3, 24.94° for 4). Cu1 is shifted by 0.259(1) Å (0.324(2) Å for 2, 0.316(2) Å for 3, 0.306(2) Å for 4) from the mean equatorial plane toward the axial position. Pzdc<sup>3-</sup> connects the Cu1 and Cu2 ions in a  $\mu_5$ - $\eta^1$ O,  $\eta^2$ N',O', η<sup>2</sup>N",O", η<sup>1</sup>O", η<sup>1</sup>O" coordination mode (Fig. S1†) to form a two-dimensional (2D) cationic Cu(II) layered coordination polymer in the ac crystallographic plane. The layer consists of a 13-membered macrocycle enclosed by three Cu(II) ions and four pzdc<sup>3-</sup> with the closest Cu···Cu distance of 3.914 (1) Å (Fig. 2). Also, the  $\mu_2$ -dpe spacers connect adjacent layers along the b crystallographic axis constructing a 3D cationic pillarlayer coordination framework (Fig. 4). The two pyridine rings of bipyridyl moieties are not coplanar with the dihedral angle between the two planar pyridine rings of 5.06° (3.20° for 2, 2.23° for 3, 2.00° for 4). The C-CH=CH-C torsion angle of  $\mu_2$ -dpe is 178.25–179.62° for 1–4. The Cu···Cu separation *via*  $\mu_2$ -dpe is 13.418(1) Å for 1 (13.388 (1) Å for 2, 13.391(1) Å for 3, and 13.400(1) Å for 4). The 3D cationic framework of 1 contains a 1D open-channel along the c axis which is occupied by a disordered NO<sub>3</sub><sup>-</sup> lattice anion (Fig. 3). The dimension of the channel in the ab plane is about 3.95  $\times$  13.42 Å<sup>2</sup> (4.65  $\times$ 13.39  $\text{Å}^2$  for 2, 4.49 × 13.39  $\text{Å}^2$  for 3, and 4.45 × 13.40  $\text{Å}^2$  for 4). Besides electrostatic interaction between the cationic framework and anionic guest, the weak intermolecular hydrogen bonds involving the C-H of the  $\mu_2$ -dpe linker and lattice anion also stabilize the entire supramolecular frameworks of 1-3 (Fig. 4, Table S2†).

Crystal structure of {[Cu<sub>4</sub>(I)Cu(II)<sub>4</sub>(pzdc)<sub>4</sub>(dpe)<sub>6</sub>](H<sub>2</sub>O)<sub>4</sub>}<sub>2n</sub> (5). Single-crystal analysis revealed that compound 5 crystallizes in the monoclinic,  $P2_1/n$  space group. The asymmetric unit of 5 contains four Cu(II) ions (Cu1–Cu4), four Cu(I) ions (Cu5–Cu8), four pzdc<sup>3–</sup>, six dpe ligands and four lattice water molecules. All monovalent copper atoms are three-coordination completed by one carboxylate oxygen atom from pzdc<sup>3–</sup> and two pyridyl nitrogen atoms from two different  $\mu_2$ -dpe. The Cu(I)–N and Cu(I)–O distances are in the ordinary range of 1.901(4)–

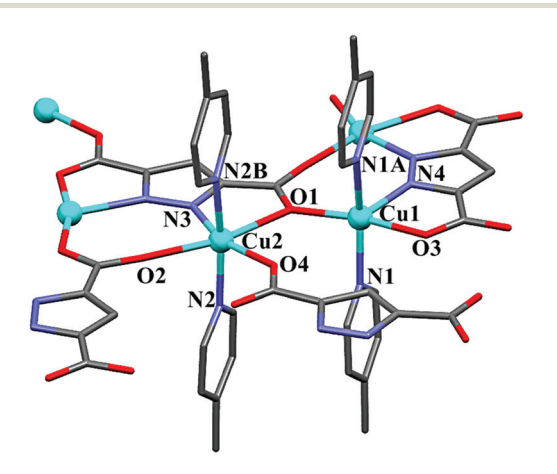


**Fig. 1** Crystal structure and atom labeling scheme of **1**. All hydrogen atoms and lattice nitrate anions are omitted for clarity (symmetry code: A = x, 0.5 - y, z; B = 1 - x, -0.5 + y, 1 - z).

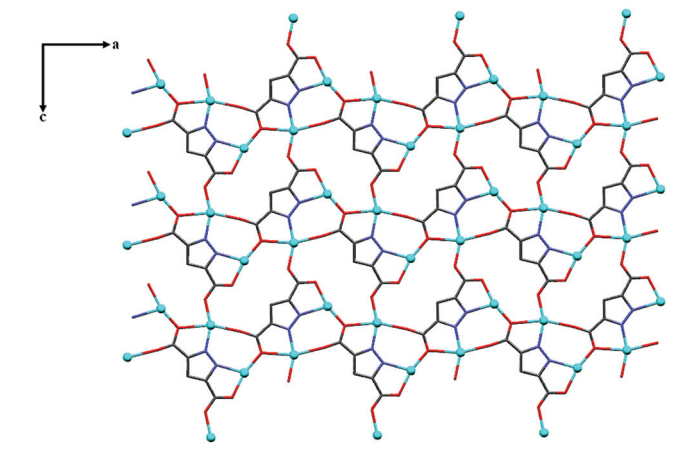


Fig. 2 The 2D layer of 1 in the ac plane constructed by Cu(11) ions and  $\mu_5\text{-pzdc}^{3-}.$ 

Paper Dalton Transactions

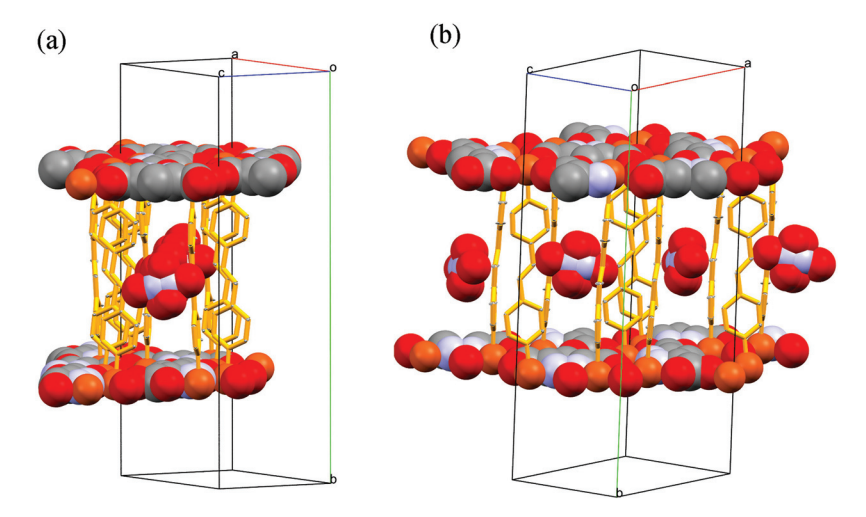


Fig. 3 The space-filling model of disordered  $NO_3^-$  anions incorporated into the 1D open-channel of the 3D cationic framework of 1 in different views.

2.345(4) Å. 39,40 While all divalent copper atoms display a square pyramidal geometry ( $\tau = 0.02-0.05$ ) and are coordinated by two carboxylate oxygen atoms and two pyrazoyl nitrogen atoms from two pzdc<sup>3-</sup> in the basal plane, the axial position is occupied by one nitrogen atom from  $\mu_2$ -dpe. The Cu(II)-N and Cu(II)-O distances are in the range of 1.921(4)-2.264(4) Å. 20,38 The CuN<sub>2</sub>O<sub>2</sub> square base is not totally planar with a tetrahedral twist between the planes of 23.29°, 22.83°, 24.77°, and 23.60° for Cu1-Cu4, respectively. Cu(II) is shifted by 0.306(1) Å, 0.298(1) Å, 0.324(1) Å, and 0.310(1) Å from the mean equatorial plane toward the axial site for Cu1-Cu4, respectively. The calculation of the bond valence sum (BVS) for copper centers in 5 was also performed using the Cu-X bond constants derived previously (see the ESI†).41-43 The BVS analysis resulted in the values of 2.10, 2.14, 2.11, 2.11 for Cu1-Cu4, respectively, and 0.93, 0.94, 0.94, and 0.93 for Cu5-Cu8, respectively, thus confirming the formal oxidation states of +2 for Cu1-Cu4 and +1 for Cu5-Cu8 ions. Two pzdc<sup>3-</sup> ligands bind two Cu(II) ions, giving a dinuclear Cu(II) unit with Cu···Cu separations of 3.957(1) and 3.950(1) Å. Each dinuclear  $Cu(\pi)$  unit is connected via double  $\mu_2$ -dpe spacers with a Cu···Cu separation of 13.876(1) and 13.891(1) Å, forming a tetranuclear Cu(II) unit. Each tetranuclear Cu(II) unit consists of two  $[Cu(II)_2(pzdc)_2]^{2-}$  conformations as A and B forms (Fig. 5). In the case of the A form, the dinuclear Cu(II) unit adopts the cis-conformation for two carboxylate bridges which are connected to two Cu(I) centers in  $\mu_3$ - $\eta^2$ N,O,  $\eta^2$ N',O',  $\eta^1$ O"-pzdc<sup>3</sup>bridging mode (Fig. S1†). For the B form, the dinuclear Cu(II) unit adopts the trans-conformation for two carboxylate bridges which are linked to two Cu(I) centers through two pzdc<sup>3-</sup> in  $\mu_3 - \eta^2 N_1 O_1$ ,  $\eta^2 N'_1 O'_2$ ,  $\eta^1 O''_3$  and  $\mu_3 - \eta^2 N_2 O_3$ ,  $\eta^2 N'_2 O'_3$ ,  $\eta^1 O'_3$  modes (Fig. S1†). Moreover, each 3-connected Cu(I) center links with two neighboring Cu(I) centers via two  $\mu_2$ -dpe and also connects with a tetranuclear Cu(II) unit giving rise to a mixed-valence Cu(I)-Cu(II) two-dimensional coordination layer (Fig. 6a). The C-CH=CH-C torsion angle of  $\mu_2$ -dpe spacers is in the range of

176.29–179.30°. Furthermore, two adjacent layers are interpenetrated to form a two-fold 2D  $\rightarrow$  2D parallel interpenetrating network as shown in Fig. 6b.

Crystal structure of  $\{[Cu_5(HPO_4)_2(pzdc)_2(dpe)_3](H_2O)_5\}_n$  (6). Compound 6 crystallizes in the triclinic  $P\bar{1}$  space group. The asymmetric unit contains three crystallographically independent Cu(II) ions, one Hpzdc<sup>2-</sup>, one-half of dpe ligands, one hydrogen phosphate, and five lattice water molecules. The coordination environment of Cu(II) centers is shown in Fig. 7. The Cu1 center exhibits a square pyramidal geometry ( $\tau$  = 0.15), coordinated by one carboxylate oxygen, one pyrazole nitrogen atom from pzdc3-, one hydrogen phosphate oxygen (O5), and one pyridyl nitrogen from  $\mu_2$ -dpe in a basal position. The axial site is occupied by an oxygen from another  $HPO_4^{2-}$ . The Cu1N2O2 square plane is not totally planar with tetrahedral distortion between the planes of 9.87°. Cu1 is shifted by 0.010(1) Å from the mean equatorial plane toward the axial position. Cu2 is four-coordinated with a square planar geometry ( $\tau_4$  = 0.20, four-coordinate geometry index  $\tau_4$  = 0 for a perfect square planar and  $\tau_4 = 1$  for a perfect tetrahedron).<sup>44,45</sup> The copper(II) center is completed by one carboxylate oxygen and one pyrozole nitrogen atom from pzdc3-, oxygen from  $HPO_4^{2-}$  and one pyridyl nitrogen from  $\mu_2$ -dpe. The  $Cu2N_2O_2$ square base is not completely planar with tetrahedral distortion between the planes of 16.69°. The Cu3 center lies on a crystallographic inversion center and adopts a perfect square planar geometry which is bonded with two pyridyl nitrogen from  $\mu_2$ -dpe and two oxygen atoms from two different HPO<sub>4</sub><sup>2-</sup>. The Cu-N and Cu-O distances are in the range of 1.890(3)-2.382(2) Å. The Cu1 and Cu2 ions are connected by  $\mu_2 - \eta^2 N_1 O_1$ , η<sup>2</sup>N',O'-pzdc<sup>3-</sup> (Fig. S1†) forming a Cu(II) dimer with a Cu···Cu separation of 4.315(1) Å. Then, two hydrogen phosphate anions connect two adjacent dinuclear Cu(II) units and two Cu3 centers generating a 1D chain of Cu3-HPO<sub>4</sub>-[Cu1Cu2]<sub>2</sub>-HPO<sub>4</sub> along the crystallographic b axis (Fig. 8a). Moreover, each 1D chain of 6 is linked together by six  $\mu_2$ -dpe spacers in a

Dalton Transactions Paper

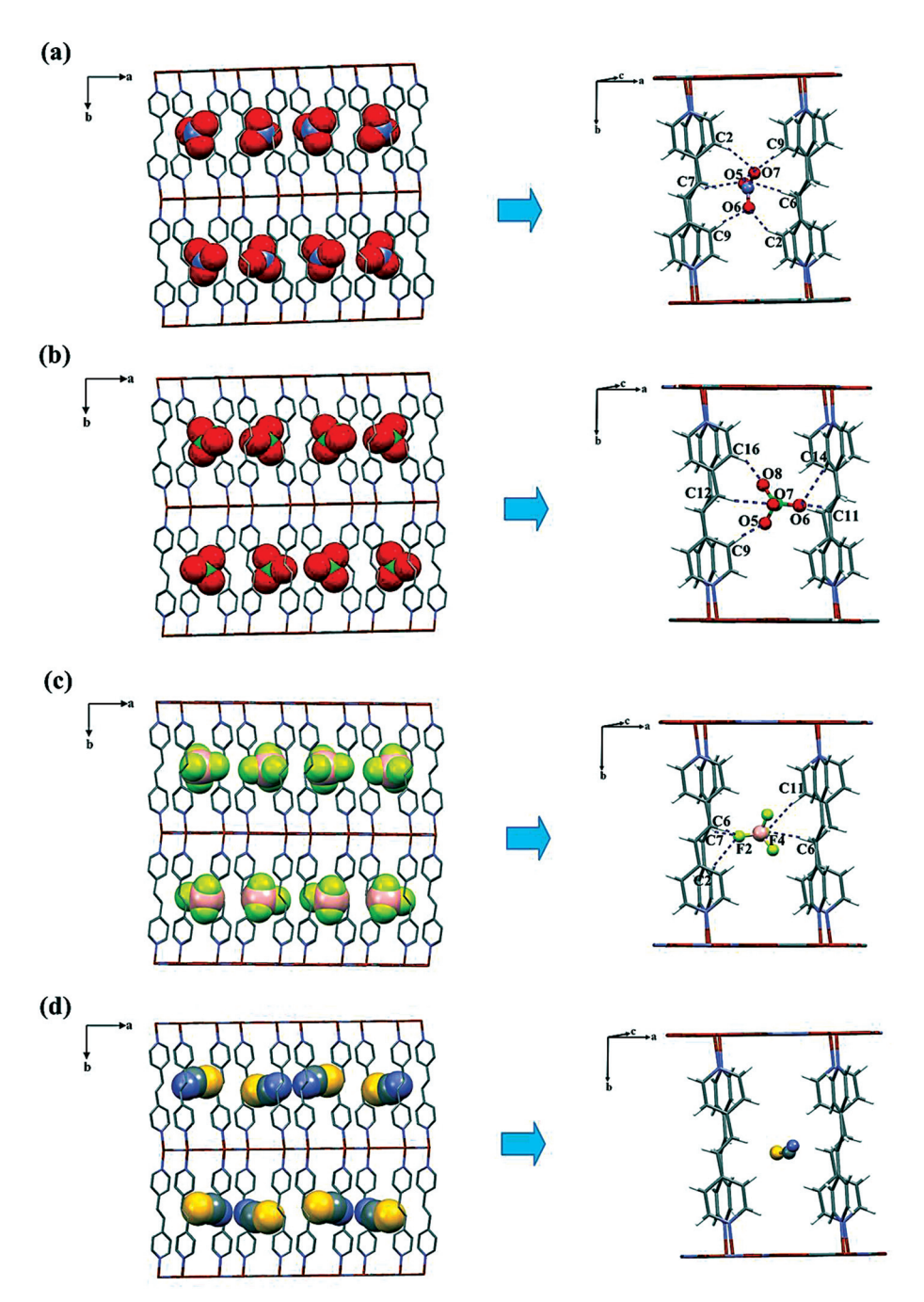


Fig. 4 The 3D porous cationic frameworks in the ab plane containing NO<sub>3</sub><sup>-</sup> for 1 (a), ClO<sub>4</sub><sup>-</sup> for 2 (b), BF<sub>4</sub><sup>-</sup> for 3 (c), and SCN<sup>-</sup> for 4 (d) in the pores. The insets present the weak hydrogen bonds between C-H of the dpe linker and lattice anions. The disordered positions of all anions are omitted for clarity.

different direction to generate a 3D framework as shown in Fig. 8b (Fig. S4 $\dagger$ ).

## Thermal analyses

Thermogravimetric analysis (TGA) of all compounds except compound 2 was performed under a  $N_2$  atmosphere from 30–750 °C. Compound 2 contains a perchlorate anion which may be potentially explosive at high temperature. The isostruc-

tures of 1–4 are stable up to about 300 °C. Then the structures collapsed. Compound 5 shows a gradual weight loss of 3.2% from 30–260 °C corresponding to the escape of eight water molecules (calcd 3.2%). Then the structure is decomposed. Compound 6 reveals a gradual weight loss of 6.0% in the range of 30–280 °C corresponding to the release of five water molecules (calcd 6.2%). Then the structures decompose to  $[Cu_3(PO_4)_2]_2$  (found, 54.0%, calcd 52.4%) (Fig. S6†).

Paper Dalton Transactions

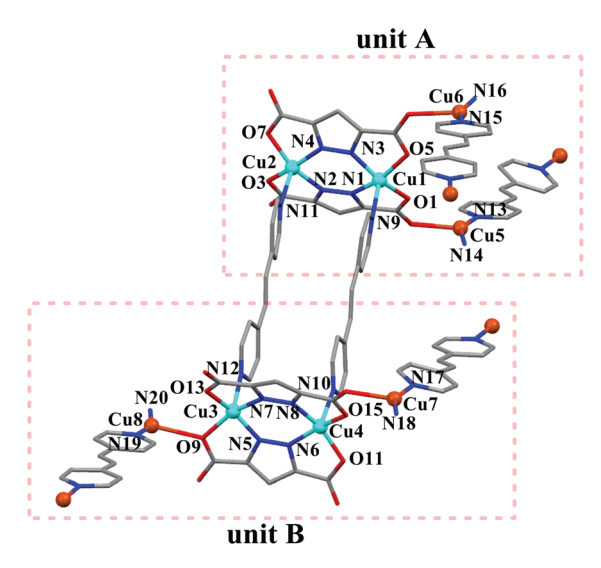


Fig. 5 View of the coordination environments of Cu(I) and Cu(II) ions in 5 with atom labels. All hydrogen atoms are omitted for clarity.

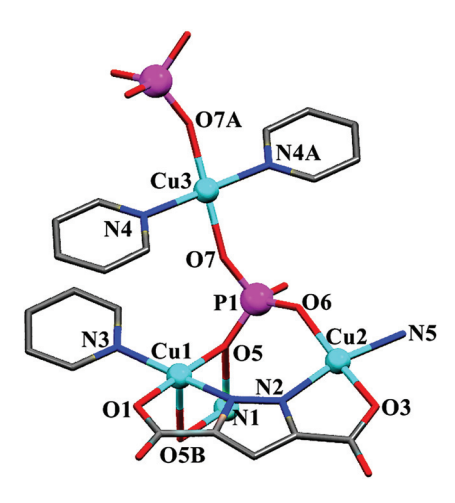


Fig. 7 The coordination environments of Cu(II) ions in 6. All hydrogen atoms are omitted for clarity (symmetry code: A = -x, 1 - y, 1 - z; B = -x, 2 - y, 1 - z).

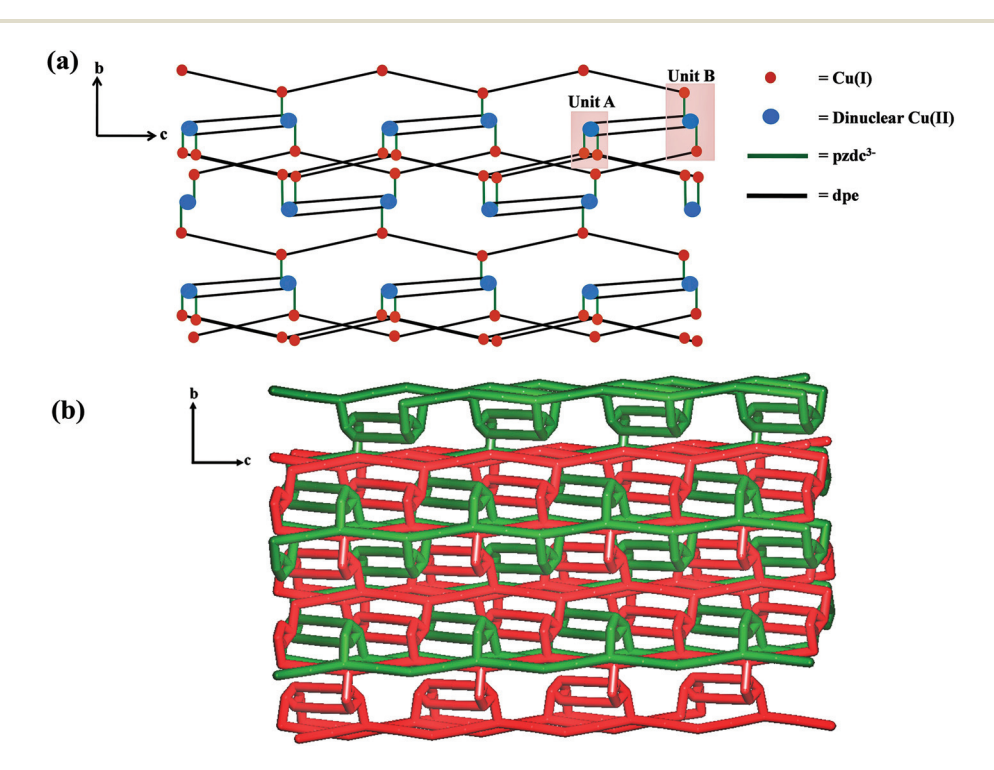


Fig. 6 (a) The mixed-valence Cu(I,II) 2D coordination polymer of 5 in the bc plane. (b) The two-fold 2D  $\rightarrow$  2D parallel interpenetrated network of 5.

#### Anion exchange studies and SCN sorption of 1-4

As demonstrated by the X-ray structures, the counteranions  $(NO_3^-(1), ClO_4^-(2), BF_4^-(3))$  and  $SCN^-(4)$  occupy the 1D channel of the 3D pillar-layered cationic frameworks of 1–4. In addition, compounds 1–4 are insoluble in common organic solvents and water. Consequently, these metal organic frameworks are potentially expected to exhibit anion exchange properties. The anion exchange of 1–4 was verified by IR and UV-Vis reflectance spectra and X-ray powder diffraction

(PXRD). When a suspension of crystalline powder of 1 in a saturated aqueous solution of KSCN was stirred continuously for 1 day at room temperature, the blue color of the crystalline solid changed to greenish blue. The IR spectrum of 1-SCN (Fig. 9) shows the identical intensity and position of the original  $\nu(NO_3^-)$  at 1338 cm<sup>-1</sup> along with increasing peak intensity at 2105 cm<sup>-1</sup>, which is an indication of the  $\nu(CN)$  of thiocyanate. The UV-Vis reflectance spectrum of 1-SCN shows a broad absorption band around 15 060 cm<sup>-1</sup> which is slightly blue-shifted in comparison with those of 1 implying that the

Dalton Transactions Paper

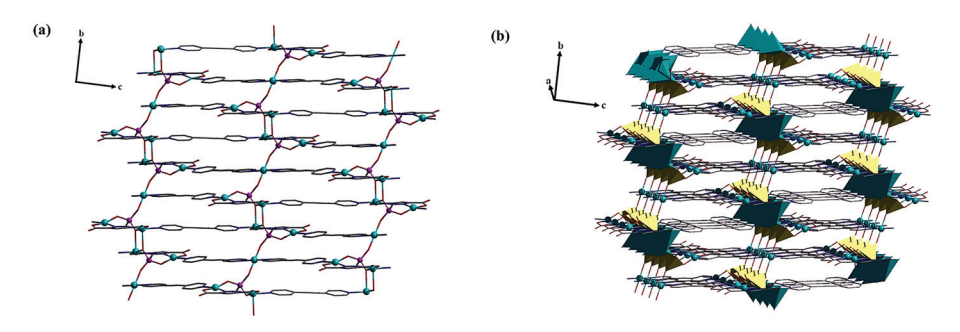


Fig. 8 (a) View of a 2D layer of 6 in the bc plane. (b) The 3D framework of 6. The yellow and blue polygons represent HPO<sub>4</sub><sup>2-</sup> and Cu(II) centers, respectively.

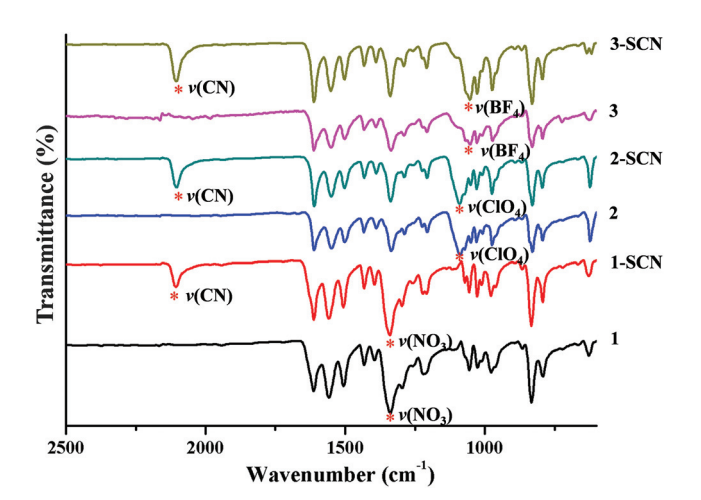


Fig. 9 IR spectra of the anion exchange products with the SCN<sup>-</sup> anion.

coordination environment around  $Cu(\pi)$  ions is varied (Fig. S8†). The PXRD pattern of **1-SCN** (Fig. 10) is identical to that of **1** which could be evidence for nonstructural transformation during the exchange process. In contrast, the  $NO_3^-$  in **1** could not be exchanged by  $ClO_4^-$  and  $BF_4^-$  anions which was confirmed by IR spectra.

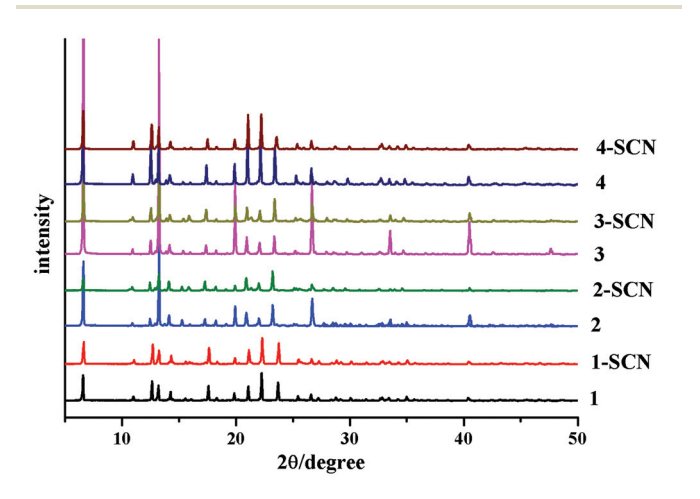


Fig. 10  $\,$  PXRD patterns of the anion exchange products with the SCN  $^-$  anion.

The above anion exchange procedure can be extended to other anions. When the blue crystalline solids of 2-3 were continuously stirred in a saturated aqueous solution of KSCN for 1 day, their colors were also changed to greenish blue. The IR spectra (Fig. 9) of the products of exchange also show the original peaks of  $\nu(\text{ClO}_4^-)$  at 1089 cm<sup>-1</sup> for 2, and  $\nu(\text{BF}_4^-)$  at 1051 cm<sup>-1</sup> for 3 and the appearance of new peaks at 2100 cm<sup>-1</sup>, being the same as 1-SCN. The UV-Vis reflectance spectra of 2-3-SCN exhibit blue-shifted absorption bands around 14 970-15 015 cm<sup>-1</sup> (Fig. S8†). The PXRD patterns of 2-3-SCN confirm that their crystallinities are still the same as the original crystalline phase during the anion exchange process (Fig. 10). In contrast, the ClO<sub>4</sub> in 2 is not exchanged by either NO<sub>3</sub> or BF<sub>4</sub> anions, and also the BF<sub>4</sub> in 3 is not exchanged by NO<sub>3</sub><sup>-</sup> and ClO<sub>4</sub><sup>-</sup>. Inversely, crystalline solids 1-3-SCN, and compound 4 cannot be replaced by other anions. According to the IR spectroscopic data that are used widely to monitor anion exchange, they reveal that the intensity of the vibrational peak of the original counteranion within the framework is not decreased after the anion exchange process, but the new peak of  $\nu(CN)$  around 2100 cm<sup>-1</sup> appears. It indicates that isostructures 1-3 exhibit the sorption properties of the SCN<sup>-</sup> anion without any anion exchange process. To confirm the sorption of the thiocyanate anion in these isostructural series, compound 4, which contains lattice SCN within the pores, was constantly stirred in a saturated aqueous solution of KSCN under the same conditions. Interestingly, the IR spectrum of **4-SCN** exhibits two characteristic peaks of  $\nu$ (CN). The new one appears at 2100 cm<sup>-1</sup> and the original one is at 2053 cm<sup>-1</sup> (Fig. S7†). The first peak of  $\nu$ (CN) that is identical to those of 1-3-SCN indicates Cu-SCN, thiocyanato complexes (2100-2120 cm<sup>-1</sup>), 46,47 whereas those peaks of lattice SCN<sup>-</sup> anions exhibit  $\nu$ (CN) at 2053 cm<sup>-1</sup>. <sup>34,47</sup> The crystalline phase of 4-SCN is identical to that of 4 which is verified by PXRD. The above results imply that isostructures 1-4 display chemisorption of thiocyanate without the destruction of their crystalline framework. Moreover, to balance the charge of the overall frameworks during chemisorption of the thiocyanate anion, we used atomic absorption spectroscopy (AAS) for the detection of K<sup>+</sup> ions in 1-4-SCN. The observed K<sup>+</sup> amount in the analytes is 0.13-0.16 mol K<sup>+</sup> per mol 1-4. The observed small amount of K<sup>+</sup> in 1-4-SCN suggests that the chemisorption of

Paper Dalton Transactions

SCN<sup>-</sup> may occur on the surface of 3D frameworks of **1–4** which agree with no observed solvent accessible voids for **1–4**, calculated by the PLATON program. The chemisorption of SCN<sup>-</sup> may be attributed to the unsaturated 5-coordination Cu(II) center in **1–4** which may play a crucial role in the chemisorption of SCN<sup>-</sup> without the collapse of their crystalline frameworks.

To further study the effect of the stronger coordinating ability of the anion, N<sub>3</sub> was used to examine the anion exchange properties of 1-4. The IR spectra of 1-4-N<sub>3</sub> show the disappearance of intense peaks of  $\nu(NO_3^-)$ ,  $\nu(ClO_4^-)$ ,  $\nu(BF_4^-)$ and  $\nu(CN^-)$  for 1-4, respectively, and exhibit the growth of a new N<sub>3</sub><sup>-</sup> peak at 2070 cm<sup>-1</sup> (Fig. S9†). 12,48 The UV-Vis reflectance spectra of 1-4-N3 show blue-shifted absorption bands around 16 367-15 870 cm<sup>-1</sup> which are in agreement with the alteration of color from blue to green (Fig. S10†). Moreover, 1-4-N<sub>3</sub> do not contain any number of Na<sup>+</sup> ions and this was verified by AAS, confirming the exchange process that the samples undergo. The PXRD patterns of  $1-4-N_3$  are different from those of the original 1-4 implying the anion-induced structural transformation (Fig. S11†). The resulting IR spectra and PXRD of the exchanged products differ significantly from that of the original compounds, suggesting that it is not only the original ions that are quantitatively displaced by N<sub>3</sub><sup>-</sup> but also the solid-state topology that is fully changed. It seems that the variation of their structures upon anion exchange may be related to the coordinating ability of the different anions. Therefore, the exchange of the lattice anion by a strong coordinating anion can produce a structural change. Notably, both the sorption of SCN and anion-exchange of N<sub>3</sub><sup>-</sup> mentioned above are irreversible processes which may involve the dissociation of Cu(II)-SCN or Cu(II)-N3 bonds. Therefore, they cannot be easily exchanged by other weak coordinating anions.

#### **Luminescent properties**

The solid-state emission spectra at room temperature of compounds 1-6, chemisorption samples 1-4-SCN, exchanged samples 1-4-N3, H3pzdc, and dpe ligands have been investigated. The free ligand dpe displays a strong emission peak at 368 nm and a small one at 509 nm ( $\lambda_{ex}$  = 320 nm) whereas H<sub>3</sub>pzdc displays two insignificant emission peaks at 368 and 472 nm ( $\lambda_{ex}$  = 285 nm) (Fig. S12†). The emission behavior of the ligands can be assigned to  $\pi^* \to \pi$  and  $\pi^* \to n$  transitions. Upon excitation of solid samples 1-6 and 1-4-SCN at 320 nm, they exhibit two emission bands with the main peak at 468 nm and the minor peak at about 362-370 nm (Fig. S12†). In comparison with the dpe ligand, the emission intensity of all compounds shows a quenching phenomenon at 368 nm. However, an enhancement of the intensity at around 468 nm was observed. The luminescent behavior may probably be ascribed to the ligand-to-ligand charge transfer (LLCT) and/or ligand-tometal charge transfer (LMCT). 49-54 Some differences in the emission intensity of 1-6 may relate to the distinct structures, coordination environments, and counteranions. The emission intensity of chemisorption samples 1-4-SCN is slightly increased compared with 1-4 (Fig. S13†), which may be attributed to the distinct copper(II) geometry and the adsorption of KSCN. In contrast to the emission spectra of exchanged samples 1–4- $N_3$ , they exhibited slightly shifted and quenching emission peaks which also confirm the structural transformation when exchanged by an azide anion.

## Conclusions

By the solvothermal reaction of different starting Cu(II) salts, H<sub>3</sub>pzdc and dpe coligands, three unique distinct structures of ternary coordination networks were obtained. In the case of monoanions, 1-4 are isostructural and exhibit a 3D porous pillar-layered cationic coordination framework stabilized by counteranions within their channels. The various sizes and shapes of anions somewhat affect the torsion angles of the  $\mu_2$ -dpe spacer and the channel's dimension. When using a sulfate dianion, compound 5 shows a mixed-valence Cu(I,II)  $2D + 2D \rightarrow 2D$  parallel interpenetrated layer without the incorporation of SO<sub>4</sub><sup>2-</sup> in the structure. At a vigorous reaction temperature, the species arising from  $SO_4^{\ 2-}$  may play a key role in the reduction of the Cu(II) ion. Finally, compound 6 exhibits a 3D coordination framework including a coordinated HPO<sub>4</sub><sup>2-</sup> bridge which is generated by starting with PO<sub>4</sub><sup>3-</sup>. The distinct coordination modes of pzdc<sup>3-</sup> also play a fundamental role in the structural assemblies of these CPs. The anion exchange between weak coordinating anions, NO<sub>3</sub><sup>-</sup>, ClO<sub>4</sub><sup>-</sup> and BF<sub>4</sub><sup>-</sup> was not observed, but the chemisorption of SCN on frameworks 1-4 balanced by K<sup>+</sup> with color change was found instead. The unsaturated 5-coordination Cu(II) center in 1-4 may play a crucial role in the chemisorption of SCN without the collapse of their crystalline frameworks. In addition, the anion-induced structural transformation was observed when exchanging by using the powerful coordinating ability of N<sub>3</sub>-.

## Acknowledgements

Funding for this work is provided by The Thailand Research Fund: Grant No. MRG5980237 (for Boonmak, J.) and BRG5980014 (for Youngme, S.), the Higher Education Research Promotion and National Research University Project of Thailand, through the Advanced Functional Materials Cluster of Khon Kaen University, and the Center of Excellence for Innovation in Chemistry (PERCH-CIC), Office of the Higher Education Commission, Ministry of Education, Thailand.

## References

- 1 S. K. Elsaidi, M. H. Mohamed, J. S. Loring, B. P. McGrail and P. K. Thallapally, *Appl. Mater. Interfaces*, 2016, **8**, 28424–28427.
- 2 K. Sarkar and P. Dastidar, Chem. Eur. J., 2016, 22, 1-13.
- 3 S. Suckert, M. Rams, M. Böhme, L. S. Germann, R. E. Dinnebier, W. Plass, J. Werner and C. Näther, *Dalton Trans.*, 2016, **45**, 18190–18201.

Dalton Transactions Paper

- 4 N. M. Khatri, M. H. Pablico-Lansigan, W. L. Boncher, J. E. Mertzman, A. C. Labatete, L. M. Grande, D. Wunder, M. J. Prushan, W. Zhang, P. S. Halasyamani, J. H. S. K. Monteiro, A. d. Bettencourt-Dias and S. L. Stoll, *Inorg. Chem.*, 2016, 55, 11408–11417.
- 5 S. Roy, H. M. Titi, B. K. Tripuramallu, N. Bhunia, R. Verma and I. Goldberg, Cryst. Growth Des., 2016, 16, 2814–2825.
- 6 Z.-X. Wang, L.-F. Wu, H.-P. Xiao, X.-H. Luo and M.-X. Li, *Cryst. Growth Des.*, 2016, **16**, 5184–5193.
- 7 F.-Y. Cui, K.-L. Huang, Y.-Q. Xu, Z.-G. Han, X. Liu, Y.-N. Chi and C.-W. Hu, *CrystEngComm*, 2009, **11**, 2757–2769.
- 8 P. Kang, S. Jung, J. Lee, H. J. Kang, H. Lee and M.-G. Choi, *Dalton Trans.*, 2016, 45, 11949–11952.
- 9 Y.-Y. Jia, G.-J. Ren, A.-L. Li, L.-Z. Zhang, R. Feng, Y.-H. Zhang and X.-H. Bu, *Cryst. Growth Des.*, 2016, **16**, 5593–5597.
- 10 N. P. Martin, C. M. Falaise, C. Volkringer, N. Henry, P. Farger, C. Falk, E. Delahaye, P. Rabu and T. Loiseau, *Inorg. Chem.*, 2016, 55, 8697–8705.
- 11 Z. Zhang, Y. Yang, H. Sun and R. Cao, *Inorg. Chim. Acta*, 2015, **434**, 158–171.
- 12 Y. Ma, A.-L. Cheng, B. Tang and E.-Q. Gao, *Dalton Trans.*, 2014, 43, 13957–13964.
- R. A. Agarwal and P. K. Bharadwaj, Cryst. Growth Des., 2014, 14, 6115-6121.
- 14 C.-P. Li, J. Guo and M. Du, *Inorg. Chem. Commun.*, 2013, 38, 70–73.
- 15 S. Hou, Q.-K. Liu, J.-P. Ma and Y.-B. Dong, *Inorg. Chem.*, 2013, **52**, 3225–3235.
- 16 H. Lü, Y. Mu, J. Li, D. Wu, H. Hou and Y. Fan, *Inorg. Chim. Acta*, 2012, 387, 450–454.
- 17 L. Pan, X. Huang and J. Li, *J. Solid State Chem.*, 2000, **152**, 236–246.
- 18 P. King, R. Clérac, C. E. Anson and A. K. Powell, *Dalton Trans.*, 2004, 852–861.
- 19 J.-H. Yang, S.-L. Zheng, X.-L. Yu and X.-M. Chen, *Cryst. Growth Des.*, 2004, 4, 831–836.
- 20 P. King, R. Clérac, C. E. Anson, C. Coulon and A. K. Powell, *Inorg. Chem.*, 2003, **42**, 3492–3500.
- 21 J. Xia, B. Zhao, H.-S. Wang, W. Shi, Y. Ma, H.-B. Song, P. Cheng, D.-Z. Liao and S.-P. Yan, *Inorg. Chem.*, 2007, 46, 3450–3458.
- 22 C.-B. Liu, L. Liu, S.-S. Wang, X.-Y. Li, G.-B. Che, H. Zhao and Z.-L. Xu, *J. Inorg. Organomet. Polym.*, 2012, 22, 1370–1376.
- 23 S. Barman, H. Furukawa, O. Blacque, K. Venkatesan, O. M. Yaghi, G.-X. Jinc and H. Berke, *Chem. Commun.*, 2011, 47, 11882–11884.
- 24 APEX2, Bruker AXS Inc., Madison, WI, 2014.
- 25 SAINT 4.0 Software Reference Manual, Siemens Analytical X-Ray Systems Inc., Madison, WI, 2000.
- 26 G. M. Sheldrick, *SADABS*, *Program for Empirical Absorption correction of Area Detector Data*, University of Göttingen, Göttingen, Germany, 2000.
- 27 G. M. Sheldrick, Acta Crystallogr., Sect. A: Fundam. Crystallogr., 2015, 71, 3–8.

28 G. M. Sheldrick, Acta Crystallogr., Sect. A: Fundam. Crystallogr., 2008, 64, 112–122.

- 29 A. L. Spek, J. Appl. Crystallogr., 2003, 36, 7-13.
- 30 A. L. Spek, Acta Crystallogr., Sect. C: Cryst. Struct. Commun., 2015, 71, 9–18.
- 31 A. L. Spek, *Acta Crystallogr.*, *Sect. D: Biol. Crystallogr.*, 2009, **65**, 148–155.
- 32 M. Pait, E. Colacio and D. Ray, Polyhedron, 2015, 88, 90-100.
- 33 S. Y. Moon, M. W. Park, T. H. Noh and O.-S. Jung, *J. Mol. Struct.*, 2013, **1054–1055**, 326–330.
- 34 E. Melnic, E. B. Coropceanu, A. Forni, E. Cariati, O. V. Kulikova, A. V. Siminel, V. C. Kravtsov and M. S. Fonari, *Cryst. Growth Des.*, 2016, 16, 6275–6285.
- 35 P. Suvanvapee, J. Boonmak, F. Klongdee, C. Pakawatchai, B. Moubaraki, K. S. Murray and S. Youngme, *Cryst. Growth Des.*, 2015, **15**, 3804–3812.
- 36 J. Boonmak, S. Youngme, N. Chaichit, G. A. v. Albada and J. Reedijk, *Cryst. Growth Des.*, 2009, **9**, 3318–3326.
- 37 A. W. Addison and T. N. Rao, *J. Chem. Soc., Dalton Trans.*, 1984, 1349–1356.
- 38 W. L. Driessen, L. Chang, C. Finazzo, S. Gorter, D. Rehorst, J. Reedijk, M. Lutz and A. L. Spek, *Inorg. Chim. Acta*, 2003, **350**, 25–31.
- 39 G. Kang, Y. Jeon, K. Y. Lee, J. Kim and T. H. Kim, *Cryst. Growth Des.*, 2015, 15, 5183–5187.
- 40 J. Troyano, J. Perles, P. Amo-Ochoa, F. Zamora and S. Delgado, *CrystEngComm*, 2016, **18**, 1809–1817.
- 41 G. P. Shields, P. R. Raithby, F. H. Allen and W. D. S. Motherwell, *Acta Crystallogr., Sect. B: Struct. Sci.*, 2000, **56**, 455–465.
- 42 P. Smoleński, J. Kłak, D. S. Nesterov and A. M. Kirillov, *Cryst. Growth Des.*, 2012, 12, 5852–5857.
- 43 H.-Z. Zhang, Y.-M. Chen, Y.-H. Yu, G.-F. Hou and J.-S. Gao, *Polyhedron*, 2016, **110**, 93–99.
- 44 L. Yang, D. R. Powell and R. P. Houser, *Dalton Trans.*, 2007, 955–964.
- 45 L. K. Das, C. Diaz and A. Ghosh, *Cryst. Growth Des.*, 2015, 15, 3939–3949.
- 46 L. Song, C. Jiang, C. Ling, Y.-R. Yao, Q.-H. Wang and D. Chen, *J. Inorg. Organomet. Polym.*, 2016, **26**, 320–325.
- 47 K. Nakamoto, *Infrared and Raman spectra of inorganic and coordination compounds*, John Wiley & Sons, Inc., 2008.
- 48 X.-M. Zhang, Y.-Q. Wang, Y. Song and E.-Q. Gao, *Inorg. Chem.*, 2011, **50**, 7284–7294.
- 49 A. Vogler and H. Kunkely, *Coord. Chem. Rev.*, 2007, **251**, 577–583.
- 50 M. Du, X.-J. Jiang and X.-J. Zhao, *Inorg. Chem.*, 2006, 45, 3998–4006.
- 51 X.-L. Wang, F.-F. Sui, H.-Y. Lin and G.-C. Liu, *Aust. J. Chem.*, 2015, **68**, 1076–1083.
- 52 X. Cao, B. Mu and R. Huang, *CrystEngComm*, 2014, **16**, 5093–5102.
- 53 G. Liang, Y. Liu, X. Zhang and Z. Yi, *CrystEngComm*, 2014, **16**, 9896–9906.
- 54 Y. Feng, D.-B. Wang, B. Wan, X.-H. Li and Q. Shi, *Inorg. Chim. Acta*, 2014, 413, 187–193.



Contents lists available at ScienceDirect

## Polyhedron

journal homepage: www.elsevier.com/locate/poly



# Copper(II) coordination polymers containing neutral trinuclear or anionic dinuclear building units based on pyrazole-3,5-dicarboxylate: Synthesis, structures and magnetic properties



Fatima Klongdee <sup>a</sup>, Jaursup Boonmak <sup>a,\*</sup>, Boujemaa Moubaraki <sup>b</sup>, Keith S. Murray <sup>b</sup>, Sujittra Youngme <sup>a</sup>

- <sup>a</sup> Materials Chemistry Research Center, Department of Chemistry and Center of Excellence for Innovation in Chemistry, Faculty of Science, Khon Kaen University, Khon Kaen 40002. Thailand
- <sup>b</sup> School of Chemistry, Monash University, Building 23, 17 Rainforest Walk, Melbourne, Victoria 3800, Australia

#### ARTICLE INFO

#### Article history: Received 28 October 2016 Accepted 10 January 2017 Available online 18 January 2017

Keywords: Coordination polymer Pyrazole-3,5-dicarboxylic acid Secondary building unit Magnetic properties Copper(II)

#### ABSTRACT

Four novel copper(II) coordination polymers, namely  $\{[Cu_3(pzdc)_2(pyz)(H_2O)_6](H_2O)\}_n$  (1),  $\{[Cu_3(pzdc)_2(bpy)(H_2O)_8](H_2O)_6\}_n$  (2),  $\{[Cu_4(Hpzdc)_2(pzdc)_2(bpy)_2][Cu(bpy)(H_2O)_4]_n(H_2O)_4\}_n$  (3), and  $\{[Cu_3(pzdc)_2(ampy)(H_2O)_5](H_2O)_3\}_n$  (4)  $(H_3pzdc = pyrazole-3,5$ -dicarboxylic acid, pyz = pyrazole, pyz = 4,4'-bipyridine and ampy = 2-aminopyrazine) were synthesized and characterized. Compounds 1, 2 and 4 were synthesized by layering method at room temperature while 3 was prepared under solvothermal reaction. Compounds 1 and 2 are one-dimensional (1D) chain coordination polymers, while 3 shows 1D cationic chain coordination polymer with anionic tetranuclear Cu(II) cluster. Compound 4 exhibits 1D ladder-like chain structure. Compounds 1, 2 and 4 consist of neutral trinuclear  $[Cu_3(pzdc)_2]$  building unit which is constructed by  $\mu_2$ -pzdc<sup>3-</sup> bridging (5-6-5), (6-6-6), and (6-5-5) sequences of Cu(II) geometries for 1, 2 and 4, respectively. Each trinuclear unit is extended via N,N'-linkers giving polymeric chain structure. In contrast, anionic tetranuclear cluster of 3 is built up from two anionic dinuclear metallacyclic  $[Cu_2(Hpzdc)(pzdc)]^-$  building units and double  $\mu_2$ -bpy spacers. The magnetic properties of 1, 2 and 4 exhibit weak antiferromagnetic interactions among Cu(II) centers.

© 2017 Elsevier Ltd. All rights reserved.

#### 1. Introduction

In the last few decades, coordination polymers (CPs) have attracted wide attention due to their diverse structures and many potential applications in the areas of gas storage, catalysis, ionexchange, luminescence, and magnetism [1-10]. CPs have been constructed by primary building unit, i.e., metal ions and organic bridging ligands, and it is well known that metal center, ligand, pH, temperature, and solvent have strongly affected on construction and versatile structures of CPs [11-16]. CPs with short bridging ligands such as azide, pyrazole, and carboxylate are especially favorable for creating new magnetic materials because they are able to efficiently transfer magnetic interactions between neighboring magnetic centers [17-20]. Pyrazole-3,5-dicarboxylic acid (H<sub>3</sub>pzdc) is a multifunctional ligand and exhibits diverse coordination modes [21,22]. It has six potential coordination sites consisting of four carboxylate oxygen atoms from two carboxylate groups and two nitrogen atoms from pyrazole ring when it is fully

deprotonated. A variety of coordination compounds based on H<sub>3</sub>-pzdc have been reported [23–26]. Generally, incorporation of Cu (II) ions with H<sub>3</sub>pzdc ligands can generate metallacyclic dinuclear [23,27] and trinuclear secondary building units [28,29] (Fig. 1), such as  $(Et_3NH)_2[Cu_2(pzdc)_2(H_2O)_2]$ , [23]  $[Cu_3(pzdc)_2(MeOH)_6(H_2O)_4]$  [28] and  $[Cu_3(2,2'-bipy)_2(pzdc)_2(H_2O)_2](H_2O)_2$  [29] complexes. In addition, the pyrazole-3,5-dicarboxylic acid can also provide the extended structures, such as, 3D frameworks of  $\{[Na_2(\mu-H_2O)_2](Cu_2(pzdc)_2]\}_n$  [23] and  $[Cu_3(pzdc)_2(H_2O)_4]_n$  [30]. However the structures and properties of the ternary Cu(II)-CPs containing both H<sub>3</sub>pzdc and organic coligands have been less documented [31]. In this work, N,N'-ditopic coligands were used to build the extended structures of Cu(II) pyrazole-3,5-dicarboxylate based on tri- and dinuclear secondary building units.

Based on above consideration, we synthesized four novel ternary copper(II) coordination polymers with  $H_3$ pzdc and N,N'-ditopic ligands (Scheme 1), namely {[Cu<sub>3</sub>(pzdc)<sub>2</sub>(pyz)(H<sub>2</sub>O)<sub>6</sub>](H<sub>2</sub>O)<sub>3</sub>, (1), {[Cu<sub>3</sub>(pzdc)<sub>2</sub>(bpy)(H<sub>2</sub>O)<sub>8</sub>](H<sub>2</sub>O)<sub>6</sub>}<sub>n</sub> (2), {[Cu<sub>4</sub>(Hpzdc)<sub>2</sub> (pzdc)<sub>2</sub> (bpy)<sub>2</sub>][Cu(bpy)(H<sub>2</sub>O)<sub>4</sub>]<sub>n</sub>(H<sub>2</sub>O)<sub>4</sub>}<sub>n</sub> (3), and {Cu<sub>3</sub>(pzdc)<sub>2</sub>(ampy) (H<sub>2</sub>O)<sub>5</sub>](H<sub>2</sub>O)<sub>3</sub>}<sub>n</sub> (4) (pyz = pyrazine, bpy = 4,4'-bipyridine, and ampy = 2-aminopyrazine). Combining Cu(II) ions and  $H_3$ pzdc

<sup>\*</sup> Corresponding author.

E-mail address: Jaursup@kku.ac.th (J. Boonmak).

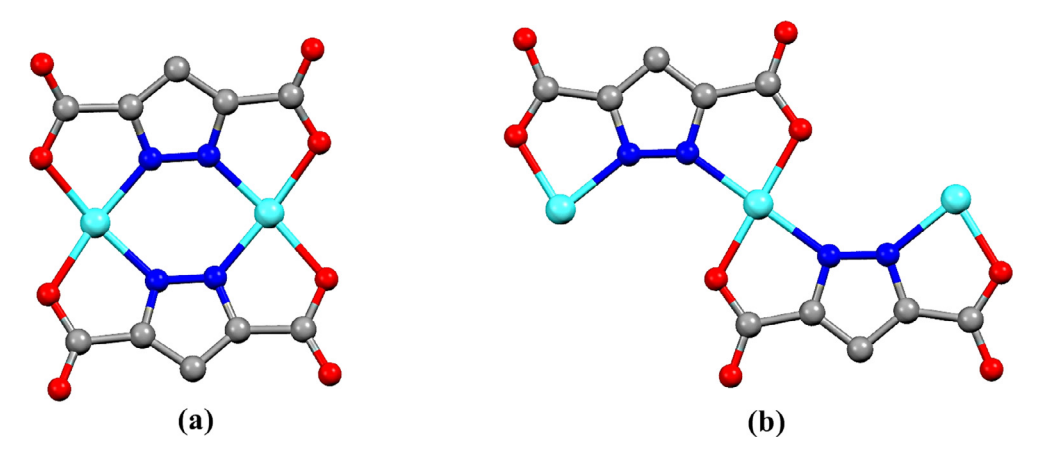
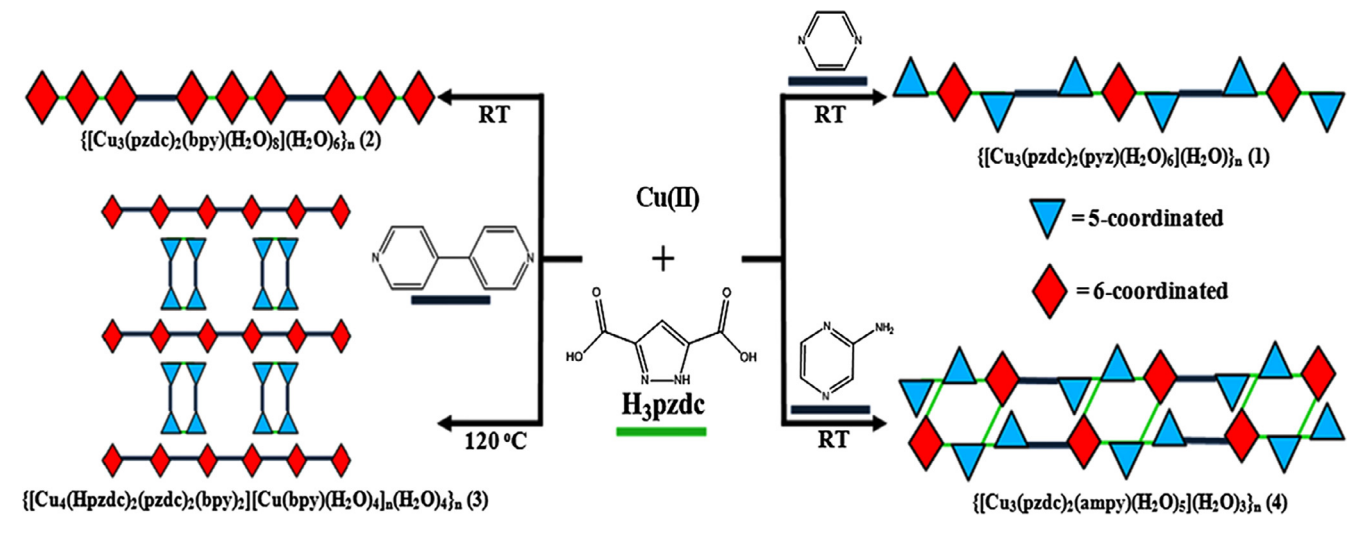


Fig. 1. (a) Metallacyclic dinuclear Cu(II) secondary building unit (b) trinuclear Cu(II) secondary building unit.



Scheme 1. A series of Cu(II) coordination polymers 1-4.

ligands can generate neutral trinuclear  $[Cu_3(pzdc)_2]$  secondary building unit for **1**, **2** and **4** and anionic dinuclear metallacyclic  $[Cu_2(Hpzdc)_2]^-$  building unit for **3**. A variety of coordination geometries and distinct sequences of Cu(II) geometries in each building unit has been demonstrated. Moreover, each building unit was extended by N,N'-ditopic coligands, giving rise to 1D chain CPs for **1** and **2**, tetranuclear anionic cluster for **3**, and ladder-like chain structure for **4**. The effects of coligands, geometry of Cu(II) center, reaction temperature and various coordination modes of  $H_3pzdc$  play an important role in the construction of chain coordination polymers. In addition the magnetic properties of **1**, **2** and **4** containing trinuclear Cu(II) building unit have been studied.

#### 2. Experimental

## 2.1. General

All chemicals and solvents used for synthesis were obtained from commercial sources and were used without further purification. FT-IR spectra were obtained in KBr disks on a PerkinElmer Spectrum One FT-IR spectrophotometer in 4000–450 cm<sup>-1</sup> spectral range. Solid-state (diffuse reflectance) electronic spectra were measured as polycrystalline samples on a PerkinElmer Lambda2S spectrophotometer, within the range 400–1100 nm. Elemental analyses (C, H, N) were carried out with a PerkinElmer PE

2400CHNS analyzer. The X-ray powder diffraction (XRPD) data were collected on a PANalytical EMPYREAN using monochromatic CuKα radiation, and the recording speed was  $0.5 \, \mathrm{s/step}$  over the  $2\theta$  range of  $5-50^{\circ}$  at room temperature. Thermogravimetric analyses (TGA) were performed using a TG-DTA 2010S MAC apparatus between 35 and 750 °C in N<sub>2</sub> atmosphere with heating rate of  $10^{\circ}$ -C min<sup>-1</sup>. Magnetic susceptibility measurements (2–300 K) were carried out using a Quantum design MPMS-5S SQUID magnetometer. Measurements carried out using a 1 kOe dc field. Accurately weighed samples of  $\sim$ 25 mg were contained in a gel capsule that was held in the center of a soda straw that was attached to the end of the sample rod. Data were corrected for magnetization of the sample holder and for diamagnetic contributions, which were estimated from Pascal constants.

## 2.2. Synthesis

## 2.2.1. Synthesis of $\{[Cu_3(pzdc)_2(pyz)(H_2O)_6](H_2O)\}_n$ (1)

The deionized water (3 mL) was slowly dropped over the mixture solution containing  $\text{Cu}(\text{NO}_3)_2 \cdot 3\text{H}_2\text{O}$  (0.2 mmol, 48 mg) and pyrazine (0.2 mmol, 16 mg) in water and DMF (4 mL, 1:1 v/v) in 15 mL of glass vial. Then, the solution of pyrazole-3,5-dicarboxylic acid (0.2 mmol, 35 mg) in deionized water and ethanol (5 mL, 1:1 v/v) was carefully layered over the mixture layer. Then, the vial was sealed and allowed to stand undisturbed at room temperature.

The blue crystals of **1** were obtained after 2 days. Yield: 16 mg (34%) based on copper salt. *Anal.* Calcd for  $Cu_3C_{14}H_{20}N_6O_{15}$ : C, 23.92; H, 2.87; N, 11.95. Found: C, 24.40; H, 2.80; N, 11.73%. FT-IR peaks (KBr, cm<sup>-1</sup>): 3367br ( $\nu$ (OH)), 1622s ( $\nu$ <sub>as</sub>(OCO)), 1609s ( $\nu$ (C=N)), 1509m, 1423w, 1395m ( $\nu$ <sub>s</sub>(OCO)), 1341s, 1330s, 1297s, 1157w, 1127w, 1100w, 1063w, 1028w, 1017w, 930w, 828w, 797w. UV-vis (diffuse reflectance, cm<sup>-1</sup>): 14049.

## 2.2.2. Synthesis of $\{[Cu_3(pzdc)_2(bpy)(H_2O)_8](H_2O)_6\}_n$ (2)

The preparation of **2** was similar to that of **1**, except 4, 4′-bipyridine (0.2 mmol, 31 mg) replaced pyrazine. After 2 days, light blue crystals of **2** were obtained. Yield: 14 mg (23%) based on copper salt. *Anal.* Calcd for Cu<sub>3</sub>C<sub>20</sub>H<sub>38</sub>N<sub>6</sub>O<sub>22</sub>: C, 26.54; H, 4.23; N, 9.28. Found: C, 26.37; H, 4.00; N, 9.30%. FT-IR peaks (KBr, cm<sup>-1</sup>): 3405br ( $\nu$ (OH)), 1620s ( $\nu$ <sub>as</sub>(OCO)), 1615s ( $\nu$ (C=N)), 1520m, 1415w, 1390m ( $\nu$ <sub>s</sub>(OCO)), 1339s, 1293m, 1223m, 1127w, 1060w, 1028w, 1015w, 828w, 781m, 643w. UV-Vis (diffuse reflectance, cm<sup>-1</sup>): 14384.

# 2.2.3. Synthesis of $\{[Cu_4(Hpzdc)_2(pzdc)_2(bpy)_2][Cu(bpy)(H_2O)_4]_n(H_2O)_4\}_n$ (3)

The mixture solution of Cu(NO<sub>3</sub>)<sub>2</sub>·3H<sub>2</sub>O (0.2 mmol, 48 mg), 4,4′-bipyridine (0.2 mmol, 31 mg) and pyrazole-3,5-dicarboxylic acid (0.2 mmol, 35 mg) in the deionized water (7 mL), DMF (2 mL) and ethanol (3 mL) was sealed in a 20 mL glass vial. Then, the mixture was heated at 120 °C for 1 day and then slowly cooled down to room temperature. The blue crystals of **3** were obtained. Yield: 10 mg (16%) based on copper salt *Anal*. Calcd for Cu<sub>5</sub>C<sub>50</sub>H<sub>46</sub>N<sub>14</sub>O<sub>24</sub>: C, 38.88; H, 3.00; N, 12.69. Found: C, 38.79; H, 2.85; N, 13.00%. FT-IR peaks (KBr, cm<sup>-1</sup>): 3368br ( $\nu$ (OH)), 1646s ( $\nu$ <sub>as</sub>(OCO)), 1599s ( $\nu$ (C=N)), 1533w, 1481w, 1407w, 1387m ( $\nu$ <sub>s</sub>(OCO)), 1288s, 1224m, 1065w, 1020w, 817w, 806w, 778 m. UV-vis (diffuse reflectance, cm<sup>-1</sup>): 14407.

#### 2.2.4. Synthesis of $\{[Cu_3(pzdc)_2(ampy)(H_2O)_5](H_2O)_3\}_n$ (4)

The preparation of **4** was similar to that of **1**, except aminopyrazine (0.2 mmol, 19 mg) replaced pyrazine. The dark green crystals of **4** were obtained after 2 days. Yield: 17 mg (35%) based on copper salt. *Anal.* Calcd for  $\text{Cu}_3\text{C}_{14}\text{H}_{23}\text{N}_7\text{O}_{16}$ : C, 22.97; H, 3.17; N, 13.39. Found: C, 23.10; H, 3.11; N, 13.10%. FT-IR peaks (KBr, cm<sup>-1</sup>): 3336br ( $\nu$ (OH)), 1635s ( $\nu$ <sub>as</sub>(OCO)), 1607s ( $\nu$ (C=N)), 1541m, 1511m, 1383m ( $\nu$ <sub>s</sub>(OCO)), 1327s, 1314s, 1282s, 1229m, 1078w, 1028w, 1012w, 850w, 785m. UV–Vis (diffuse reflectance, cm<sup>-1</sup>): 14389.

#### 2.3. X-ray structure determination for 1-4

The X-ray reflection data of 1-4 were collected on a Bruker D8 Quest PHOTON100 CMOS detector with graphite-monochromated Mo Kα radiation using the APEX2 program [32]. Raw data frame integration was performed with SAINT, [33] which also applied correction for Lorentz and polarization effects. An empirical absorption correction by using the sadabs program [34] was applied. The structure was solved by direct methods and refined by full-matrix least-squares method on  $F^2$  with anisotropic thermal parameters for all non-hydrogen atoms using the SHELXTL software package [35]. All hydrogen atoms were placed in calculated positions and refined isotropically, with the exception of the hydrogen atoms of all water molecules in 1-4 were found via difference Fourier maps, then restrained at fixed positions and refined isotropically. The hydrogen atoms on the disordered lattice water molecules in 2(08), and 3 (04) could not be located. The highly disordered lattice water molecules in 3 (O4) and 4 (O14) could not be resolved. The pzdc/Hpzdc ligand in 3 lies across a mirror plane so the disordered hydrogen atom (H2) on carboxylic oxygen was refined with quarter occupancy. The details of crystal data, selected bond lengths and angles for compounds **1–4** are listed in Tables 1 and S1.

#### 3. Results and discussion

## 3.1. Structural description of $\{[Cu_3(pzdc)_2(pyz)(H_2O)_6](H_2O)\}_n$ (1)

X-ray crystallographic analysis reveals that 1 crystalizes in the triclinic system with  $P\bar{1}$  space group. Asymmetric unit of 1 consists of two independent Cu(II) centers (Cu1 and Cu2), one pzdc<sup>3-</sup> ligand, a half of pyz ligand, three coordination water molecules and one lattice water molecule. Each Cu1 ion lies on a crystallographic inversion center adopting an elongated octahedral CuN2O4 geometry which is coordinated by two oxygen atoms and two nitrogen atoms from two different pzdc<sup>3-</sup> ligands in the equatorial plane. The axial position is occupied by two oxygen atoms from two coordination water molecules. Whereas the terminal Cu2 center is five-coordinated showing distorted square pyramidal CuN<sub>2</sub>O<sub>3</sub> geometry ( $\tau$  = 0.33, Addison's parameter  $\tau$  = 0 for square pyramid and  $\tau = 1$  for trigonal bipyramid) [36]. The basal plane is surrounded by carboxylic oxygen and pyrazoyl nitrogen atoms from pzdc<sup>3-</sup> ligand, one pyrazine nitrogen atom and one oxygen atom from coordination water molecule, while the apical position is occupied by oxygen atom from another coordination water molecule (O5). The Cu-N and Cu-O distances are in the range of 1.9619(11)-2.1734(15) Å, while the axial Cu1-O distance of 2.4957(14) Å is significantly longer, indicating the presence of a common Jahn-Teller effect in the Cu(II) ion [30]. The Cu2N<sub>2</sub>O<sub>2</sub> square plane is not completely planar with tetrahedral twist between the planes of 29.64°. The Cu2 is shifted by 0.3268(2) Å from the mean equatorial plane toward the apical position. The Cu1 and two Cu2 ions are connected by pzdc<sup>3-</sup> in a  $\mu_2$ - $\eta^2$ N,O,  $\eta^2 N', O'$  coordination mode (type I, Fig. S1) to form a neutral trinuclear Cu(II) unit containing (5-6-5) sequences of Cu(II) geometries with the Cu1···Cu2 distance of 4.4102(2) Å (Fig. 2a). Each trinuclear Cu(II) unit is linked by  $\mu_2$ -pyrazine spacer to form a 1D chain structure of 1 with the Cu2···Cu2 distance of 6.8462(3) Å (Fig. 2b). Furthermore, the 3D packing motif of 1 is stabilized by various interchain hydrogen bonding interactions between pzdc<sup>3-</sup>, pyz, coordination and lattice water molecules (Fig. S2 and Table S2).

## 3.2. Structural description of $\{[Cu_3(pzdc)_2(bpy)(H_2O)_8](H_2O)_6\}_n$ (2)

Compound 2 crystallizes in monoclinic system and  $P2_1/c$  space group. The asymmetric unit contains two independent Cu(II) ions (Cu1 and Cu2), one pzdc<sup>3-</sup>, one-half of bpy, four coordination water molecules and three lattice water molecules. Both Cu(II) ions reveal an elongated octahedral geometry, Cu1 is six-coordinated surrounded by O and N atoms from pzdc<sup>3-</sup> ligand, one pyridine nitrogen atom and one oxygen atom from coordination water molecule in the basal plane. The axial position is located by two oxygen atoms from two coordination water molecules. While the Cu2 is located in crystallographic inversion center and occupied by two N atoms and two O atoms from two different pzdc3ligands in the equatorial plane. The apical site is occupied by two oxygen atoms from two coordination water molecules. The Cu-N and Cu–O distances are in the range of 1.959(3)–2.6715(3) Å which are within the range of those reported for elongated octahedral geometry of Cu(II) complexes containing pzdc<sup>3-</sup> [28,30]. The Cu1N<sub>2</sub>O<sub>2</sub> square base is not completely planar with tetrahedral twist between the planes of 5.35°. The pzdc<sup>3-</sup> ligand acting as a  $\mu_2$ - $\eta^2$ -N,O,  $\eta^2$ -N',O' fashion (type I, Fig. S1) link between two Cu1 and Cu2 ions forming a neutral trinuclear Cu(II) unit with (6-6-6) sequences of Cu(II) geometries. The Cu1···Cu2 distance is 4.5207(5) Å (Fig. 3a). In addition, each trinuclear Cu(II) unit is con-

Table 1 Crystallographic data for compounds 1-4.

| Compound  | 1                           | 2                           | 3                              | 4  |
|---|-----------------------------|-----------------------------|--------------------------------|--|
| Formula   | $Cu_3C_{14}H_{20}N_6O_{15}$ | $Cu_3C_{20}H_{38}N_6O_{22}$ | $Cu_5C_{50}H_{46}N_{14}O_{24}$ | Cu <sub>3</sub> C <sub>14</sub> H <sub>23</sub> N <sub>7</sub> O <sub>16</sub> |
| Molecular weight                                      | 702.98                      | 905.18                      | 1544.71                        | 736.01   |
| T (K)   | 293(2)                      | 293(2)                      | 293(2)                         | 293(2)   |
| Crystal system  | triclinic                   | monoclinic                  | orthorhombic                   | triclinic  |
| Space group   | ΡĪ                          | $P2_1/c$                    | Cmmm                           | $P\bar{1}$   |
| a (Å)   | 7.1902(2)                   | 8.8968(7)                   | 15.6847(5)                     | 7.8991(3)  |
| b (Å)   | 8.8370(2)                   | 10.1970(8)                  | 18.6369(7)                     | 12.9067(5)   |
| c (Å)   | 9.5076(2)                   | 18.2364(14)                 | 11.1125(4)                     | 13.6852(5)   |
| α (°)   | 72.1460(10)                 | 90                          | 90                             | 110.648(1)   |
| β(°)  | 75.8720(10)                 | 93.682(2)                   | 90                             | 97.878(1)  |
| γ (°)   | 82.1560(10)                 | 90                          | 90                             | 100.755(1)   |
| $V(Å^3)$  | 556.38(2)                   | 1651.0(2)                   | 3248.3(2)                      | 1251.0(1)  |
| Z   | 1                           | 2                           | 2                              | 2  |
| $\rho_{\rm cald}~({ m g~cm}^{-3})$                    | 2.098                       | 1.813                       | 1.571                          | 1.954  |
| $\mu$ (Mo K $\alpha$ ) (mm <sup>-1</sup> )            | 2.933                       | 2.014                       | 1.696                          | 2.617  |
| Data collected  | 3895                        | 4119                        | 1879                           | 5540   |
| Unique data $(R_{int})$                               | 3433(0.0172)                | 3350(0.0480)                | 1530(0.0228)                   | 3802(0.0634)   |
| $R_1^a/wR_2^b[I > 2\sigma(I)]$                        | 0.0252/0.0659               | 0.0504/0.1365               | 0.0606/0.1885                  | 0.0530/ 0.1249   |
| $R_1^a/wR_2^b$ [all data]                             | 0.0315/0.0684               | 0.0649/0.1460               | 0.0754/ 0.1994                 | 0.0941/ 0.1408   |
| GOF   | 1.102                       | 0.994                       | 1.115                          | 1.059  |
| Maximum/minimum electron density (e $\mbox{Å}^{-3}$ ) | 0.525/-0.307                | 1.392/-1.305                | 1.623/-0.843                   | 2.290/-0.518   |

 $R = \sum ||F_0| - |F_c|| / \sum |F_0|.$   $R_w = \{\sum [w(|F_0| - |F_c|)]^2 / \sum [w|F_0|^2]\}^{1/2}.$ 

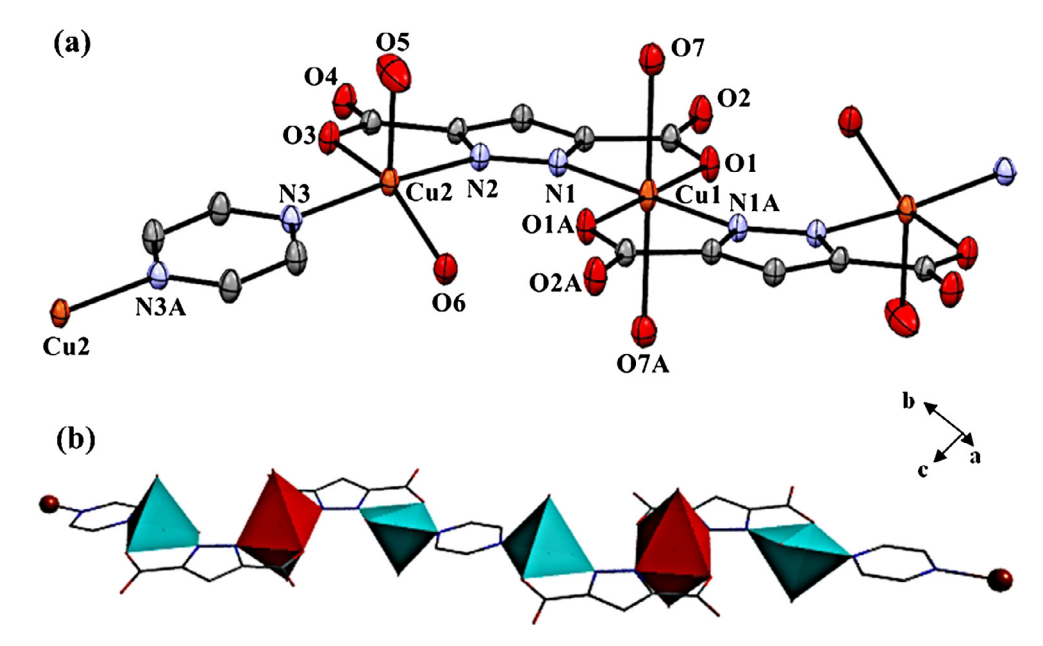
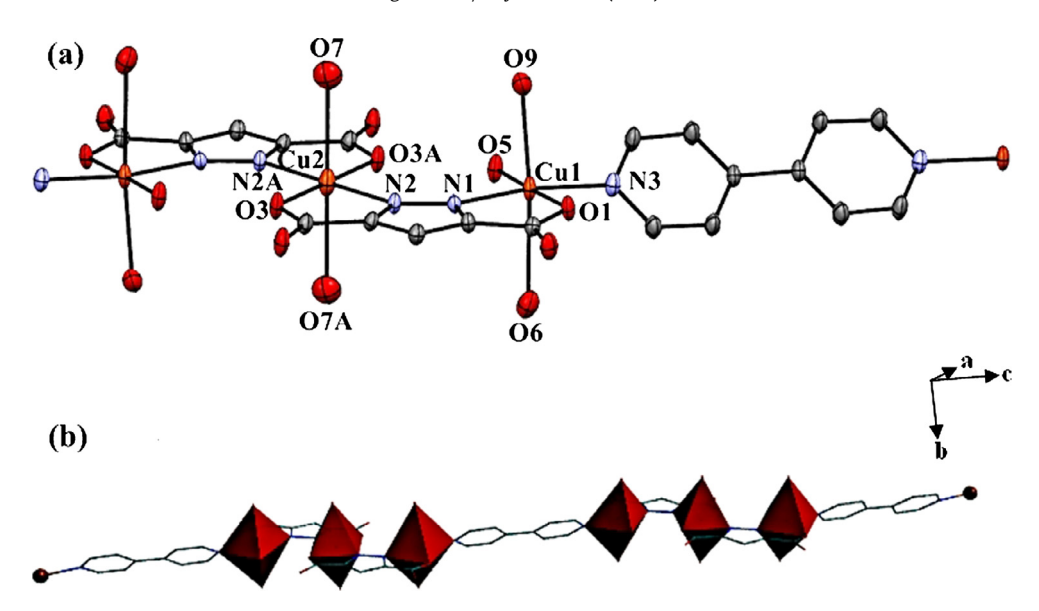


Fig. 2. (a) A trinuclear Cu(II) building unit and atom labeling scheme of 1. The ellipsoids are shown at 50% probability level. All hydrogen atoms and lattice water molecules are omitted for clarity (symmetry code: A = 1 - x, 2 - y, 2 - z). (b) The 1D coordination polymer of 1. The blue and red polygons represent five- and six-coordination geometries of Cu(II) centers, respectively. (Colour online.)

nected by  $\mu_2$ -bpy ligands to generate a 1D chain (Fig. 3b) with Cu1...Cu1 distance of 11.1146(9) Å. The two pyridine rings of bipyridyl moieties are perfectly coplanar, being located on a crystallographic center of symmetry. The 3D supramolecular structure of 2 is generated via various hydrogen bonding interactions between pzdc<sup>3-</sup>, bpy, coordination and lattice water molecules (Fig. S3 and Table S2).

## 3.3. Structural description of $\{[Cu_4(Hpzdc)_2(pzdc)_2(bpy)_2][Cu(bpy)\}$ $(H_2O)_4]_n(H_2O)_4\}_n$ (3)

Compound **3** crystallizes the orthorhombic, *Cmmm* space group which consists of cationic  $[Cu(bpy)(H_2O)_4]_n^{2+}$  chain coordination polymer and anionic  $[Cu_4(Hpzdc)_2(pzdc)_2(bpy)_2]^{2-}$  units. The anionic tetranuclear Cu(II) unit contains four Cu(II) centers (Cu1), two Hpzdc<sup>2-</sup>, two pzdc<sup>3-</sup> and two bpy ligands. Each Cu1 is located in crystallographic mirror plane adopting a distorted square pyramidal geometry. The Cu(II) center is coordinated by two carboxylate O and two pyrazoyl N atoms from two different pyrazole-3,5-dicarboxylates in equatorial plane and one N atom from  $\mu_2$ -bpy in the axial site (Fig. 4a). The Cu1N<sub>2</sub>O<sub>2</sub> square base is not completely planar with tetrahedral twist between the planes of 24.98°. The Cu1 is shift by 0.3277(7) Å from the mean equatorial plane toward the axial position. The calculation of the bond valence sum (BVS) [37,38] for Cu1 was performed. The analysis resulted in the value of 2.11, thus confirming the formal oxidation states of +2 for copper center. Two Cu1 centers are connected by Hpzdc<sup>2-</sup> and pzdc<sup>3-</sup> ligands in  $\mu_2$ - $\eta^2$ N,O,  $\eta^2$ N',O' coordination modes (type I, Fig. S1),



**Fig. 3.** (a) A trinuclear Cu(II) building unit and atom labeling scheme of **2**. The ellipsoids are shown at 50% probability level. All hydrogen atoms and lattice water molecules are omitted for clarity (symmetry code: A = 2 - x, 1 - y, 1 - z). (b) The 1D coordination polymer of **2**. The red polygon represents six-coordination geometries of Cu(II) centers. (Colour online.)

resulting to metallacyclic dinuclear Cu(II) unit with Cu···Cu distance of 3.995(1) Å. Moreover, these two dinuclear Cu(II) units are linked by two  $\mu_2$ -bpy linkers, forming tetranuclear anionic cluster (Fig. 4a). The metallacyclic anionic dinuclear Cu(II) building unit containing pzdc<sup>3-</sup> has been found in the literature, such as,  $(Et_3NH)_2[Cu_2(pzdc)_2(H_2O)_2], [23] [{Na_2(\mu-H_2O)_2}{Cu_2(pzdc)_2}]_n$ [23] and  $\{[Cu_2(pzdc)_2] (C_{10}H_{10}N_2)\}_n$  [31] While a neutral  $[Cu_2(-$ Hpzdc)<sub>2</sub>] building unit is less reported [39]. In this work, we show the first example of metallacyclic anionic dinuclear Cu(II) building unit containing both Hpzdc<sup>2-</sup> and pzdc<sup>3-</sup> ligands. In the cationic 1D coordination polymer, the Cu2 is surrounded by four O atoms from four coordination water molecules in basal plane and two N atoms from two different  $\mu_2$ -bpy linkers in apical position, adopting elongated octahedral geometry (Fig. 4b). Each Cu2 is connected by  $\mu_2$ -bpy to generate a 1D cationic linear chain (Fig. 4c). The Cu–N and Cu-O distances are in the normal range between 1.933(4)-2.201(9) Å [23]. The two pyridine rings of all bipyridyl moieties are perfectly coplanar, being located on a crystallographic mirror plane. In the 3D packing diagram of 3, besides electronic interaction between cationic chain and anionic tetranuclear unit of 3, the molecular structure hydrogen bonding interaction between bpy, pyrazole-dicarboxylate and coordination water molecule stabilize entire 3D supramolecular structure (Fig. 5 and Table S2).

#### 3.4. Structural description of $\{[Cu_3(pzdc)_2(ampy)(H_2O)_5](H_2O)_3\}_n$ (4)

Single crystal X-ray analysis reveals that compound **4** crystal-lizes in triclinic crystal system,  $P\bar{1}$  space group. Asymmetric unit of **4** contains three independent Cu(II) ions, two pzdc<sup>3-</sup>, one ampy ligand, five coordination water molecules and three lattice water molecules. Each Cu1 center is occupied by O and N atoms from pzdc<sup>3-</sup>, one pyrazine nitrogen atom from ampy ligand and one oxygen from coordination water molecule in the basal plane, while the apical positions are occupied by an O atom from coordination water molecule giving rise to square pyramidal CuN<sub>2</sub>O geometry. In addition, the semi-coordinated O4 atom from pzdc<sup>3-</sup> weakly interacts to copper center with the longest Cu1···O4 distance of 2.800(3) Å, forming an elongated octahedral geometry. The Cu2 and Cu3 centers show distorted square pyramidal geometries ( $\tau$  = 0.02 and 0.03 for Cu2 and Cu3, respectively). Each Cu2 center

is coordinated by two carboxylate oxygen and two nitrogen atoms from two different pzdc<sup>3-</sup> ligands at equatorial plane. The axial site is occupied by one oxygen from coordination water molecule. The basal plane around the Cu3 center is composed of O and N atoms from pzdc<sup>3-</sup>, one pyrazine nitrogen from ampy and one oxygen from coordination water molecule. The apical site is taken by oxygen from coordination water molecule. The Cu-N and Cu-O distances are in the range of 1.931(4)-2.472(5) Å which are well within their normal ranges for pyrazolato-bridged trinuclear Cu (II) complexes.[30] While the longest Cu1-O4 distance of 2.800 (3) Å shows very weak coordination bond [31,40]. The CuN<sub>2</sub>O<sub>2</sub> square base shows tetrahedral twists between the planes of 7.19°, 11.01°, and 17.76° for Cu1–Cu3, respectively. The pzdc $^{3-}$ ligand exhibits  $\mu_3$ - $\eta^2$ N,O,  $\eta^2$ N',O',  $\eta^1$ O bridging mode (type II, Fig. S1) connecting three Cu(II) centers to form a neutral trinuclear Cu(II) unit containing (6-5-5) sequences of Cu(II) geometries with the Cu1···Cu2, Cu2···Cu3 distances of 4.4634(5) and 4.4765(6) Å, respectively (Fig. 6a). In addition, each trinuclear Cu(II) building unit is linked together by weak  $\mu_3$ -syn,anti-pzdc<sup>3-</sup> bridging mode (Cu1-O4) forming hexanuclear Cu(II) cluster (Fig. 6b). Moreover, the adjacent hexanuclear Cu(II) units are connected by double  $\mu_2$ -ampy spacers to generate 1D ladder-like chain structure with the shortest Cu···Cu distance of 6.8089(2) Å (Fig. 6c). In addition, the intramolecular hydrogen bond between NH<sub>2</sub> group of  $\mu_2$ -ampy and coordination water molecules stabilizes the ladder-like chain structure of 4. The 3D packing structure of 4 is assembled by various weak interchain hydrogen bonding interactions between pzdc<sup>3</sup>-, ampy, coordination and lattice water molecules (Fig. S4 and Table S2).

## 3.5. Thermal analyses

Thermogravimetric analysis (TGA) of **1–4** were performed in  $N_2$  atmosphere from 35–750 °C. Compound **1** shows a weight loss of 15.50% in the range of 70–110 °C, which is due to the loss of six water molecules (calcd. 15.36%). After 250 °C, the sample gradually starts to lose the remaining water molecule and decompose to the unidentified species. Compounds **2** and **4** show the first weight loss of 17.85% and 4.66% varying from 35 to 80 °C for **2** and 35–60 °C for **4** corresponding to the loss of nine water molecules for **2** (calcd.

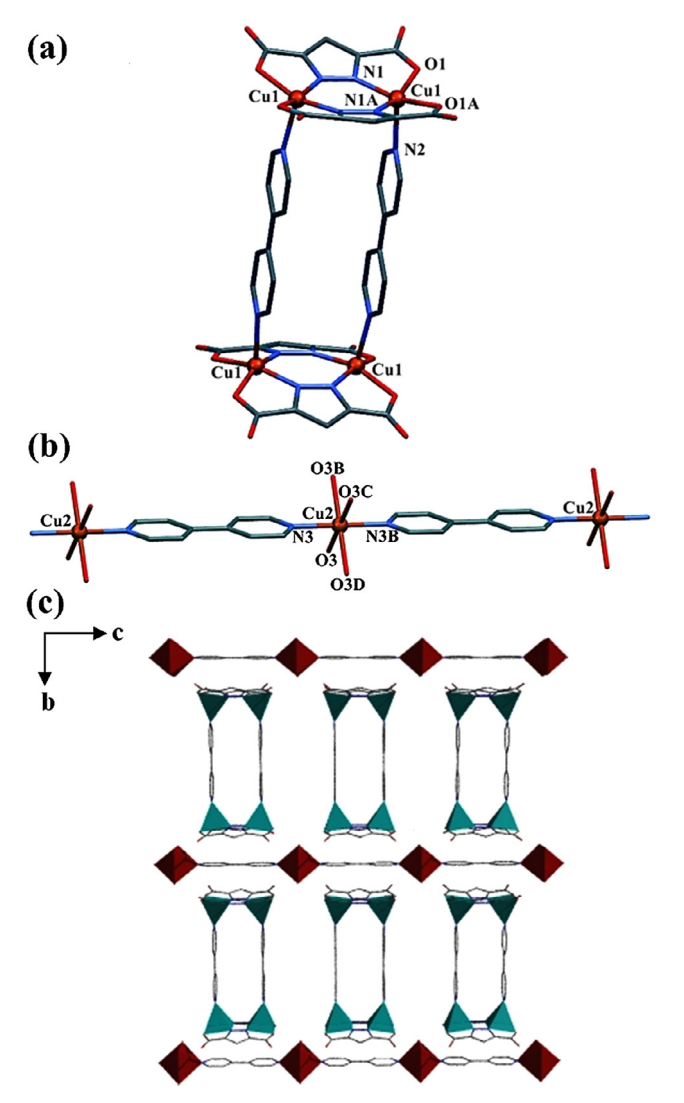


**Fig. 4.** (a) Anionic tetranuclear Cu(II) unit of  $\{[Cu_4(Hpzdc)_2(pzdc)_2(bpy)_2]^{2-}, (b)$  Cationic chain coordination polymer of  $[Cu(bpy)(H_2O)_4]_n^{2+}$  with atom labeling scheme of **3.** All hydrogen atoms and lattice water molecules are omitted for clarity (symmetry codes: A = -x, y, z; B = 1 - x, 1 - y, -z; C = x, 1 - y, z; D = 1 - x, y, -z. (c) Anionic tetranuclear Cu(II) units stabilizing with cationic 1D chain coordination polymers. The blue and red polygons represent five- and six-coordination geometries of Cu(II) centers, respectively. (Colour online).

17.91%) and two water molecules for **4** (calcd. 4.89%). Subsequently, the second weight loss process of 9.91% and 14.74% varies from 80 to 295 °C and 60–290 °C for **2** and **4**, respectively, corresponding to the removal of all remaining water molecules (calcd. 9.95% for **2** and 14.69% for **4**). Then the samples start to decompose after about 290 °C. Finally, compound **3** shows gradual weight loss of 9.51% in the range of 35–250 °C, corresponding to the escape of all coordination and lattice water molecules (calcd. 9.33%). Then the structures decompose to some unidentified species (Fig. 7).

## 3.6. XRPD patterns

To confirm whether the crystal structures of **1–4** are truly representative of the bulk materials, X-ray powder diffraction experiments have been performed at room temperature. The experimental and simulated (from the single crystal data) patterns are identical confirming the phase purity of the bulk samples (Figs. S6–S9).

### 3.7. Structural discussion

By the combination of  $Cu(NO_3)_2 \cdot 3H_2O$  with  $H_3pzdc$  and  $N_1N'$ ditopic coligands in a 1:1:1 molar ratio in the mixture solution of H<sub>2</sub>O/DMF/EtOH, the ternary Cu(II) coordination polymers **1–4** were obtained. Compounds 1, 2 and 4 were synthesized by layering method at room temperature. They exhibit 1D chain coordination polymers comprised of pyrazolato-bridged trinuclear Cu(II) building unit with the unique (5-6-5), (6-6-6) and (6-5-5) sequences of Cu(II) coordination number for 1, 2 and 4, respectively. While 3 was synthesized by solvothermal method at 120 °C that contains both anionic tetranuclear Cu(II) cluster and cationic 1D coordination polymer. The  $\mu_2$ -N,N'-bridges link Cu<sub>3</sub> secondary building unit in compounds 1 and 2 giving rise to 1D chain structure. While each trinuclear unit in 4 is assembled to hexanuclear cluster by weak syn, anti-bridging mode of pzdc<sup>3-</sup> and further extended by  $\mu_2$ ampy forming 1D ladder-like chain structure. The neutral trinuclear [Cu<sub>3</sub>(pzdc)<sub>2</sub>] building unit with various sequences of Cu(II) coordination numbers have been reported, such as, [Cu<sub>3</sub>(pzdc)<sub>2</sub>(- $Me_2en_2(H_2O)_2[(H_2O)_8, [28] [Cu_3(dien)_2(pzdc)_2CH_3OH]_2(CH_3OH)_6,$ [41]  $[Cu_3(pzdc)_2(H_2O)_4]_n$ ,[30] with (5-4-5), (5-5-5), and (5-6-5) sequences of Cu(II) coordination numbers, respectively. It can be seen that 5-coordinated Cu(II) geometry is more favorable in the neutral Cu<sub>3</sub> system, however, 6-coordinated octahedral geometry may be adopted by using long rigid bpy spacer in 2 where is less steric hindrance between neighboring Cu<sub>3</sub> units. Besides versatile of distorted coordination geometries of Cu(II) centers, and various coordination modes of H<sub>3</sub>pzdc play a key role on the construction of Cu(II) secondary building unit, the reaction temperature also have a significant influence on the structural assembly. When using the bpy as a coligand, compound 3 was synthesized at high temperature, giving the cationic 1D chain CPs with the unique anionic tetranuclear Cu(II) cluster constructed from metallacyclic dinuclear Cu(II) building unit while 2 was prepared at room temperature, generating a simple 1D chain structure. The coordination geometries of Cu(II) centers were also confirmed by electronic diffuse reflectance spectra which agree with the  ${}^{2}E_{g}$  to  ${}^{2}T_{2g}$  (parent) transition for distorted octahedral and square pyramidal geometry (Fig. S5) [7,40].

#### 3.8. Magnetic properties

The temperature dependent magnetic susceptibilities for the 1D coordination polymers **1**, **2** and **4** are all very similar and indicative of the neutral trinuclear, pyrazolato-bridged moieties showing weak antiferromagnetic coupling with little or no coupling across the N,N'-ditopic linkers in the 1D species. Taking compound **4** as a typical example (Fig. 8, the other plots are in Fis. S10–S11),  $\chi_M T$ , per Cu<sub>3</sub>, is ~1.25 cm<sup>3</sup> mol<sup>-1</sup> K at room temperature, as expected for three weakly coupled Cu(II) ions, with g on each Cu (II) of 2.1. The  $\chi_M T$  values decrease gradually between 300 K and 100 K, then more rapidly reaching a plateau at 0.4 cm<sup>3</sup> mol<sup>-1</sup> K at 10 K, indicative of a  $S = \frac{1}{2}$  ground state for the Cu<sub>3</sub> species. Below 5 K, there is a further decrease that is possible indicative of weak antiferromagnetic inter-trinuclear coupling, across the linking N, N'-ditopic coligands.

Focusing, first, on the 5–300 K data, we have used a linear trinuclear  $S = \frac{1}{2}$  model with spin Hamiltonian containing exchange and Zeeman terms: [30,42].

$$\mathbf{H} = -2J\{\mathbf{S}_1.\mathbf{S}_2 + \mathbf{S}_1.\mathbf{S}_2'\} + g\mu_{\rm B}S_{Tz}H_z$$

where the Cu(II) centers are arranged Cu2–Cu1(center)-Cu2'. J is the exchange interaction between adjacent Cu(II) ions in the trimer,  $S_i$  the spin operator for each S = 1/2 Cu(II),  $S_T$  the total spin operator of the trimer with  $S_T = S_1 + S_2 + S_2'$  and  $S_{Tz}$  is the z component of

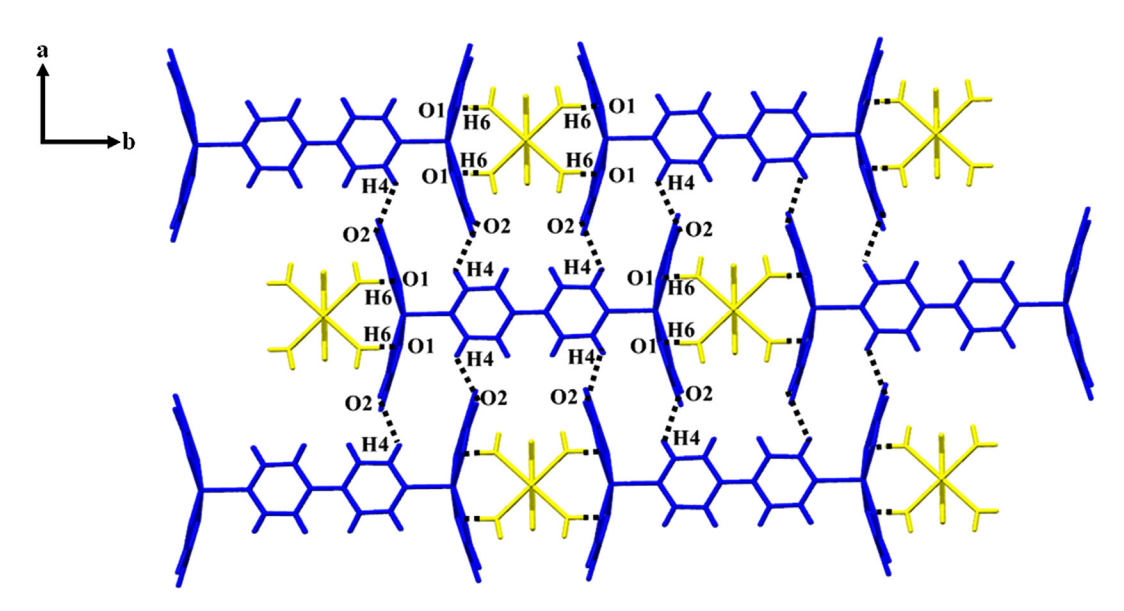
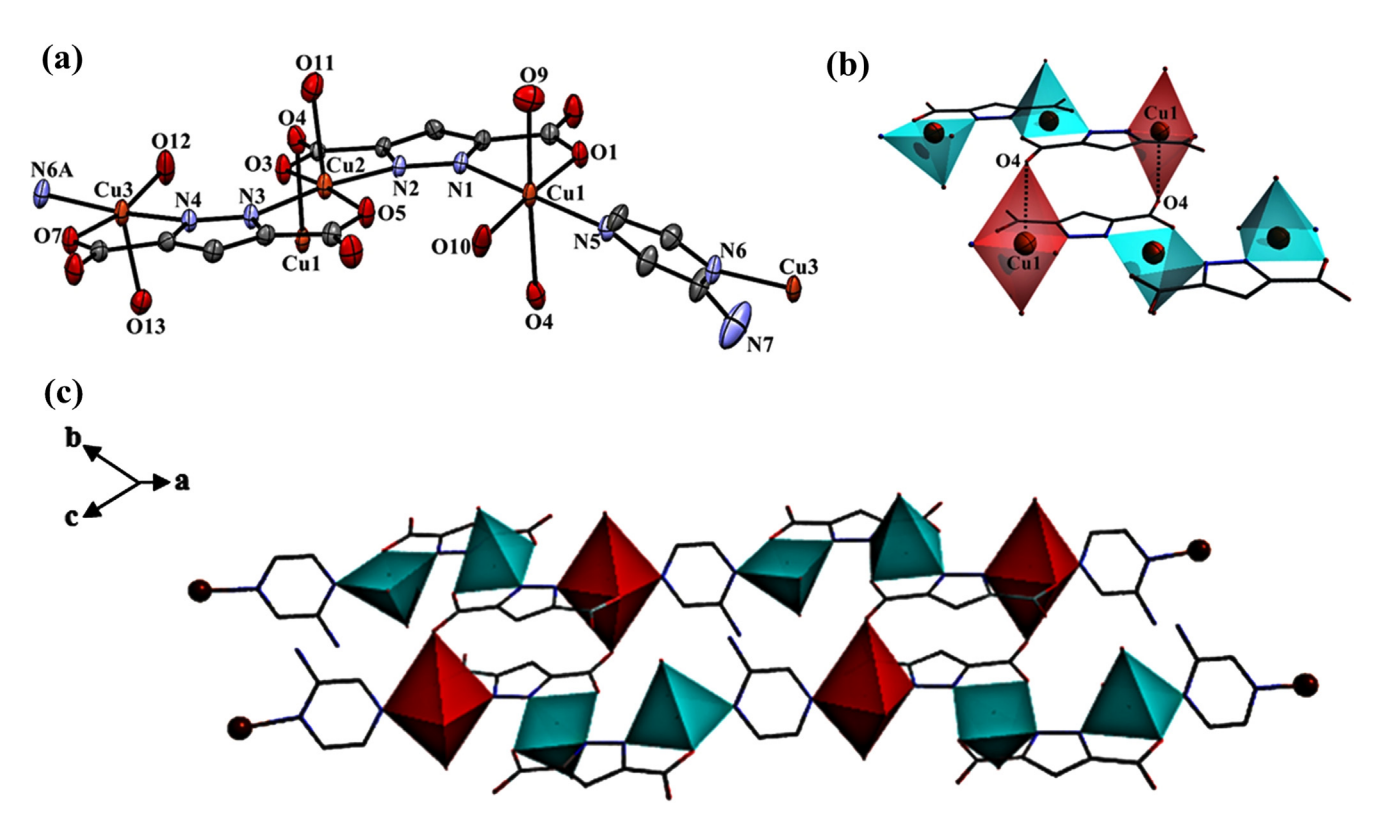


Fig. 5. 3D packing diagram of 3 formed by intermolecular hydrogen bonding.



**Fig. 6.** (a) A trinuclear Cu(II) building unit and atom labeling scheme of **4**. The ellipsoids are shown at 50% probability level. All hydrogen atoms and lattice water molecules are omitted for clarity (symmetry code: A = x, -1 + y, -1 + z). (b) A hexanuclear Cu(II) building unit composed of weak Cu1-O4 bond. (c) The 1D ladder-like chain of **4**. The blue and red polygons represent five- and six-coordination geometries of Cu(II) centers, respectively. (Colour online).

the  $\mathbf{S}_T$  operator. This leads to three energy levels  $S = \frac{1}{2}$  (energy zero);  $S = \frac{1}{2}$  (E = -2J) and S = 3/2 (E = -3J). We have also included a J' (Cu2–Cu2') term in the fitting but it is insensitive compared to setting it at zero (Table 2).

In Fig. 8 it can be seen that the best fit line (solid line) reproduces the  $\chi_M T$  values extremely well, the plateau at low temperatures indicative of population of the  $S = \frac{1}{2}$  state. Perusal of the literature of pyrazolate-bridged Cu(II) compounds reveals few singly-pyrazolate bridged examples for comparison. The 3D complex  $[Cu_3(pzdc)_2(H_2O)_4]_n$ , [30] obtained hydrothermally, shows similar

trinuclear core units to the present 1D CPs, but forms a 3D array via bridging through the carboxylate O atoms. The J value obtained in fitting the 50–300 K data to the present trinuclear model is  $-22 \, \mathrm{cm}^{-1}$ , a little higher than those found here which is agree with the shorter. Cu···Cu separation in the trinuclear moiety of  $[\mathrm{Cu_3}(\mathrm{pzdc})_2(\mathrm{H_2O})_4]_n$  (4.356 Å) comparing to 4.4102(2)–4.5207 (2) Å for **1**, **2** and **4**. A singly-bridged complex, K[Cu<sub>2</sub>L<sub>2</sub>(pz)]H<sub>2</sub>O (H<sub>2</sub>L = 6-amino-1,3-dimethyl-5-(2'-carboxy phenyl)azouracil and pz = pyrazole), with pseudotetrahedral geometry around the Cu (II) centers, showed  $J = -2.7 \, \mathrm{cm}^{-1}$  and g = 2.1, [43] J being much

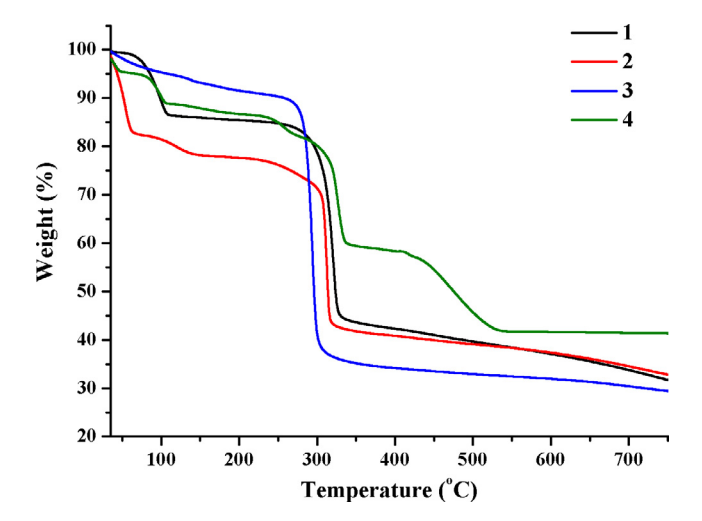
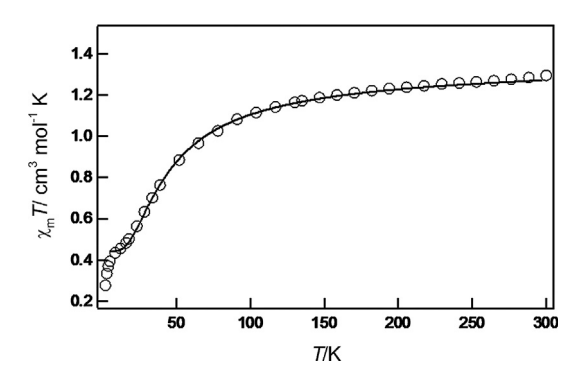


Fig. 7. TGA curves of 1-4.



**Fig. 8.** Experimental values of  $\chi_M T$ , per Cu<sub>3</sub>, (open circles) versus temperature (K) plot for compound **4.** The solid lines is the best fit using the linear  $S = \frac{1}{2}$  trimer model described in the text that does not include an inter-trimer term,  $\theta$ .

**Table 2** Best fit *J* values. A constant  $N\alpha$  (temperature independent susceptibility) of  $65 \times 10^{-6} \, \mathrm{cm^3 \, mol^{-1}}$  was fixed in the susceptibility expression.

| CPs | $J$ (cm $^{-1}$ ) | g    |
|-----|-------------------|------|
| 1   | -16.4             | 2.10 |
| 2   | -16.5             | 2.14 |
| 4   | -18.0             | 2.17 |

lower in magnitude than those in Table 2. In contrast, double-pyrazolate bridging, in (Bu<sub>4</sub>N)<sub>2</sub>[Cu<sub>2</sub>(pzdc)<sub>2</sub>], with Cu···Cu separation of 3.98 Å, [44] or mixed {pyrazolate/alkoxide} [45] or {pyrazolate/ azide} [46] bridging leads to much stronger antiferromagnetic coupling and larger negative J values ( $\geq -100 \text{ cm}^{-1}$ ) than those found here, no doubt because of the extra bridging contribution and smaller Cu---Cu separation. A marked difference is observed in the  $\chi_M T$  plots for 1, 2 and 4 compared to that of  $[Cu_3(pzdc)_2(H_2O)_4]$ n, [30] at very low temperatures. In the latter, the  $\chi_{\rm M}T$  values are similar to the present ones above  $\sim$ 50 K, but increase sharply below  $\sim$ 20 K due to long-range magnetic order of the  $S = \frac{1}{2}$  ground states  $(J(2D = +1.9 \text{ cm}^{-1}; J(3D) = -0.06 \text{ cm}^{-1})$  brought about by the carboxylate bridging that forms the 3D array. We do not see such behaviour here, the linking pyrazine and bipyridine that form the 1D chains, do not provide strong enough superexchange pathways between the Cu<sub>3</sub> units to induce long range order. Indeed, the small decrease in  $\gamma_{\rm M}T$  at very low temperatures is indicative of weak inter-trinuclear coupling.

#### 4. Conclusions

Four new copper(II) coordination polymers constructed by selfassembly of dinuclear or trinuclear building units based on pzdc ligand and auxiliary N,N'-ditopic spacers have been structurally characterized. Compounds 1 and 2 exhibit 1D chains while 3 shows 1D chain cationic coordination polymer and anionic tetranuclear Cu(II) cluster. Compound 4 exhibits 1D ladder-like chain structure. Compounds 1 and 2 consist of trinuclear Cu(II) building units constructed by Cu(II) ions and pzdc<sup>3-</sup> ligands with (5-6-5), (6-6-6) sequences of Cu(II) geometries, respectively. These Cu<sub>3</sub> units are extended via pyz or bpy linkers giving 1D chain structures. In 4, the hexanuclear Cu(II) cluster is generated by the combination of two Cu<sub>3</sub> units based on pzdc<sup>3-</sup> and ampy spacer extend the hexanuclear unit to 1D ladder-like chain structure. In contrast, anionic tetranuclear Cu(II) cluster of **3** is built up from two [Cu<sub>2</sub>(Hpzdc) (pzdc)]- units and two bpy linkers, stabilizing with 1D chain of  $[Cu(bpy)(H_2O)_4]_n^{2+}$ . This result demonstrated that various distorted geometries of Cu(II) centers, diverse coordination modes of H<sub>3</sub>pzdc and, N,N'-ditopic coligands play a key role on their structural diversity. Furthermore the reaction temperature also have a great influence on the structural assembly of 2 and 3. The magnetic studies of 1, 2 and 4 revealed weak antiferromagnetic coupling interactions within Cu(II) trimer.

#### Acknowledgments

Funding for this work is provided by The Thailand Research Fund: Grant No. MRG5980237 (for Boonmak, J.) and BRG5980014 (for Youngme, S.), the Higher Education Research Promotion and National Research University Project of Thailand, through the Advanced Functional Materials Cluster of Khon Kaen University, and the center of Excellence for Innovation in Chemistry (PERCH–CIC), Office of the Higher Education Commission, Ministry of Education, Thailand. KSM thanks the Australian Research Council for a Discovery grant.

#### Appendix A. Supplementary data

CCDC 1507699–1507702 contains the supplementary crystallographic data for **1–4**. These data can be obtained free of charge via <a href="http://www.ccdc.cam.ac.uk/conts/retrieving.html">http://www.ccdc.cam.ac.uk/conts/retrieving.html</a>, or from the Cambridge Crystallographic Data Centre, 12 Union Road, Cambridge CB2 1EZ, UK; fax: (+44) 1223-336-033; or e-mail: deposit@ccdc.cam.ac.uk. Supplementary data associated with this article can be found, in the online version, at <a href="http://dx.doi.org/10.1016/j.poly.2017.01.015">http://dx.doi.org/10.1016/j.poly.2017.01.015</a>.

## References

- [1] M. Arıcı, O.Z. Yeşilel, M. Taş, H. Demiral, Inorg. Chem. 54 (2015) 11283.
- [2] L. Bromberg, X. Su, T.A. Hatton, Chem. Mater. 26 (2014) 6257.
- [3] E. Lee, H. Ju, S. Kim, K.-M. Park, S.S. Lee, Cryst. Growth Des. 15 (2015) 5427.
- [4] J.-J. Liu, Y.-F. Guan, M.-J. Lin, C.-C. Huang, W.-X. Dai, Cryst. Growth Des. 15 (2015) 5040.
- [5] G. Kang, Y. Jeon, K.Y. Lee, J. Kim, T.H. Kim, Cryst. Growth Des. 15 (2015) 5183.
- [6] H.-Y. Wang, Y. Wu, C.F. Leong, D.M. D'Alessandro, J.-L. Zuo, Inorg. Chem. 54 (2015) 10766.
- [7] P. Suvanvapee, J. Boonmak, F. Klongdee, C. Pakawatchai, B. Moubaraki, K.S. Murray, S. Youngme, Cryst. Growth Des. 15 (2015) 3804.
- [8] J. Wu, L. Zhao, M. Guo, J. Tang, Chem. Commun. 51 (2015) 17317.
- [9] C. Wang, S.-Y. Lin, W. Shi, P. Cheng, J. Tang, Dalton Trans. 44 (2015) 5364.
- [10] J. Wu, L. Zhao, L. Zhang, X.-L. Li, M. Guo, A.K. Powell, J. Tang, Angew. Chem., Int. Ed. 55 (2016) 15574.
- [11] B. Mohapatra, S. Verma, Cryst. Growth Des. 16 (2016) 696.
- [12] L. Liu, C. Huang, X. Xue, M. Li, H. Hou, Y. Fan, Cryst. Growth Des. 15 (2015) 4507.
- [13] J.-X. Yang, X. Zhang, J.-K. Cheng, J. Zhang, Y.-G. Yao, Cryst. Growth Des. 12 (2012) 333.
- [14] G.G. Sezer, O.Z. Yeşilel, M. Arıcı, H. Erer, Polyhedron 102 (2015) 514.

- [15] M. Felloni, A.J. Blake, P. Hubberstey, C. Wilson, M. Schröder, Cryst. Growth Des. 9 (2009) 4685.
- [16] I.M.L. Rosa, M.C.S. Costa, B.S. Vitto, L. Amorim, C.C. Correa, C.B. Pinheiro, A.C. Doriguetto, Cryst. Growth Des. 16 (2016) 1606.
- [17] X. Liu, P. Cen, H. Li, H. Ke, S. Zhang, Q. Wei, G. Xie, S. Chen, S. Gao, Inorg. Chem. 53 (2014) 8088.
- [18] A.K. Singh, J.I.V.D. Vlugt, S. Demeshko, S. Dechert, F. Meyer, Eur. J. Inorg. Chem. (2009) 3431.
- [19] K. Hassanein, O. Castillo, C.J. Gómez-García, F. Zamora, P. Amo-Ochoa, Cryst. Growth Des. 15 (2015) 5485.
- [20] Y.M. Litvinova, Y.M. Gayfulin, D.G. Samsonenko, A.S. Bogomyakov, W.H. Shon, S.-J. Kim, J.-S. Rhyee, Y.V. Mironov, Polyhedron 115 (2016) 174.
- [21] L. Pan, X. Huang, J. Li, J. Solid State Chem. 152 (2000) 236.
- [22] J.-H. Yang, S.-L. Zheng, X.-L. Yu, X.-M. Chen, Cryst. Growth Des. 4 (2004) 831.
- [23] P. King, R. Clérac, C.E. Anson, A.K. Powell, Dalton Trans. (2004) 852.
- [24] J. Zhao, L.-S. Long, R.-B. Huang, L.-S. Zheng, Dalton Trans. (2008) 4714.
- [25] X.-H. Zhou, X.-D. Du, G.-N. Li, J.-L. Zuo, X.-Z. You, Cryst. Growth Des. 9 (2009) 4487.
- [26] D. Saha, T. Maity, S. Das, S. Koner, Dalton Trans. 42 (2013) 13912.
- [27] S. Barman, H. Furukawa, O. Blacque, K. Venkatesan, O.M. Yaghi, G.-X. Jin, H. Berke, Chem. Commun. 47 (2011) (1884) 11882.
- [28] W.L. Driessen, L. Chang, C. Finazzo, S. Gorter, D. Rehorst, J. Reedijk, M. Lutz, A.L. Spek, Inorg. Chim. Acta 350 (2003) 25.
- [29] C.-Z. Xie, R.-F. Li, L.-Y. Wang, Q.-Q. Zhang, Z. Anorg, Allg. Chem. 636 (2010) 657.
- [30] P. King, R. Clérac, C.E. Anson, C. Coulon, A.K. Powell, Inorg. Chem. 42 (2003) 3492.

- [31] Q.-Q. Dou, Y.-K. He, L.-T. Zhang, Z.-B. Han, Acta Cryst. E63 (2007) m2908.
- [32] APEX2; Bruker AXS Inc., Madison, WI., 2014.
- [33] SAINT 4.0 Software Reference Manual; Siemens Analytical X-Ray Systems Inc., Madison, WI., 2000.
- [34] G.M. Sheldrick, SADABS, Program for Empirical Absorption correction of Area Detector Data; University of Gottingen: Gottingen, Germany. 2000.
- [35] G.M. Sheldrick, Acta Crystallogr., Sect. A A64 (2008) 112.
- [36] A.W. Addison, T.N. Rao, J. Chem. Soc., Dalton Trans. (1984) 1349.
- [37] G.P. Shields, P.R. Raithby, F.H. Allen, W.D.S. Motherwell, *Acta Crystallogr.* B 56 (2000) 455.
- [38] P. Smoleński, J. Kłak, D.S. Nesterov, A.M. Kirillov, Cryst. Growth Des. 12 (2012) 5852.
- [39] J.-L. Tian, S.-P. Yan, D.-Z. Liao, Z.-H. Jiang, P. Cheng, Inorg. Chem. Commun. (2003) 1025.
- [40] J. Boonmak, S. Youngme, N. Chaichit, G.A.V. Albada, J. Reedijk, Cryst. Growth Des. 9 (2009) 3318.
- [41] F.-M. Nie, Z.-Y. Dong, F. Lu, G.-X. Li, J. Coord. Chem. 63 (2010) 4259.
- [42] O. Kahn, Molecular Magnetism, Chapter 10, 1993.
- [43] J.-M. Dominguez-Vera, E. Colacio, J. Ruiz, J.M. Moreno, M.R. Sundberg, Acta Chem. Scand. 46 (1992) 1055.
- [44] J.C. Bayoń, P. Esteban, G. Net, P.G. Ramussen, K.N. Baker, C.W. Hahn, M.M. Gumz, Inorg. Chem. 30 (1991) 2572.
- [45] S.-F. Huang, Y.-C. Chou, P. Misra, C.-J. Lee, S. Mohanta, H.-H. Wei, Inorg. Chim. Acta 357 (2004) 1627.
- [46] J.-C. Liu, D.-G. Fu, J.-Z. Zhuang, C.-Y. Duan, X.-Z. You, J. Chem. Soc., Dalton Trans. (1999) 2337.